ISSN 0252-1075
Research Report No. RR-096

Acc. No. RR-96
Date 24.4.03

Contribution from
Indian Institute of Tropical Meteorology

EVIDENCE OF TWIN GYRES IN THE INDIAN OCEAN: NEW INSIGHTS USING REDUCED GRAVITY MODEL FORCED BY DAILY WINDS.

by

P. RAHUL CHAND REDDY, P.S. SALVEKAR,
D.W. GANER and A.A. DEO

PUNE – 411 008
INDIA

FEBRUARY 2003

Contents

411 008.
RR-96
24.4.03

Evidence of Twin Gyres in the Indian Ocean: New Insights using reduced gravity model forced by daily winds.

P.Rahul Chand Reddy, P.S.Salvekar, D.W.Ganer & A.A.Deo.

Indian Institute Of Tropical Meteorology, Pune, India.

Abstract

Westward straddling anticyclonic mesoscale Twin (T) Gyres are discovered to form even before the Somali Gyres during the South West monsoon months May through mid September, every year over the Equatorial Indian Ocean as revealed from the analysis of surface circulations by the Reduced Gravity Model with daily forcing. The Seasonal and the Monthly forcing fail to capture this finer aspect. The Twin Gyres (T1-Northen Gyre, T2-Southern Gyre) move westwards (from 90E) between 5^0N and 5^0S. T1 forms first and dissipates first by July end at 65E, T2 dissipates later at the Somali coast at 45E by mid September. World Ocean Circulation Experiment observations in 1995 catch the dissipating stage of such gyres. TOPEX Sea Surface Height observations in the Indian Ocean (90E) from May to July by *Subrahmanyam et.al* [2001] also support the Twin Gyres formation and westward movements. 'Conjunction Theory' is proposed to explain the formation, westward movement of the Gyres. The results reveal new dynamics in the Indian Ocean and stress the need of using daily data in modeling studies as monthly data hides such significant modes.

Keywords - Data Spectrum, Equatorial Indian Ocean, Conjunction Hypothesis, Twin gyres.

1.Introduction

Indian Ocean enacts a very active and independent role (*Webster,* 1999) in climate variability but is independent of forcing by external phenomena such as ENSO [*Meehl(1994,1997),Nicholls(*1983, 1997)]. The surface circulations play an important role in the exchange of mass, momentum and energy between the atmosphere and ocean *Kendall et al*(2002). In fact, the surface circulations predominantly govern the ocean state. Wind driven upper circulation gives rise to massive near surface flows such as Gulf Stream, Khuroshio and Antartic circumpolar currents, *Carlwunsch* (2000). Ocean numerical models have become quite realistic as recognized by *Semnter* (1995) in simulating the seasonal and interannual large-scale surface circulations. It is now being realized that very simple models, which can be run on relatively inexpensive computers, can provide results different from, but just as useful as those produced by high resolution simulations, *Pillard* (2002). The basin scale Reduced Gravity 1½ layer ocean model also called as the IITM Reduced Gravity (IRG) model, has been proven to simulate realistic observed surface currents on both monthly and seasonal scales as seen by *Behera et al.* (1996, 1998). Earlier studies by *Luther et a.l* (1985), *Woodberry et, al* (1989) *Potemra et al.* (1991) and by *Jensen* (1993) with monthly and seasonal winds fail to simulate the Twin gyres. This is first time the impact of daily winds in model simulations is being studied Using Reduced Gravity model. *Rahul et al*. (2002 a, b) have shown that these model-simulated currents can be treated equivalent to observations in the data sparse regions. Indian ocean has been extensively studied using seasonal or the monthly forcing, what happens to the model simulations when the time scale is fractured to daily forcings? As expected, the results encompass all the features that are simulated with Seasonal and Monthly forcing plus something that the Seasonal and the Monthly forcing had been missing since the past 4 to 5 decades. Daily climatologically simulated upper layer currents reveal westward advecting anticyclonic Twin (T) Mesoscale gyres on either side of the equator in the well-studied equatorial Indian Ocean, *Wyrtki* (1973) during midmonsoon months. A "Conjunction Theory" is proposed to probe into the details of the T-Gyres. A "Data Spectrum" that explains the role of daily data in simulating finer aspects of Mesoscale circulations is also proposed. The small-scale processes, whose influence on large-scale processes is just beginning to emerge and would bring radical changes in ocean modeling *Quadfasel* (2002). Relation of such small-scale processes to the dynamics of the Indian Southwest monsoon and its subsequent impact on the global climate needs to be further investigated. In the following sections the model details, data & methodology, results & discussion and finally the conclusions are provided.

2. Model and Methodology

The model used in this study has one active layer, overlying a deep motionless inactive layer, i.e., zero pressure gradient in the lower layer that effectively filters the fast barotropic mode. The model equations are based on vertically integrated shallow water equations over a layer, assuming no vertical shear in the horizontal fields.

The model equations in Cartesian co-ordinate are:

$$U_t + (UU/H)_x + (UV/H)_y - fV + (g'/2)(H^2)_x = A_H \nabla^2 (U) + \tau_{xz} / \rho_1 \quad (1)$$

$$V_t + (UV/H)_x + (VV/H)_y + fU + (g'/2)(H^2)_y = A_H \nabla^2 (V) + \tau_{yz} / \rho_1 \quad (2)$$

$$H_t + U_x + V_y = We \quad (3)$$

Where U and V are zonal and meridional components of transport obtained from vertically integrating upper layer velocity field, f is the Coriolis parameter. H is the upper layer thickness, $g' = g\ (\rho_2 - \rho_1)/\rho_2$ is the reduced gravity ($0.03 ms^{-2}$). A_H is the horizontal eddy viscosity coefficient ($2250\ m^2 s^{-1}$) and 'τ_{xz} ' 'τ_{yz}' are the components of the wind stress applied as a body force. w_e is a source term representing entrainment from deep motionless layer to the upper active layer. This entrainment is introduced only to prevent the interface from surfacing that happens when a small initial upper layer thickness is considered. This term is positive for upper layer when the layer thickness becomes less than a pre-set minimum depth *Hmin* (100 m). The term is determined through a simple function as suggested by *McCreary and Kundu* (1988). The effect of this entrainment on the upper layer density, momentum and kinetic energy balance has been neglected. It is assumed that the entrained water engulfed into the upper layer, has zero velocity and is instantaneously adjusted to the density ρ_1. The model equations are solved numerically on a finite difference mesh staggered in space (Arakawa C-grid) and integrated with respect to time (Δt=30 min) using leapfrog finite-difference scheme. An Euler scheme is applied at every 49th step to eliminate the spurious growth that usually arises due to time splitting in leapfrog scheme. The horizontal domain used in the model extends from 35°E to 115°E and from 24°S to 23°N. Boundary conditions are no slip ($U = V$ =0) at land boundaries and modified radiation boundary condition by *Camerlengo and O'Brien* (1980), *Jensen* (1990) is applied at the open boundaries. The reduced gravity model has realistically simulated most of the circulation features in the Indian Ocean as referred by *Luther et al.* (1989), *Simmons et al.* (1988), *Luther and O'Brien*.(1985). The model is integrated by using daily climatology of NCEP winds, interpolated to the model grid resolution (0.5° X 0.5°) from 1992- 2001 and the spin up time to reach the steady state is 10 years. Model is further integrated from Jan 1992 to Dec2001 using daily interannual surface forcings. The detection and measurement of small changes in the Earth's climate require extremely precise observations on a daily scale *Frank et al* (2000) from the satellites. To see the impact of still more reduced time scales than the daily data, IRS P4 MSMR (OCEANSAT) derived 6 hourly surface winds over the north Indian ocean are acquired during the mid monsoon month of July for three years 1999,2000 & 2001.These winds having an initial grid resolution of 1.48° × 1.48° are interpolated to reduced gravity model resolution of 0.5° × 0.5°. The steady state solution for June using daily reanalysis NCEP climatology is considered as the initial condition and the model is further integrated for the month of July using interannual MSMR winds. These results are similar with those obtained by NCEP daily climatology for July.

3. Overview of the Observational and other modeling studies in the Indian Ocean

A sketch of the various modeling and observational studies that have been carried out since the last 30 years are presented here. The details of the Indian Ocean are presented in three sections, Bay of Bengal, Equatorial region and the Arabian Sea.

3.1 Bay of Bengal circulation:

The Bay of Bengal is boarded by the Indian Subcontinent, Burma, Thailand Malay Peninsula and Sumatra, east coast currents and equatorial currents characterize the circulation of the bay. The Bay seasonally experiences reversing monsoons and depressions, severe cyclonic storms and also receives a heavy amount of rainfall coupled with the river run off.

The bay of Bengal is subjected to strong seasonal reversal of wind stress forcing.5N along Srilanka and Sumatra can be taken as the southern boundary line of the Bay.*Legeckis* (1987) proposed a basin scale anti cyclonic circulation pattern during winter months using NOAA AVHRR thermal infra red images. Four stages of flow in the Bay have been suggested by *Potmera et al* (1991),an anti cyclonic gyre across the whole bay during Dec-March, followed by two gyre systems (anti cyclonic on the western and cyclonic on the eastern side) during April– July. July-august is characterized by a basin wide gyre followed by another two-gyre system in the full season, which is opposite to its counterpart. The generation of these patterns has been explained by *Yu et al* (1991) using the concept of remote effect caused by the equatorial Kelvin waves. Successful simulations of the BOB surface circulations have also been carried out by *Mc Creary* (1993), *Behara et al* (1992) along with the observational work by *Eigenheer & Quadfasel*(2000)(Fig 5). Further, *Verkey etal* (1996) explained the seasonal circulation using a 3-gyre circulation pattern in a schematic way of two monsoons, South West and North East monsoon (Fig 4 a,b). A northern gyre (G1) at 13N, 89E is clockwise during winter and anticlockwise in summer. (G2) at 11N is clockwise during both winter and summer. (G3) is a gyre in the Andaman Sea having clockwise and anti clockwise flows in winter and summer respectively.

3.1.1 The East India Coastal Current.

Major part of the circulation in the BOB stems from the circulation along the coasts. The western boundary current in the BOB has been named as EICC(Fig 2,3). *Shanker* (1996); *McCreary* (1996) have shown that the EICC changes its direction twice a year, flowing north-eastward from Feb. to sep with a strong peak in March-April and southwestward from Oct-Jan with a strongest flow in Nov. This western boundary current is also part of an eddy field like the Somali current in SW monsoon *Shetya*(1993). The recent study by *Ratna Reddy* (1995) using NOAA AVHRR imagery reveled that this current is about 900 km in length and usually lies to the coast but sometimes shifts offshore *Shetya et al*(1993) with an average speed of 30-55cm/s. The EICC and its driving mechanisms have been further probed by hydrographic studies *Shetya*(1993, 1996),*Sanil kumar*(1997).Beginning in late September, the EICC begins to flow southward by November, at this time *Eigenheer and Quadfasel*(2000) through the. *TIP* altimetry have shown that, a slow cyclonic circulation around the Bay of Bengal, breaks up into several cells as the monsoon season develops. Due to the EICC it was found the geostrophic transports between the northern end of the Bay and 10N increase southward from 2Sv to about 8 Sv, *Shetye et at.* (1996).

3.1.2.West Indian Coastal Current (WICC)

Cutler and Swallow(1984); *Shetya and Shenoy*(1988) using the ship drift observations suggested of a southward flow that appears along the west coast of India in march, reaches a maximum in July (Fig 2) and vanishes by October. This is called the WICC.These features were also confirmed by *Shetya et al*(1990).

WICC flows northward during the winter monsoon (Fig 2), Shetye *et al.* (1991) found the surface current to decrease in width from about 400 km off South India near 10°N to just 100 km in the north at 22°N.The ship-drift currents indicated that the northward WICC at this time is the strongest west coastal current throughout the year , and yet the coastal winds are very weak or absent at this time. This property lends strong support for the importance of remote forcing.

The West Indian Coastal current (WICC) in the Arabian sea changes its direction seasonally. Pole ward in NE Monsoon and Equator ward during SW Monsoon and turn around Srilanka and join the eastward southwest Monsoon Current (SMC) *Shetye etal*(1990, 1993, 1996) (Fig 2).

3.2.Equatorial Regime:

3.2.1. The South Equatorial Current (SEC)

The SEC(Fig 2,3) flows westward between 10S and 20S and is the most persistent and present in most part of the year. At 20S it branches off in northward and southward directions near the Madagascar Coast. The northward branch again separates into two branches at the African Coast. One branch feeds the northward flowing EACC that is very important for SC, the southern branch feeds the Mozambique current.

3.2.2.The North Equatorial Current (NEC)

The NEC or the NEMC (Fig 3) flows west during winter with much weaker flow between 8N and the Equator (Pickard and Emery, 1982). Further south between Equator and 8S is the eastward flowing Equatorial Counter current (ECC). The NEC never reverses the direction during the summer monsoon but joins the ECC to form the Southeast monsoon current (SMC) or the Indian Monsoon current (IMC). This is more persistent along the south of equator. After the NE monsoon the NEC currents return to the westward flow.

Woodberry et al (1989) demonstrated the importance of SEC as a source of the EACC and the SC. *Potemera etal* (1991) and *Yu etal* (1991) showed that the equatorial waves remotely alter the circulation of the Bay of Bengal.

3.2.3. Wyrtki Jet or Equatorial Jet (EJ)

Theoretical studies on the equatorial jet have been reported by several authors (e.g Yoshida, 1959,O'Brain and Hurlbert, 1974,Gill, 1975 and cane, 1980). *Cane and More*(1981) theoretically proved the equatorial modes are basically composed of long Kelvin and Rossby waves. *Kindle and Thompson* (1989) showed that 26-day oscillation in the E.I.O is due to Yanai waves that are generated during the southwest monsoon. *Wyrtki* (1973) reported a jet like stream called a Wyrtki jet(Fig 2). Reverdin 1987, Rao 1989 have shown that the Wrytki jet is strongest between 60^0 E and 90^0 W and has a velocity 80 cm/s and a width 500 km. The Equatorial under current flows from East of 60^0 E during boreal winter *Cane* (1980). The Wyrtki jet transports surface waters over a time of two months. After reaching the Eastern end of the Basin the Wyrtki jet is reflected as Rossby waves and a part propagates pole ward as Eastern boundary waves. These Eastern boundary waves generate slowly propagating mid latitude Rossby waves that move into the BOB and eastern Arabian Sea is a *Perigaud and Delecsive*(1992). The existence of complex deep jets has also been reported by *Lutem and Swallow* (1976). Further it has been seem that the Indian Ocean – jets are more pronounced at depth than those in the Pacific below 2000m *Muenchctal*(1994)

3.3 .Arabian Sea

The Arabian Sea is a unique environment for studying the forced upper ocean response with strong and distinct atmospheric forcing regimes and a clear separation in the time domain between mesoscale oceanic variability and variability in the atmospheric forcing. It is influenced by unique monsoon seasonal cycle, with strong reversing wind forcing. Over the Arabian Sea Which is bounded by the land masses of the East Africa, the Arabian peninsula and the Indian Sub continent and the Indian Ocean to the South, the monsoon circulation leads to seasonal cycle of cold, dry northeasterly winds during the winter northeast monsoon and warm moist and very strong westerly winds during the summer southwest monsoon.

3.3.1. Somali Current

A Unique feature of the SW Monsoon winds out the Arabian Sea is the development of remarkably strong and steady wind jet . The dramatically changing forcing over the Arabian Sea leads to a dramatic response in the Basins boundary current/Somali current. During the SW monsoon the northward flowing Somali current has a strong transports e.g. 65 Sv, mostly confined to the upper 20 m, and posses a speed upto 3.7m/sec (Scott, 1983, swallow etal, 1983).During the NE monsoon the surface current is southwards, but is weaker and more diffuse (knox, 1987). During the SW monsoon, this current gives side to mesoscale eddy field *Bruce* (1979), *Bran* (1980), *Evans and Bran*(1981), *Bruce and Beatly* (1985), *Simma* (1988). These Eddies are important component of the short-term variability in this region.

The Somali current transports volumes of water mass comparable to the Gulf stream but changes direction during the SW monsoon. *Schott et al* (1990) showed that the Somali current during the SW monsoon decays monotonically in the vertical where as no deep reaching boundary current exists during winter monsoon. In March a northward surface current establishes north of 5^0 N *Quadfasel and Schott*(1983). The development and dissipation of the Somali gyres has been illustrated by *Schott et al*(1990) (Fig 6). During April, May the Somali current moves to the North. A southward return flow develops offshore and the eddy called the Southern gyre (SG) forms between 0-5N, 53E with a diameter ~200-300Km(Bruce1983, Schott, 1983,Subramanyam et al 1996). With strong winds blowing parallel to the coast a northern eddy system called the Great whirl (GW) forms between 5-10N, 58E with a diameter ~400-600 km (Bruce, 1970,1979: Swallow et al, 1983).*Dengler et al*(2001mkpap) recently concluded that the depth of monsoon response of GW in the WOCE observations was less than 1500m rather then 2000m as proposed by *Quadfasel*(1982). *Bruce* (1973) showed that the two gyre system is stable till Aug-Sep, when SG propagates northward and merges with the GW.After which the Somali current becomes stationary flowing from 4S to 10 N *Swallow and Fieux* (1982), Some of years there is also formation of a third warm eddy called Socotra eddy northeast of the GW.*Bruce and Beatty* (1985); *Fischer et al* (1996). *Luther & O'Brien* (1989) using 23 year mean monthly wind data *Cadet and Diehl*(1984) simulated the intraseasonal variability in the current sytem,they had found that the SG was absent in two of the 23 years. The coalescence of the SG with the GW did not take place in 7 years, *McCreary and Kundu* (1988) using a 21/2 layer reduced gravity model examined the different mechanisms responsible for the generation of SC and the associated gyres. These eddies along the Somali coast seem to be controlled by the wind forcing and topographic features *Cagle and Whritner* (1981). Significant interannual differences in the system of cold and upwelling wedges off Somali and their movements during the course of the Southeast Monsoon had already been reported by *Evans and Brown*,(1981);*Schott*,(1983).

4. IRG model simulations using monthly winds

The IRG model simulations of surface circulations in the Indian Ocean are presented below.

4.1 Bay of Bengal

The model simulated surface currents also reveal a 4-stage mode of the circulation patterns in the Bay of Bengal. A large basin wide anticylonic gyre(Fig 7,a) dominates the entire Bay, as observed in the climatological and the other model studies, *Potemera etal* (1991). This gyre(Fig 7 b,d) circulates all along the east coast of India north of 13N from January to May as observed by *Cutler and Swallow* (1984) and by *Legeckis* (1987) .The basin gets divided into two gyres during the transition months of March –May, a dominant anticylonic gyre to the west and another weak cyclonic gyre to the east with northward flow along both the boundaries(Fig 7 b,d). The coastally trapped Kelvin waves originating from the Reflected equatorial Kelvin waves at the eastern boundary cause a northward flow along the eastern side of the bay. This northward flow in turn radiates Rossby waves that dictate the flow in the Bay during the subsequent months.By late May and June a single Cyclonic gyre dominates the bay,this is replaced by two weak gyre sytems by Jul-Nov(Fig 7 f,h).

4.2.Equatorial Currents.

4.2.1 South Equatorial Current

A broad westward flowing SEC (Fig. 7,a) is seen in most of the Climatological charts between 8S and 205 almost through out the year. The same feature is well simulated by the model as well, a westward current between 105 and 205 is found to exists all through the year. The seasonal variability of the SEC is also reproduced in the model simulations in the sense that the SEC is more broader and towards the north of its mean position during the boreal summer and is narrow and to its south during the winter, this also tallies well with the climatologies that reproduce the seasonal variability of SEC. *Woodberry*(1989)has explained this seasonal variability as the consequence of the annual cycle of the wind stress curl further east, which gives rise to westward propagating Rossby waves.

Since the small islands east of Madagascar are not included in the model geometry, the simulated SEC flows directly to the east coast of Madagascar, splitting near Madagascar coast around 17S and is in agreement with the observations *Schott et al*(1988). The Northern branch, the Northeast Madagascar current, flows past the north east tip of Madagascar at Cape Amber and feeds into the EACC, the other branch flows southward as the Mozambique current. The annual cycle of the wind fields causes the basin wide southern hemisphere gyre to be flanked by SEC to the south, ECC to the north, EACC to the west (Fig 7 a to h). The model simulated ECC remains around equator between 3N and 75 and is by the westward propagating equatorial Rossby waves. During Mar-Apr and Oct-Nov, the transition months of the monsoon winds and, model simulates stronger ECC around the equator, which is comparable to the observed Equatorial Jet (EJ). The model simulates EJ in March and October, earlier to the observed occurrence during May and November respectively *Wyrtki* (1973)

4.2.2. North Equatorial Current (NEC)

The model simulated NEC is seen to change direction four times in a year, flowing eastward during southwest monsoon. There is a shift of the eastward Monsoon Current (MC) to the north and this is observed in summer months occurring because of the northward push of the westward propagating Rossby waves. This is mainly caused as the reported observed currents are wind driven surface currents whereas the model currents are mean upper layer averaged flow (100 m).

4.3. Arabian Sea.

The winds are north easterly in the Indian ocean during the Northern Hemisphere winter, the Somali current along the Somali coast has southward flow as seen in the model simulations for January(Fig 7,a).

The model simulated surface currents show a southward flow from 10N to Equator in December and then flow further south till 2S by Jan-March. An anticyclonic gyre south of the equator is simulated in the January circulation, this gyre forms when the Somali Current that flows southward joins the northward flowing East African Coastal Current (EACC). The model simulations of the features so far discussed are in perfect qualitative agreement with the observed climatological atlases *Wyrtki* (1971), *Hasternath & Greischar* (1989), Rao *et al,* (1991) and with the model results of *Luther & O' Brien* (1989) and *Woodbery et al* (1989).Before the onset of the southwest monsoon or rather during the transition period, the somali current starts to flow northward. Model results show a northward flow north of 5N fed by an onshore flow around 5N by late March (Fig 7,b)and the northward all along the coast in April (1,c). This is in good agreement with the climatological charts and also with the results of Schott and *Quadfasel* (1982). The northward flow, north of 5N occurring in March is reported as a result of the local negative wind stress curl. With the southward flowing Somali Current disappearing in April and the winds start blowing from southwest, the EACC reaches equator. The recirculated water from the EACC forms a cyclonic gyre south of equator in April. This attains strength by May (Fig. 7,d) and is found to be present through out the monsoon season. With the monsoon onset in June(Fig 7,e)an anticyclonic gyre ,the Great Whirl develops from 4-10N with a second cold wedge at the latitude where it turns off shore(10-12N) by July.

The cross equatorial flow continuous this time, it leaves the coast south of 4N, where it partially turns eastward and as well flows back across the equator resulting in a circulation pattern referred to as the Southern Gyre.Water mass signatures of both the gyres indicate a very little exchange between the Great whirl and the Southern gyre, thus the water that crosses the equator with the shoreward part of the southern gyre does not continue to flow up the Somali coast but rather bends eastward and partially recirculates southwards across the equator as seen (Fig 7,f).In the late phase of summer monsoon the Great whirl has become an almost closed circulation cell. Even though observational evidences *Swallow & Fieux*(1982) suggest a northward migration of the Southern Gyre and its subsequent merging with the Great Whirl in late August (Fig 7,g) and early September and also shown by the modeling simulations of *Luther et al*(1985), the model simulations of the present study, do not show northward migration of the Southern Gyre but eddies from the gyre migrates northward to merge with the Great Whirl. In September (Fig 7,h) the magnitude of south westerly wind decreases but the circulation features of July are retained, except for the weakening of the Southern Gyre and northward migration of the Great Whirl. When the southwest west monsoon dies down, the cross equatorial Somali current turns offshore again at 3N,while the great whirl continues to spin in its original position, the great whirl is even discernible underneath the developing Northeast Monsoon circulation well towards the end of the year, this feature is well simulated in the present study tallying with the finding of *Bruce et al* (1981).

5.IRG model simulations using Daily winds

5.1 Bay of Bengal

All the features simulated in the monthly simulations are well simulated even in the daily simulations. Every five-day simulation of the Bay of Bengal circulations for the Southwest monsoon months from May to September are shown (Fig 8 a to z')

5.2 Arabian Sea.

The model simulations in the Arabian Sea (Fig 9 a to z') from May to September with 5-day intervals using the daily forcing reveal almost all the features obtained by monthly simulations. Noticeably as seen from the seasonal and monthly simulations, 3 gyres are simulated in the month of August, two of them constitute the Somali Gyres (Southern Gyre and the Great whirl), and the presence of the third gyre has not been satisfactorily accounted for. The third Gyre woes its existence to a series of drastic changes that take place along the equatorial belt. These changes are discussed in the next section.

5.3. Equatorial regime

The effect of using daily data over the seasonal and monthly data can be best in the model simulations over the equatorial region during the southwest monsoon months. These features have never been reported earlier in the entire history of the Indian Ocean. These features lay hidden as Seasonal and monthly data fail to simulate the finer and the moving aspects of mesoscale phenomena, which in turn may hold the key for the large-scale phenomenal changes. The model simulations reveal a Twin (T) Gyre system that forms an intrinsic signal of the Indian South West Monsoon .The fundamental point of importance is that the T-Gyres form before the Somali Gyres. As stated earlier, the Somali gyres have been extensively studied but the T-Gyres form much before the Somali gyres. Even though a lot of work needs to be carried over the T-Gyres, we present below a detailed note on the T-Gyres.

6. Discovery of the T-Gyres

Model simulations with the daily forcing.

The model reveals completely hidden dynamics along the equatorial region when daily winds are used as forcings. The month wise developments along the equator during the Southwest monsoon are disused below.

6.1 Results

May.

The equatorial jet (EJ) gains maximum speeds by mid May. Along the equator at about90E, with the increase in the EJ speeds, the reflected wave speed (reflected Rossby waves) also increases. As seen in Fig10 (a) the EJ splits at about 90E into three branches, the Northward branch(NB) flowing towards the west coast of the Bay of Bengal, Equatorial branch(EB) flowing straight to the Northern tip of Sumatra and the Southward branch(SB) along the Sumatra coast. By the 15th of May (Fig 10 b) the conjunction of the reflected Rossby wave from the Sumatra coast and the EJ starts to take the form of a gyre. At this stage a Northern gyre (T1) appears first, giving no sign of a Southern Gyre.20th May (Fig 10 c) has the Twin Gyres formed at about 88E.T2, the Southern gyre is formed by the conjunction of the reflected Rossby wave from the Sumatra coast and EJ. By May end (Fig 10 d) the Twin (T) Gyres T1 and T2 are well formed, T1 is slightly inclined to the Northeast where as T2 is almost horizontal along the Equator. By the 30th May (Fig10 e) the T-Gyres have moved westwards till 82E.Both T1 and T2 have anticyclonic circulations patterns.

June.

The T – Gyres continue their westward movement, T1 is more elliptical and still inclined Northeast to the Equator than T2 (Fig 10 f, g, h, i) that is semi-elliptic (more circular). By June end (Fig 10 j, k) T1 and T2 (1100Km length, 550Km width) are elliptic in shape (T1 is more elliptic) and aligned horizontally along the Equator, they move more westward till 74E.

July.

The T-Gyres reach till 68E(Fig 10 l to O), the intensity of T1 is lesser than T2.By the 25th July (Fig 10 p), T1 becomes diffused and finally it dissipates at about 65E.T2 also enters a diffuse state but retains the shape of the gyre.

August.

There is no trace of T1, T2 is still persistent in its diffusive form of the gyre (Fig 10 q). T2 continues westward propagation towards the Somali coast. By 8th August T2 moves to till 55E coming into contact with the Southern gyre of the Somali gyres (Fig 10 r). T2 moves still westward slightly displacing the Southern Gyre northward by August end (Fig 2 s to v). The seasonal and monthly simulations also reveal a 3 gyre structure of which 2 are the Somali gyres, the remaining 1 extra gyre could not fit into a logical explanation. Now it is seen that T2 is the 3rd Gyre along the Somali coast in month of August.

September.

A very diffused T2 reaches the Somali coast at about 40E displacing the Southern gyre of the Somali gyres to the North (Fig 10 w to z). By mid September T2 also dissipates (Fig 10 z').

The T –Gyres are not found to be simulated in any other part of the year. These form exclusively during the Southwest monsoon.

6.1. IRG model simulations using satellite daily winds

The model simulations and the Upper Layer Thickness Depths (ULTD) for 3 years when MSMR daily winds are used are shown in (Figs 11, 12, 13 a, b, c) for 5^{th} ,15^{th} ,25^{th} of July respectively. A positive ULTD's indicate a downwelling and negative ULTD's indicate upwelling. The gyres are absent when the model is forced by monthly winds as seen in (Fig 14 a, b, c, d). Irrespective of the El Nino, La Nina and the Dipole years the Twin gyres are found to occur as shown in (Fig15 a, b).

7. Validation of the Gyres

7.1. WOCE results.

The Reduced Gravity model simulated surface currents have been found to tally with WOCE observed surface currents *Rahul et al.* (2002), hence the model simulations can be treated equivalent observations in the data sparse regions. Since WOCE observations were available for 1995, the twin gyre system of 1995 is examined carefully. The observations of R/V Malcom Baldridge Figure 16(a) in the Tropical Indian Ocean near 64E-70E,Eq-5N from 1/08/1995 to 3/08/1995, at 25-35m depth support the model simulated currents of 3/08/995 using NCEP forcing as seen in Figure 16(c) with a slight shift of positions. The currents as seen from a closer view from Figure 16(b) in the region 65-70E, 5S-5N clearly show the Northern gyre between Eq-5N (the eastward moving currents turning westwards) and the Southern gyre (the Westward moving currents turning Eastwards) between Eq-5S, the Northern gyre is well observed than the Southern gyre. The complete gyre structures are not revealed in the WOCE observations as the Cruise did not move along the gyres, since the objective of Cruise was not to study the gyres. The complete picture of the gyres is simulated by the model is shown in the Figure 16(c). The maximum speed of simulated current of the Northern gyre is 60cm/s and the observed magnitude is about 80cm/s.

7.2. Observed Daily Sea Surface Heights.

A very strong evidence regarding the occurrence of the gyres comes from a recent case study by *Subrahmanyam et al.* (2001) for the year 1993, which reported that the TOPEX/POSEIDON observed Sea Surface Heights rise dramatically between 85 to 95E in the eastern Indian Ocean by the end of May, and reaches maximum by the middle of June. The model-simulated currents during May-July 1993 account for this drastic rise of TOPEX SSHs noticed by *Subrahmanyam et al.* (2001), it is seen from the model results that the Twin gyres to start form by May end and are well established by mid June at 85-95E and subsequently move westwards till July end, hence it can be said that the anticyclonic Twin gyres are responsible for downwelling and causing an dramatic increase of the TOPEX SSH. In Figure 17(A to F) the TOPEX SSH residuals computed by *Subrahmanyam et al.* (2001) are compared with the model simulations, this clearly shows that it is the evolution and the westward propagation of the Twin gyres that contributes the Observed increase and westward movement of the SSH.

Also as an example, the ULTD fields for 20th July 1999 described in the previous section (Figure8) can be compared with the observed SSH plots of ERS2, Topex Poseidon and GFO satellites which show positive anomalies over the Indian Region 5S-5N between 60-100E showing warmer surface waters.

8. Conjunction Theory.

Having adequate observational support we propose a Conjunction Theory, associating the westward movement of the gyres to the reflected Rossby wave movement. We try to explain the formation, westward propagation and dissipation of the Twin gyres. A mathematical formulation needs to taken up at a later stage, initially since this is the first time the twin gyres are noticed; we take in the observational proof to be strong enough on which we can propose the theory of Conjunction.

One of the characteristics of the tropical ocean is the relatively rapid and efficient channel of communication, through Kelvin waves and Rossby waves *Anderson*(1999). Specially the Rossby waves provide the means for westward intensification of circulation gyres and they play a critical role in the transient adjustment of ocean circulation to changes in large – scale atmospheric forcing *Dudley* (1996). Formulation and physical implication of these waves are well summarized *Gill* (1982); *Lelond*(1978); *Pedlosky*(1979). The conjunction theory is proposed in three stages.

Stage 1. The latitudinal structure of sea level associated with the dominant tropical Rossby waves has a local minimum at the equator with symmetric maxima at about 4°N and 4°S*delcroix*(1994); *Boulanger*(1995). The westward propagation is therefore much more apparent along 4°N and 4°S than along the equator *Dudley* (1996) thereby a conjunction of Kelvin and Reflected Rossby waves takes the form of a gyre as shown (Fig 18 a, b). EJ first hits the Northern tip of the Sumatra coast at 95E, with the increase in EJ speeds by mid-May the reflected Rossby waves speeds from the Northern tip of Sumatra also becomes stronger resulting the formation of T1 first. By May end the EJ has maximum speeds, the Southward branch (SB) of the EJ along the Sumatra coast also reflects back giving rise to T2.T1 is inclined slightly towards the northeast since it is bounded above by Srilanka (Fig 10 f). The horizontal shear between the westward moving Rossby waves and eastward propagating Kelvin waves is responsible for the elliptical shape of the T-gyres, inhibiting a complete circular shape. T1 is more elliptical because it gets sought of compressed by the Srilankan Island (Fig 10 h). Once the Srilankan Island is crossed T1 and T2 have the same semi-elliptical shape.

Stage 2.The westward movement of the T-Gyres is due to the combination of the energy of reflected equatorial Rossby wave (gained from the Kelvin wave, EJ) and the reflected monsoon current. This has been proved in the Pacific Ocean by *Delcroix, J.Picaut and G.Eldin.* (1991). Even the β effect (latitudinal variation of the local vertical component of the earth's angular rotation vector) contributes to the over all westward movement of the T-Gyres.

Stage 3. We propose that the reflected Rossby wave looses energy as it travels to the west, but if this is the case T1 and T2 should have simultaneously dissipated, as contrary to the simulated results. T1 dissipates first and then after 40 days, T2 dissipates at the Somali coast, the probable reason for T1 to dissipate faster may be due to the lack of larger water mass on the Northern side of the equator as compared to the Southern side of the equator that subsequently helps T2 sustain for a longer time.

9. The Data Spectrum.

The data spectrum is formulated in order to project the performance of the IRG with Seasonal, Monthly, Daily and Hourly forcings. The model has the ability to simulate circulations of different scales depending on the scale of input. Hence when Seasonal and Monthly forcings are used as input [e.g.*Luther et al* (1985), *Woodberry et, al* (1989) and by *Jensen* (1993)] large scale features like the Equatorial jet and the Somali gyres are well simulated, but to simulate Mesoscale features like the Twin Gyres the daily data plays a very crucial role. The model has single active layer, the numerical experiments with daily data as well with six hourly data are carried out. But it is noticed that the results are unaltered .In short the use of 6 hourly data did not add any extra features. This concept is graphically represented (Fig 19).

10. Conclusions

Occurrence of the Twin Gyres in EQI during mid monsoon months is shown for the first time in this study. WOCE and Topex observations confirm the occurrence of the Twin gyres. The results show that the Indian Ocean exhibits a strong ocean–atmosphere interactions that are self-maintaining and may produce significant perturbations. The periodic occurrences of the gyres suggest that the ocean is not wholly chaotic and unpredictable *Jacobs* (1994) as generally believed. The results strongly emphasize the role of daily data in understanding the details of surface circulation, which is an important component in understanding the air-sea interactions. The "Data Spectrum" shows that daily data is a minimum requirement if one wishes to study the Meso scale features by the Reduced gravity models. Based on these results we wish to recommend a closer look into using the daily data to understand the complex phenomena like ENSO. This is because an unexpected change of the ocean state in an hour can trigger an unpredictable climatic change over a decade. The results concerning the Rossby wave speeds also provide important consistency checks for evaluating the performance of Ocean General Circulation Models for studying the role of the ocean (a major component in earths climate) in the inter-annual and inter-decadal climate variability.

References:

Anderson, D., Extremes in the Indian Ocean, *Nature, 401*,337 – 339,1999.

Behera, S.K., P.S. Salvekar, Development of Simple reduced gravity ocean model for the study of upper North Indian Ocean, *IITM Research Report – 072*,1996.

Behera, S.K., P.S. Salvekar, Numerical investigation of Coastal Circulation around India, *Mausam 49*, 345 – 360,1998.

Behera, S.K , Salvekar, P.S. & Sawant, H.J. 1992, Simulation of north Indian Ocean circulation using a simple barotropic model and some sensitivity studies, -*Mausam,* 43, 353-360.

Boulanger, J.P., Propagation and reflection of long equatorial waves in the Pacific Ocean during 1992 – 1993 ElNino, *J.Geophy.Res, 100*, 25041 – 25059,1995.

Bruce, J.G., Notes on the Somali Current system during the southwest monsoon, J. Geophys. Res., 75, 4170-4173, 1970. .

Bruce, J.G., Large scale variations of the Somali Current during the southwest monsoon, Deep-Sea Res., 20, 837-846, 1973.

Bruce, J.G., Eddies off the Somali coast during the southwest monsoon, J. Geophys. Res., 84,7742- 7748, 1979.

Bruce, J.G., The wind field in the western Indian Ocean related ocean circulation, Mon. Weather. Rev., **Ill**, 1442-1453, 1983.

Bruce, J.G., W.H. Beatty,. Some observations of the coalescing of Somali eddies and a description of the Socotra eddy, Oceanologica Acta, 8,207-219, 1985.

Bruce, *I.* G., Fieux, M., & Gonella., A note on the continuance of the Somali eddy after the cessation of the Southwest monsoon. *Oceanologica Acta,* 4, 7-9,1981.

Carlwunsch., Moon, Tides and climate, *Nature, 405*,743-744,2000

Camerlengo., O'Brien, Open boundary conditions in rotating fluid, *J.Comp.Phys*, 35,12-35,1980.

Cagle, B.J., and R. Whritner., Arabian Sea project of 1980- Composites of infrared images, 61 pp., Technical report, U.S Office of Naval Research, Western Regional Office, Pasadana, CA, 1981.

Cane, M..A., 'On the Dynamics of equatorial, current, with application to the Indian ocean.,

Deep Sea. Res., 27 A, 525-4,1980.

Cane, M. A., and 'Moore, D. W ., A note on low frequency equatorial basin modes., ,. *Phys. Oceanogr.,* 11,1578-1584,1981.

Cutler, A.N., and 1.C. Swallow, Surface currents of the Indian Ocean (to 25°S, 100°E): Compiled from historical data archived by the Meteorological Office, Bracknell, UK, Rep. 187, 8pp., 37 charts, Inst. Of Oceanogr., Wormley, England, 1984.

Dudley Chelton, B., and G.Michel Schlax., Global observations of Oceanic Rossby waves. *Science, 272*,234 – 238,1996.

Delcroix, T.et al., Geosat-derived sea level and surface current anomalies in Equatorial Pacific during the 1986-1989 ElNino and LaNina, *J.Geophy.Res, 99*, 25093 – 25107,1994.

Delcroix, T.J., J.Picaut and Eldin.G., Equatorial Kelvin and Rossby waves evidenced in the Pacific Ocean trough Geosat Sea level and Surface current anomalies, *J.Geophys.Res, 96,3249*-3362,1991.

Dengler, M., Quadfasel, D., Schott, F., & Fischer, I., Abyssal circulation in the Somali Basin. *Deep-sea Res. II,* (in press), 2002.

Evans, R.M., and O.B. Brown, Propagation of thermal fronts in the Somali Current system, Deep-Sea Res., 28, 521-527, 1981.

Frank, J., Precise monitoring using complementary satellite data sets, *Nature*, *403*,414,2000.

Gill, A.E., *Atmosphere Ocean Dynamics, Academic Press*., p.*622* ,1982.

Hasternath, S. and Greischar, L., Climate atlas of the Indian Ocean, Part-Ill, Upper ocean structure, The University Of Wisconsin Press, 247 charts,1989.

Jacobs, G.A., et al. Decade scale trans pacific propagation and warming effects of ElNino anomaly, *Nature, 370*, 360 – 363,1994.

Jensen, T.D., A numerical study of the seasonal variability of the Somali current, PhD dissertation, and Florida state university pp, *21*,1990.

Jensen, T. D., Equatorial variability and Resonance in a wind driven Indian Ocean model, *J.Geophy.Res*.98., 22533-22552,1993.

Kendall, W., Distribution of breaking waves at the ocean surface, *Nature, 417*,58,2002.

Kindle, J. C., Thompson, J. D., The 26- and 50-day oscillation in the Western Indian Ocean., Model Result, *Geophys. Res.*, 94,4721-4736,1989.

Knox, R. A., & Anderson, D. L. T., Recent advances in the study of the low-latitude ocean circulation. *Progress in Oceanogra- phy,* 14,259-317,1985.

Lelond, P.H., *Waves in the Ocean, Elsevier*, p.602, 1978.

Legeckis, R., Satellite Observations of a western boundary current in the Bay of Bengal, J. Geophys. Res., 92, 12974-12978, 1987.

Luther and O'Brien., Morphology of the Somali current system during southwest monsoon: couples ocean – atmosphere models, Ed.J.C.J, Nihoul, Elsevier Science publication, 1985.

Luther et.al., Modeling the variability in Somali current, Mesoscale /synoptic coherent structure in Geophysical turbulence: Ed.J.C.J, Nihoul and B.M.Jamart, Elsevier Science publication,1989.

Luther and O'Brien ., Morphology of the Somali current system during southwest monsoon: couples ocean – atmosphere models, Ed.J.C.J. Nihoul, Elsevier Science publication ,1985.

Meehl, G.A., Coupled Ocean - Atmosphere-land process and the south Asian monsoon variability, *Science, 265,*263 – 267,1994.

Meehl, G.A., The south Asian monsoon and the tropical bineal oscillation, *J.Clim.10*, 1921 – 1943,1997.

McCreary,Kundu.,A numerical investigation of the Somali current during southwest monsoon, *J.Mareine Res, 46*,25-28,1988.

McCreary , *I* .P ., P .K. Kundu, and R.L. Molinari, A numerical investigation of dynamics, thermodynamics, and mixed layer processes in the Indian Ocean, Prog. Oceanogr., 31,181-224, 1993. (Correction, Prog. Oceanogr., 33, after pg., 248, 1994.

McCreary, *I.P.,* W. Ran, D. Shankar, and S.R. Shetye,, Dynamics of the East India Coastal Current, 2, Numerical solutions, *I.* Geophys. Res., 101, 13,993-14,010, 1996.

Muench, J. E., Kunze, E., & Firing, E., The potential vorticity structure of equatorial deep jets. *Journal of Physical Oceanogra- phy,* 24, 418-428,1994.

Nicholls, N., Air-Sea interaction and the quasi-bineal oscillations. *Mon.Weath.Rev, 106*, 1505 – 1508, 1983.

Nicholls, N., All India Summer monsoon rainfall and sea surface temperature around northern Australia and Indonesia, *J.Clim.8*, 1463 – 1467,1997.

O'Brien, J. J., -and Hurlburt, H. E., Equatorial jet in the Indian C)(:ean., *Advanced Physical, Oceanographic Numerical Modelling,* edited by J.J.*O*'Brien, Reidel, Hingam, Mass., pp 127-144,1974.

Pedlosky, J., *Geo Phys Fluid Dynamics, Springer Verlag*., p.*624* ,1979.

Perigaud, C., and Delecluse P., Simulations of dynamic topography in the northwestern Indian ocean with input of Seasat altimeter and scatterometer data., *Ocean-AirInteractionns,I,289-309,*1989.

Pickard, G.L., and *W.I.* Emery., Descriptive physical Oceanography, 249pp., Pregmon, New York, 1982.

Pillard, D., our virtual planet, *Nature, 416*,579-580,2002.

Potemra, J.T., Luther M.E and O'Brien, The seasonal circulation of the Upper Ocean in the Bay of Bengal, *J.Geophy.Res, 96*, 12667 – 12683,1991.

Quadfasel, D., & Schott, F., Water mass distribution at intermediate layers off the Somali coast during the onset of the southwest monsoon, 1979. *Journal of Physical Oceanography,* 12, 1358-1372, 1982

Quadfasel, D., & Schott, F., Southward subsurface flow below the Somali Current. *Journal of Geophysical Research,* 88, 5973-5979,1983.

Quadfasel., Ocean circulation & Climate, Observing and modeling the global ocean, *Nature, 415*,20-21,2002

Rahul, P.R *et al*., a., Real time simulations of upper ocean surface circulations by a simple ocean model, *Accepted for publication as a IITM Research Report,* 2002.

Rahul, P.R *et al*., b., Simulations of Surface Circulations over Tropical Indian Ocean using Daily surface forcing, submitted to *J. Oceanography*, 2002.

Ratna Reddy, S., A.K. Easton, S.R. Clarke, A. Narendra Nath, and M.V. Rao., Gyres off the Somali coast and western boundary currents in the Bay of Bengal during the south-west monsoon, Int. J. Remote Sens., 16, 1679-1684, 1995.

Rao, R.R., Molinari, R.L., Festa, J.F., Surface meteorological and near surface oceanographic atlas of the tropical Indian Ocean, *NOAA Tedmiazl Memorandum,* ERL AOML-69,1991.

Sanilkumar, K. V., T.V. Kuruvilla, D. Jogendranath, and R.R. Rao., Observations of the Western Boundary Current of the Bay of Bengal from hydrographic survey during March 1993, Deep-Sea Res., 44, 135-145, 1997.

Schott, F., Fieux, M., Kindle, J., Swallow, J. and Zantopp, R.. The boundary currents east and north of Madagascar, Direct measurements and model comparison, *I. Geophys. Res.*, 93,4963-4974,1988

Schott, F., Swallow, J. C., & Fieux, M., The Somali Current at the equator: annual cycle of currents and transports in the upper 1000 m and connection to neighboring latitudes. *Deep-Sea Research,* 37, 1825-1848, 1990

Schott, F., Monsoon response of the Somali Current and associated upwelling, Frog. Oceanogr., 12, 357-381,1983.

Semnter, A.J., Modeling Ocean Circulation, *Science 269*,1379 – 1385, 1995.

Simmons *et al.,* Verification of a numerical ocean model of the Arabian Sea, *J.Geophys.Res*, 96,20,449-20, 1988.

Shankar, D., J.p. McCreary, W. Han, S.R. Shetye., Dynamics of the East India Coastal Current I. Analytical solutions forced by interior Ekman pumping and local alongshore winds, J . Geophys. Res., 101, 13975-13991, 1996.

Shetye, S. R., & IShenoi, S. S. C., The seasonal cycle of surface circulation in the coastal North Indian Ocean. *Proceedings of the Indian Academy of Science (Earth & Planetary Science),* 97, 53-72. 1988

Shetye, S. R., Gouveia, A. D., Shenoi, S. S. C., Sundar, D., Michael, G. S., Almeida, A. M., & Santanam, K., Hydrography and circulation off the west coast of India during the Southwest Monsoon 1987. *Journal of Marine Research,* 48, 359-378. 1990

Shetye, S. R., Gouveia, A. D., Shenoi, S. S. C., Michael, G. S., Sundar, D., Almeida, A. M., & Santanam, K., The coastal current off western India during the northeast monsoon. *Deep-Sea Research,* 38, 1517-1529. 199I

Shetye, S. R., Gouveia, A. D., Shenoi, S. S. C., Sundar, D., Michael, G. S., & Nampoothiri, G., The western boundary current of the seasonal subtropical gyre in the Bay of Bengal. *Journal of Geophysical Research,* 98, 945-954. 1993

Shetye, S.R., A.D. Gouveia, S.S.C. Shenoi, D. Sunder, G.S. Michael, A.M. Almeida, and K. Snatanam., Hydrography and circulation off the west coast of India during the southwest monsoon 1987, J. Mar. Res., 48,359-378, 1990.

Shetye, S.R., A.D. Gouveia, S.S.C. Shenoi, D. Sunder, G.S. Michael, and G.Nampoothiri., The Western Boundary Current of the Seasonal subtropical Gyre in the Bay of Bengal, J. Geophys. Res., 98, 945-954, 1993.

Shetye, S.R., A.D. Gouveia, D. Shankar, S.S.C. Shenoi, p.N. Vinaychandran, D. Sunder, G.S. Michael, and G. Nampoothiri., Hydrography and circulation in the western Bay of Bengal during the Northeast monsoon, J. Geophys. Res., 101, 14,011-14,025, 1996.

Subrahmanyam, B *et al.*, Indian Ocean Rossby waves observed in TOPEX/POSEIDON altimeter data and in model simulations, *Int.J.of Remote Sensing, 22,141*-166,2001.

Swallow, *I.C.,* M. Fieux., Historical evidence for two gyres in the Somali Current, *I.* Mar. Res., 40, 747- 755,1982.

Swallow, *I.C.,* R.L. Molinari, *I.C.* Bruce, O.B. Brown, and R.H Evans., Development of near surface flow and watermass distribution in Somali basin in response to the southwest monsoon of 1979, *I.* Phys. Oceanog., 3, 1398-1415, 1983.

Varkey, M.J., V.S.N. Murty, and A. Suryanarayana., Physical Oceanography of the Bay of Bengal and Andaman Sea, Oceangr. and Mar. Biology: an annual review, 34,1-70,1996.

Webster, P.J., Moore, A.M, Loschneg, J.P and R.R.Leben., Coupled Ocean – atmosphere dynamics in the Indian Ocean during 1997-98, *Nature, 401,*356 – 360,1999.

Woodberry, K.E., The wind driven seasonal circulation in the Southern Tropical Indian Ocean, *J.Geophy.Res.,* 94:17985-18002,1989.

Wyrtki, K., Oceanographic atlas of the International Indian Ocean Expedition, National

Science Foundation, Washington, D.C.531pp. 1971

Wyrtki, K., An equatorial jet in the Indian Ocean, *Science, 181,*262 – 264,1973.

Yoshida, K., A theory of the Cromwell current and of the equatorial upwelling., *J..*

Oceanogr. Soc. Jpn., 15154-170,1959.

Yu, L., J.J. O'Brien, J. Yang., On the remote forcing of the circulation in the Bay of Bengal, J. Geophys. Res., 96,20449-20454, 1991.

Acknowledgements

Authors are thankful to the Director, IITM for encouragement and support. First author is grateful to the Director ISRO for the Research fellowship. Special thanks to Dr.J.P.McCreary for his comments and clarification on some of the important points.
The authors are also thankful to Dr.K.Rupa Kumar for critical review and fruitful suggestions.

Corresponding author:
Dr. (Mrs.). P.S.Salvekar,
Email: pss@tropmet.res.in and pssalvekar@hotmail.com

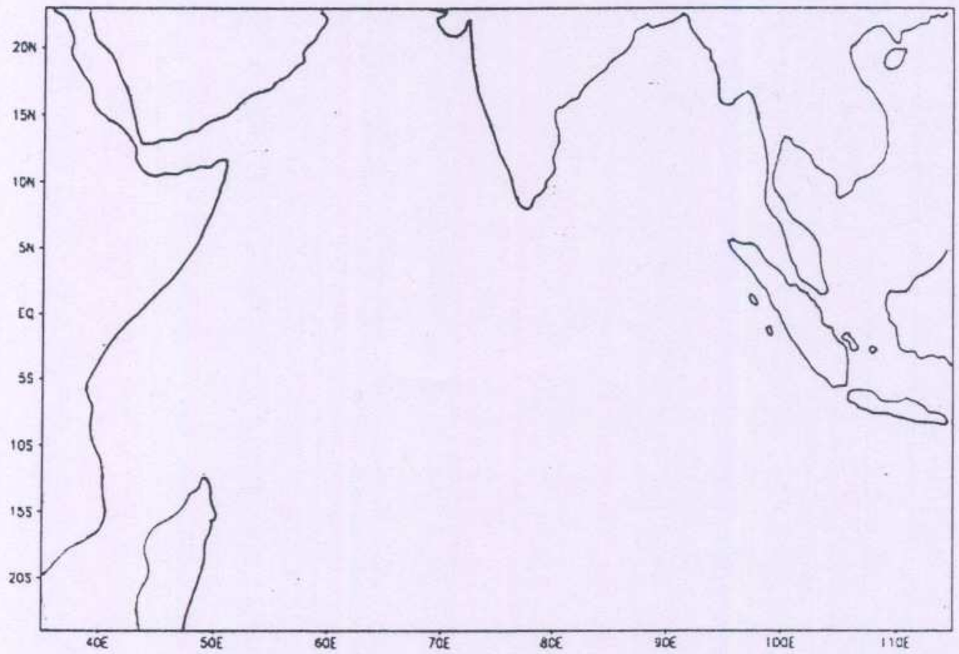

Fig.1. The Tropical Indian Ocean Model geometry.

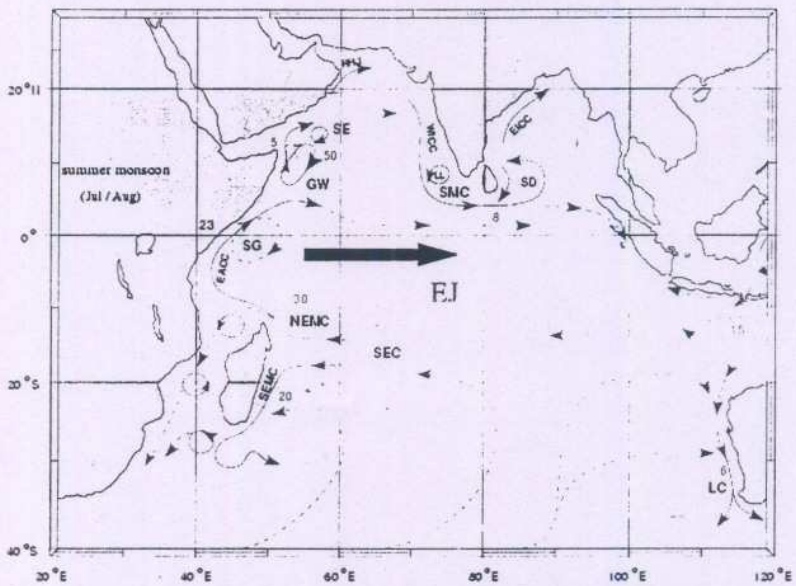

Fig .2. A schematic representation of identified current branches during the Southwest Monsoon, including some choke point trans- port numbers ($Sv=10^6 m^3 s^{-1}$). Current branches indicated are the South Equatorial Current (SEC), South Equatorial Countercurrent (SECC), Northeast and Southeast Madagascar Current (NEMC and SEMC), East African Coast Current (EACC), Somali Current (SC), Southern Gyre (SG) and Great Whirl GW) and associated upwelling wedges, Socotra Eddy (SE), Ras al Hadd Jet (RHJ) and upwelling wedges off Oman, West Indian Coast Current (WICC), Laccadive High and Low (LH and LL), East Indian Coast Current (EICC), Southwest and Northeast Monsoon Current (SMC and NMC), South Java Current (JC) ,Equatorial Jet(EJ)and Leeuwin Current(LC).

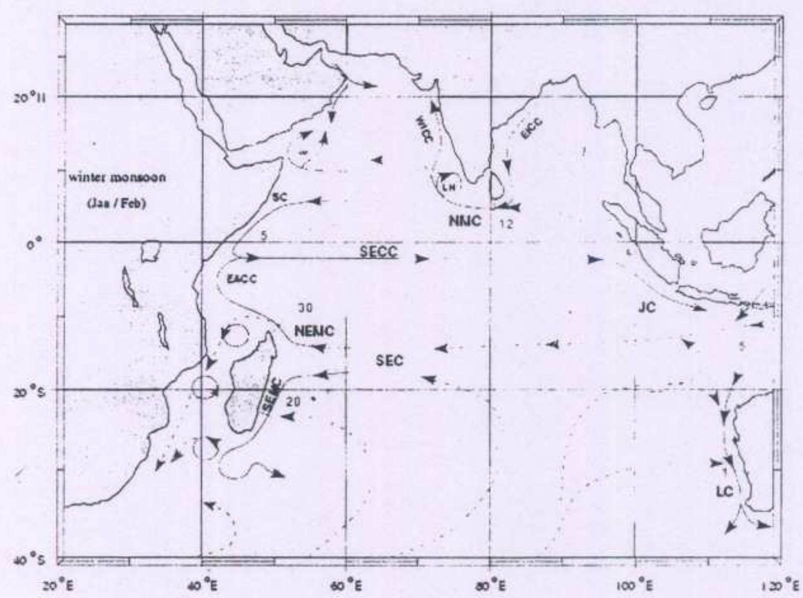

Fig 3. Same as above but for Northeast monsoon. (From Schott et al., 2001)

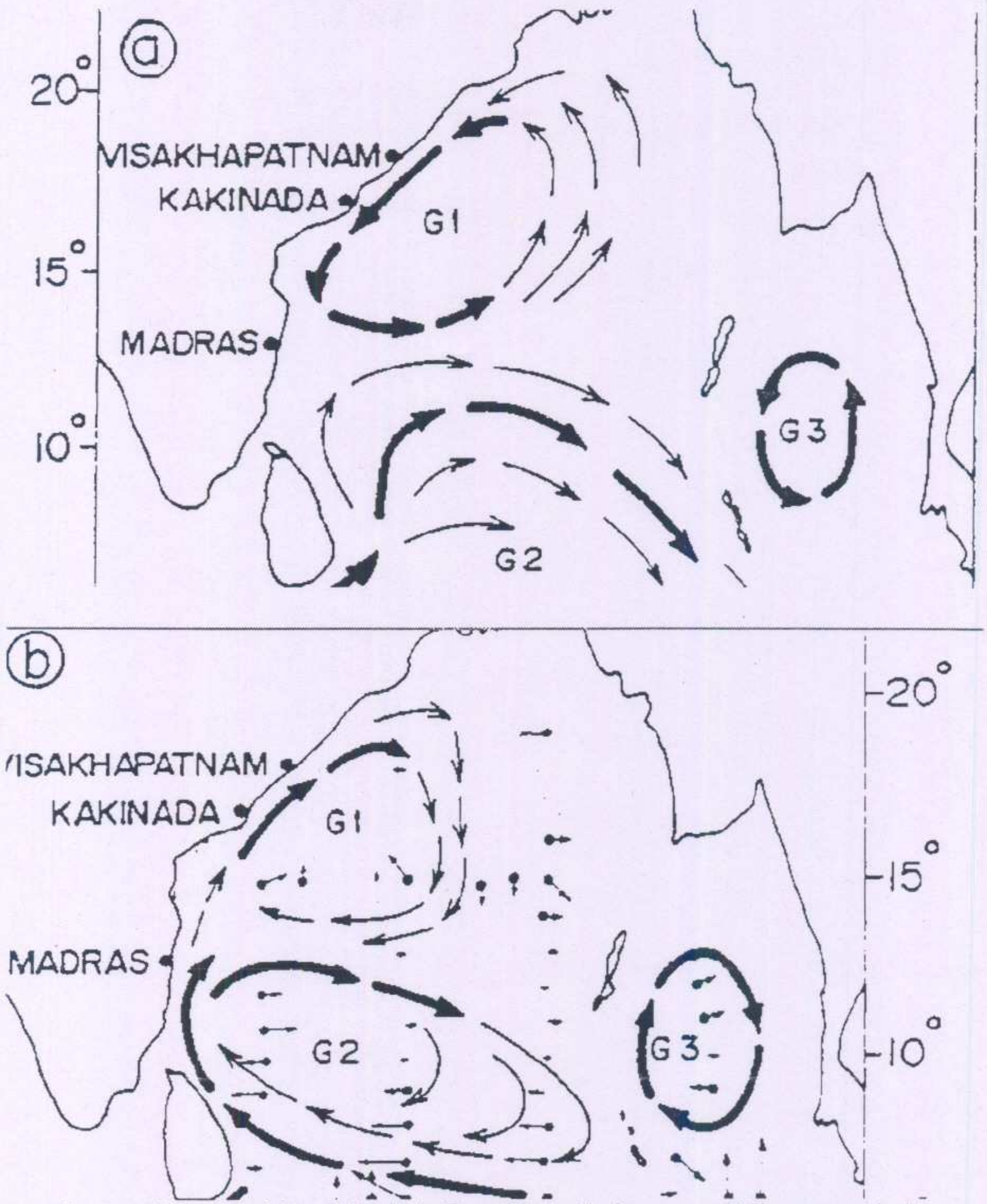

Fig 4a and b. Seasonal Circulation in the Bay of Bengal in Summer and Winter respectively. (Varkey et al., 1996)

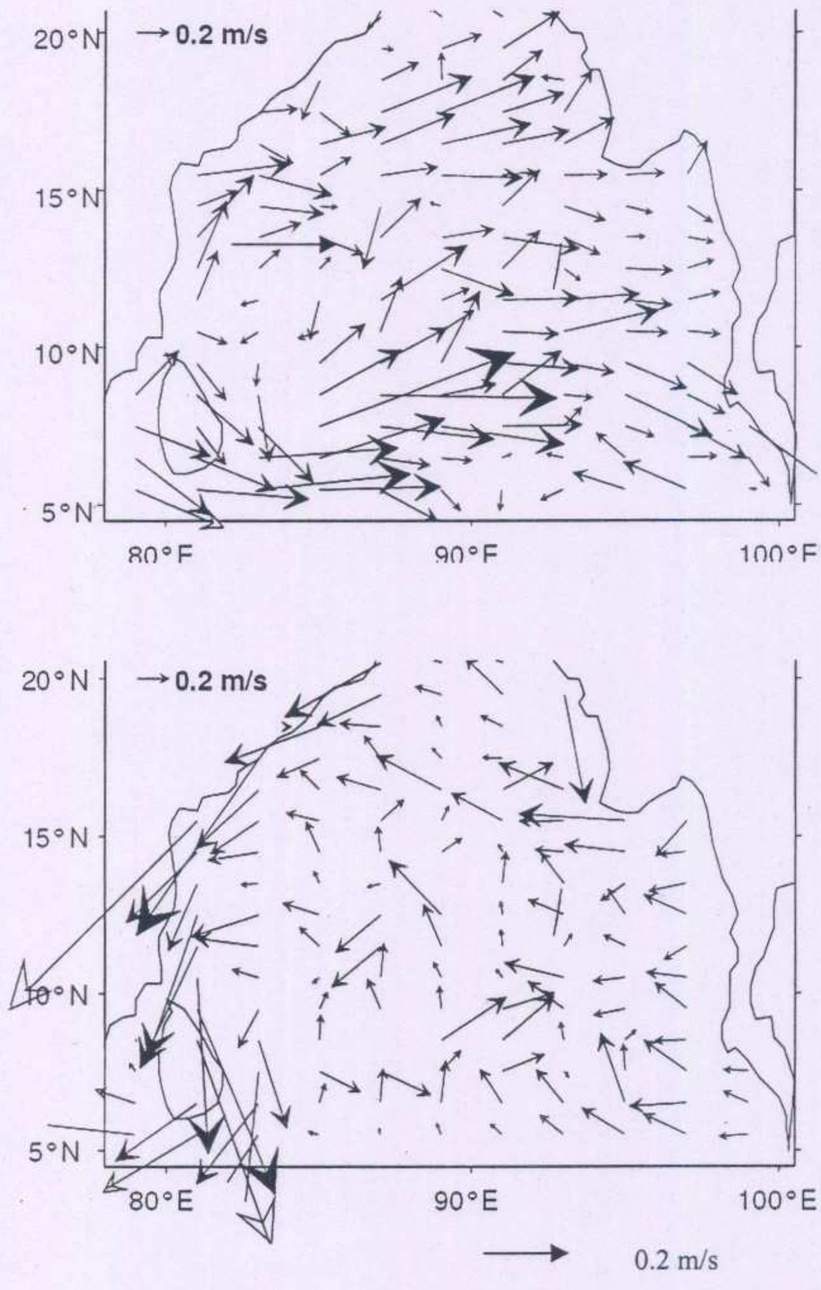

Fig 5. Surface Currents in the Bay of Bengal from the Shiip drifts.(Eigenheer & Quadfasel,2000)

SOMALI CURRENT FLOW PATTERNS

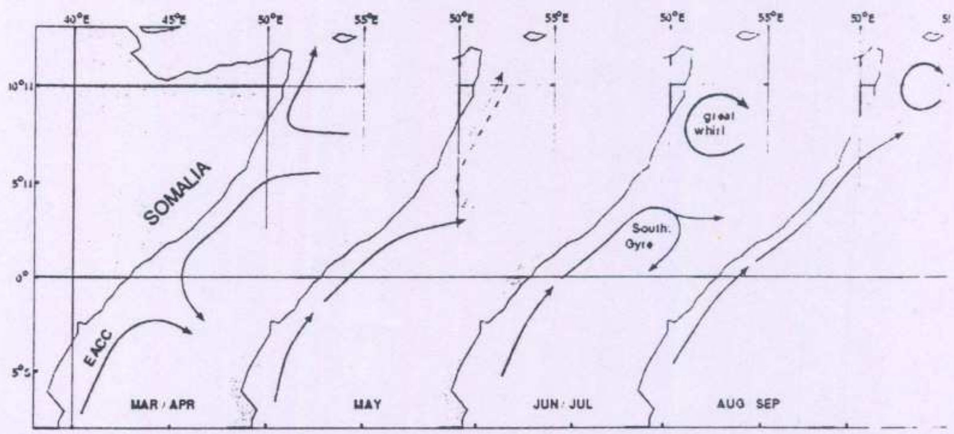

Figure 6.Somali upper layer flow patterns over the course of the year.(Schott et al.,1990)

(a)January

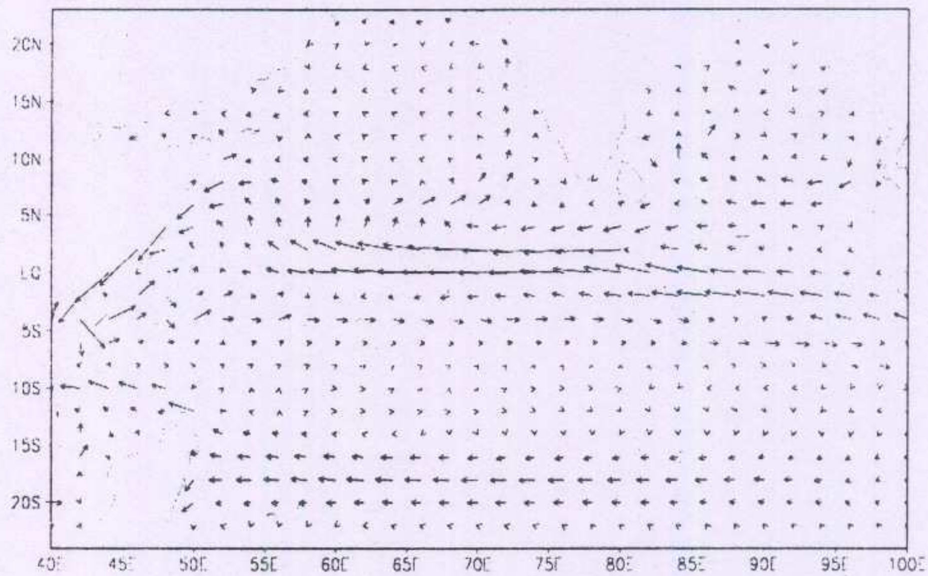

(b) March

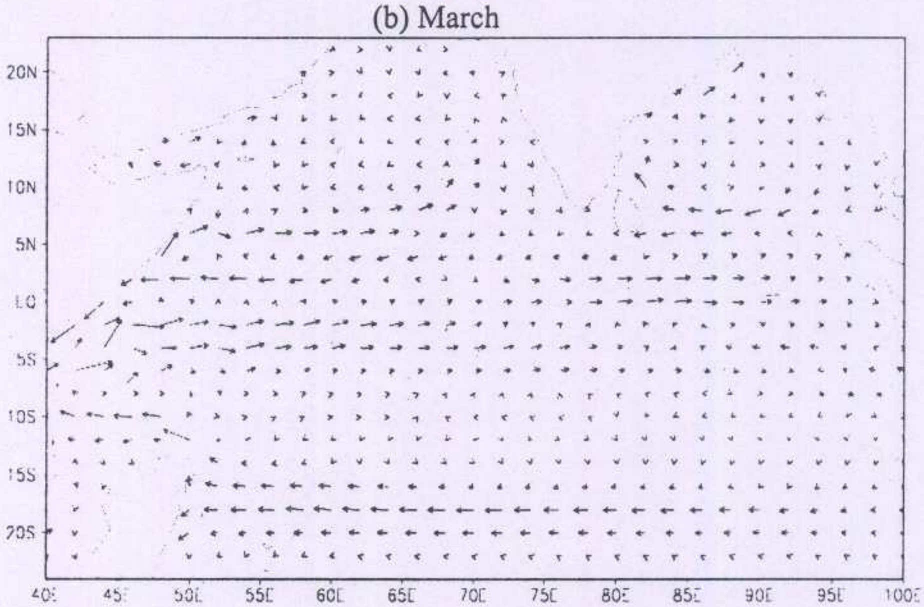

(c)April

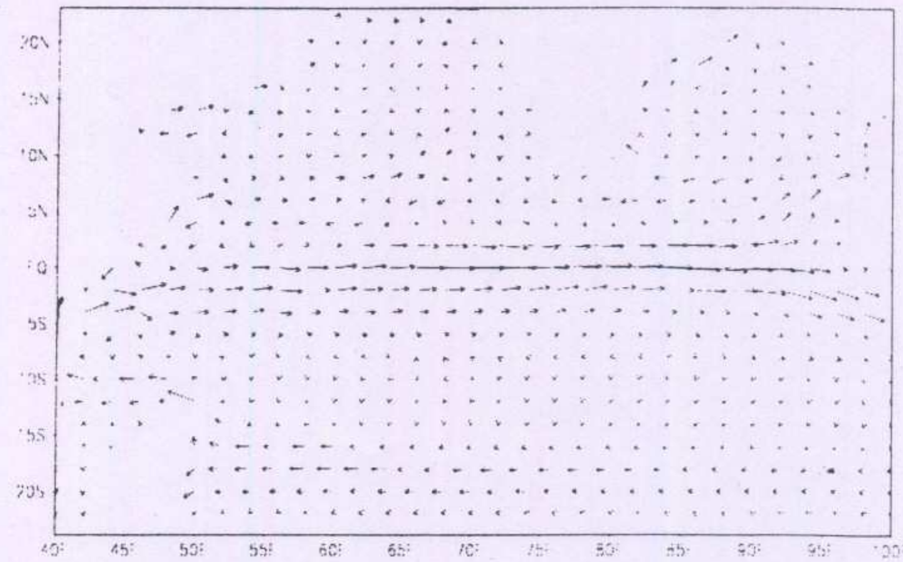

20N
15N
10N
5N
EQ
5S
10S
15S
20S
40E
45E
50E
55E
60E
65E
70E
75E
80E
85E
90E
95E
100E

(d) May

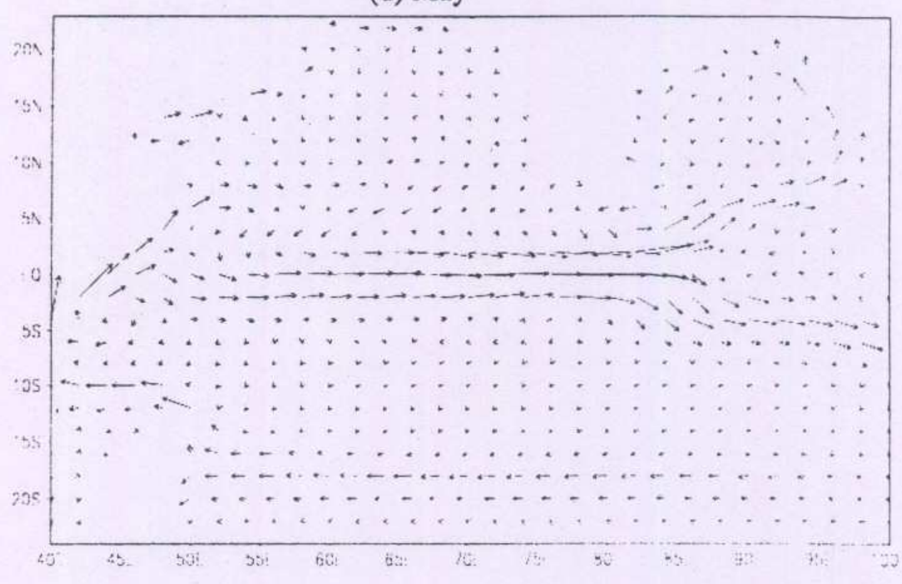

20N
15N
10N
5N
EQ
5S
10S
15S
20S
40E
45E
50E
55E
60E
65E
70E
75E
80E
85E
90E
95E
100E

(e) June

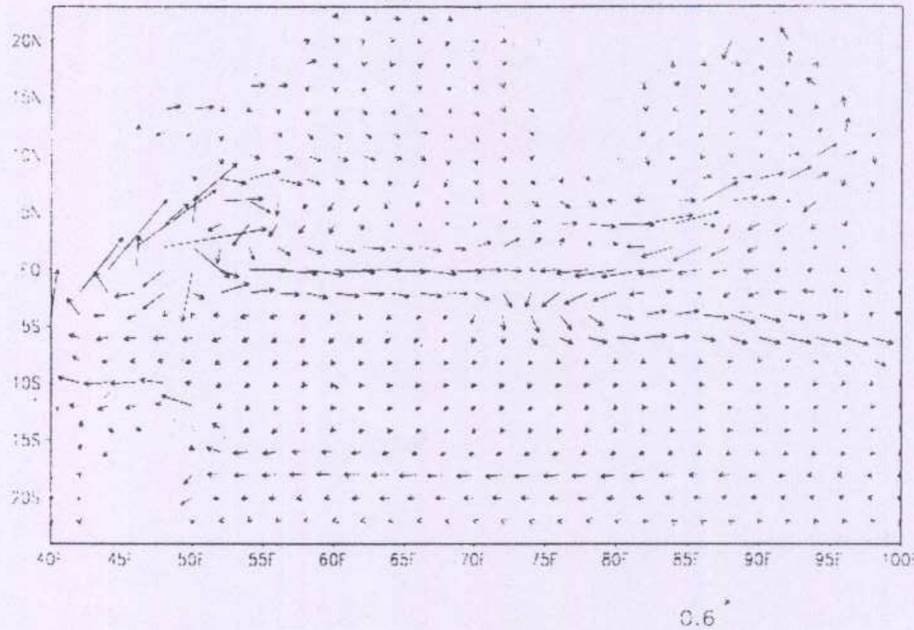
20N
15N
10N
5N
EQ
5S
10S
15S
20S
40E
45E
50E
55E
60E
65E
70E
75E
80E
85E
90E
95E
100E
0.6

(f) Jul

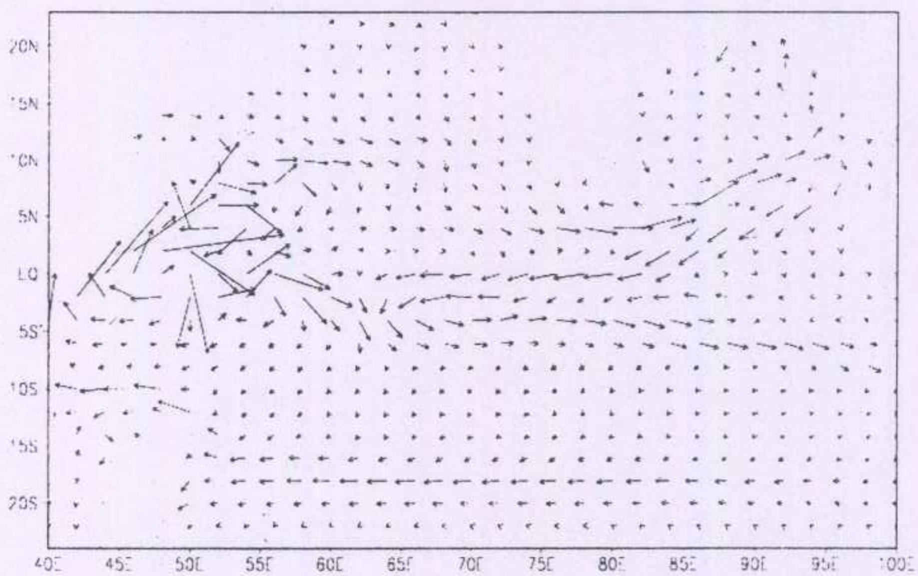
20N
15N
10N
5N
EQ
5S
10S
15S
20S
40E
45E
50E
55E
60E
65E
70E
75E
80E
85E
90E
95E
100E

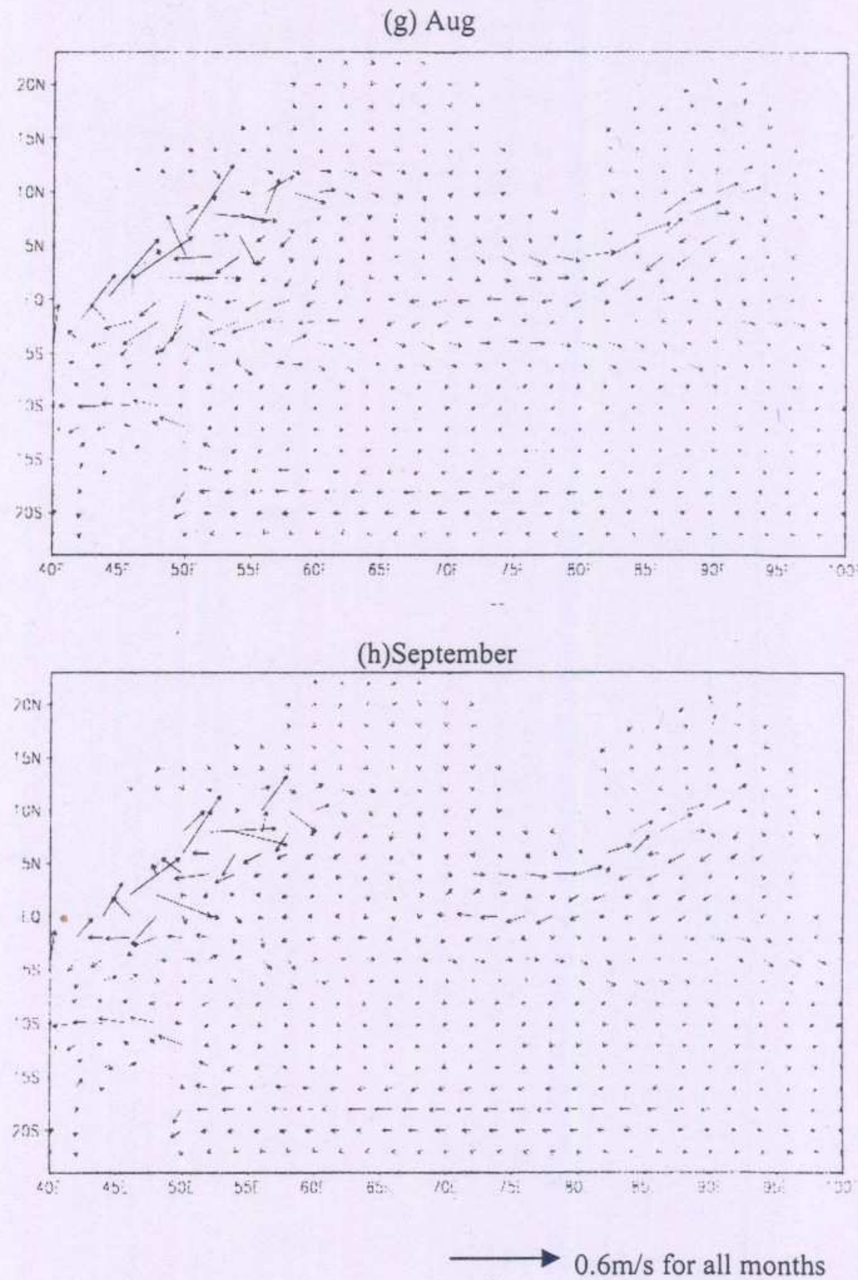

Figure 7. Simulations of surface circulations by the Reduced Gravity model with monthly forcings.

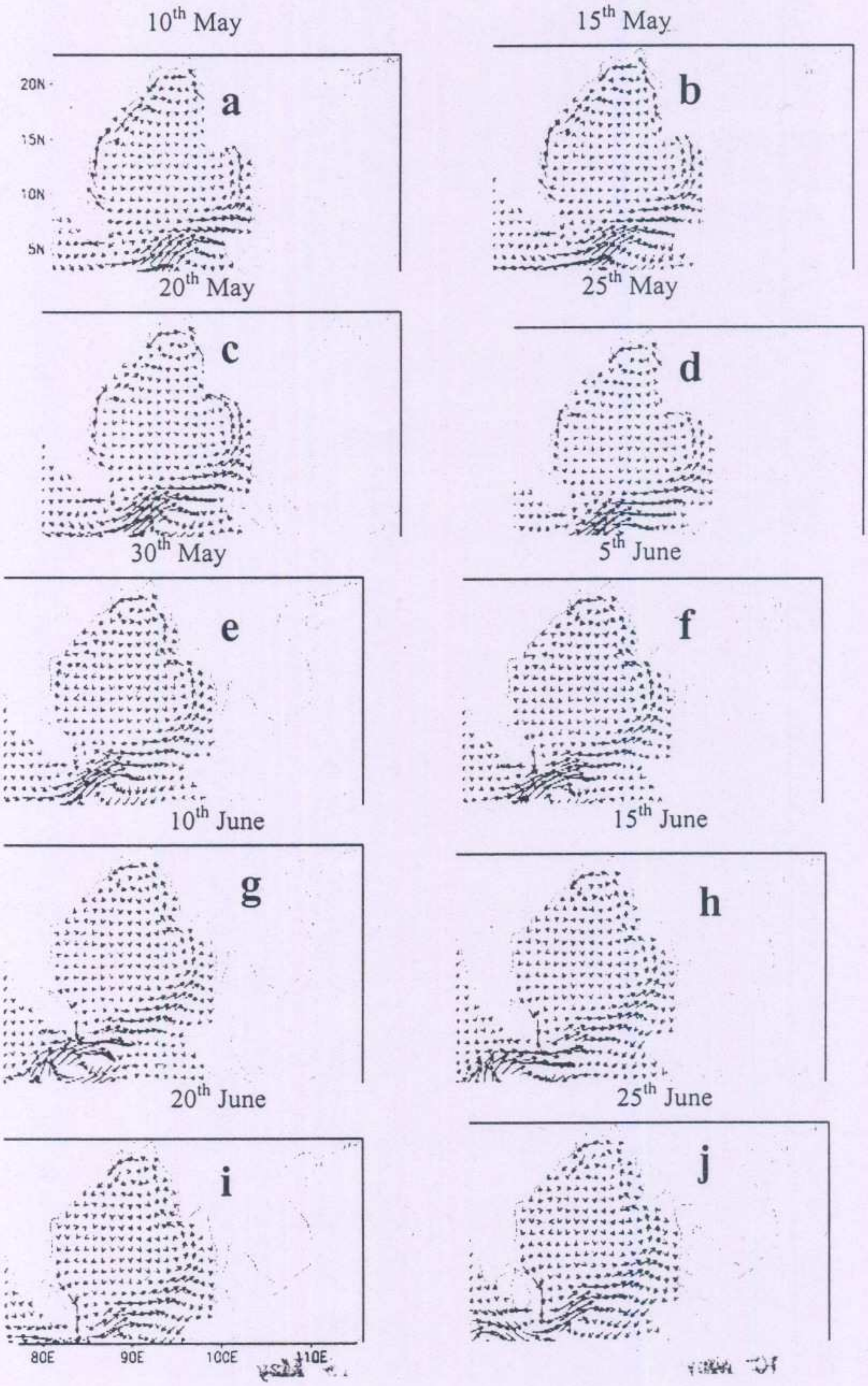
10th May
15th May
20N
15N
10N
5N
a
b
20th May
25th May
c
d
30th May
5th June
e
f
10th June
15th June
g
h
20th June
25th June
i
j
80E
90E
100E
110E

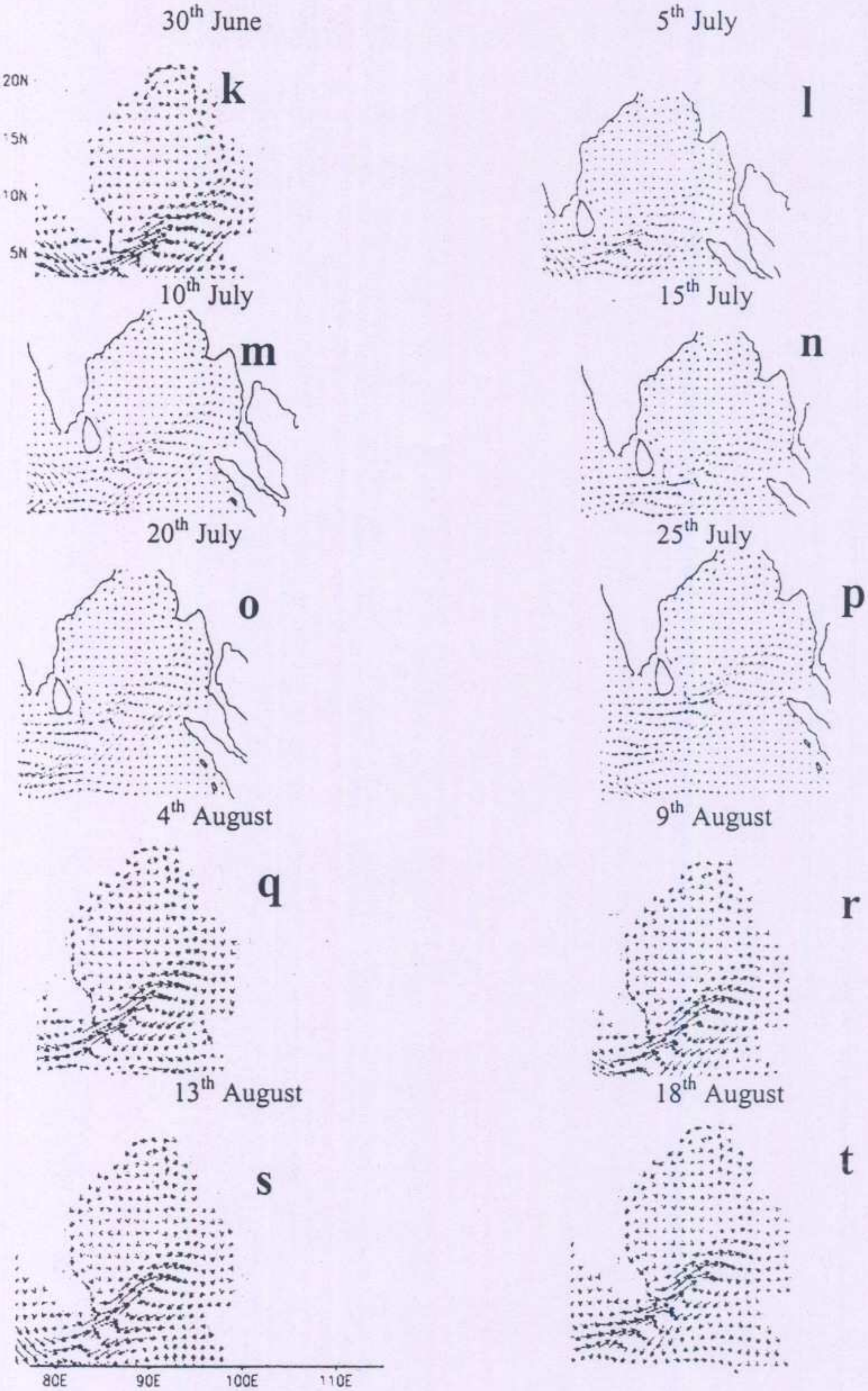
30th June
5th July
20N
15N
10N
5N
k
l
10th July
15th July
m
n
20th July
25th July
o
p
4th August
9th August
q
r
13th August
18th August
s
t
80E
90E
100E
110E

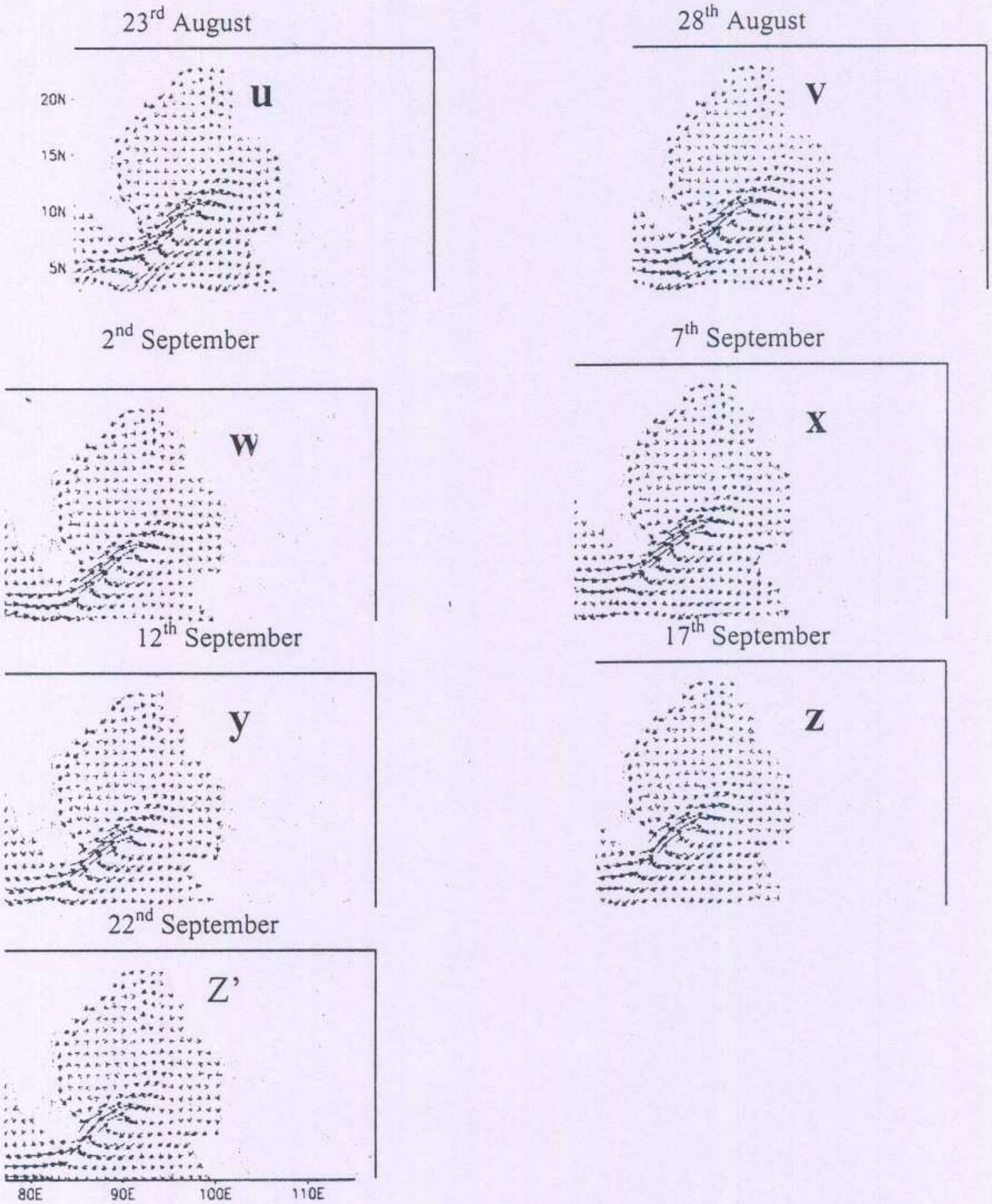

Fig 8. a to z' are the five day surface circulations simulations of IRG model in the Bay of Bengal beginning from 10th May to 22nd September, with Daily winds as forcings.

10th May to 30th May(5 day interval)

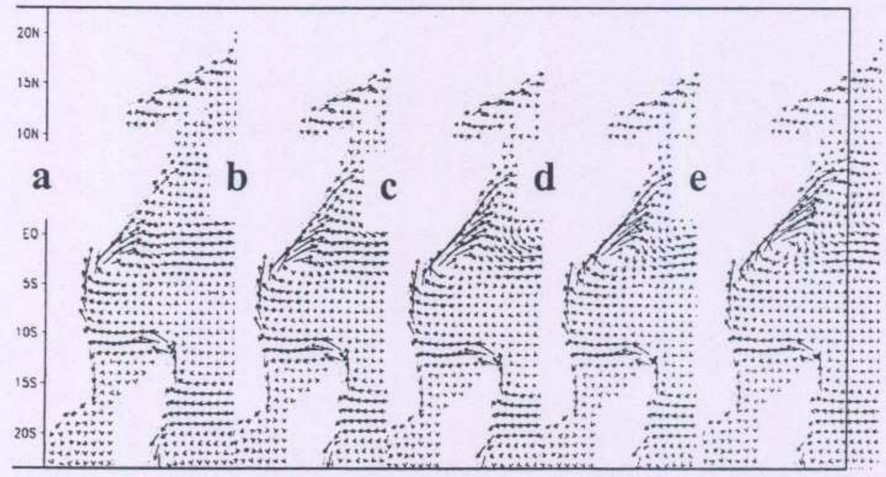

5th June to 30th June (5 day interval)

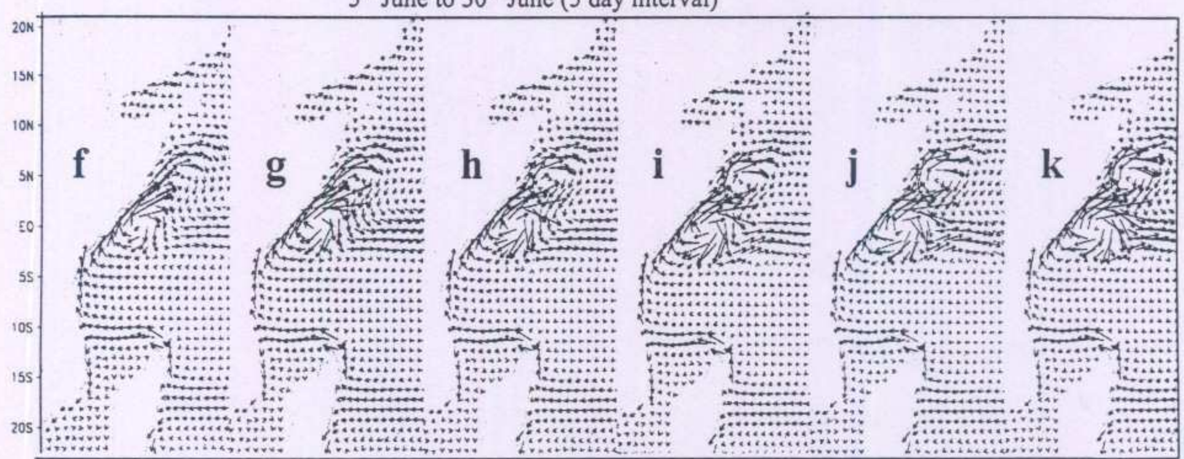

5th July to 25th July(5 day interval)

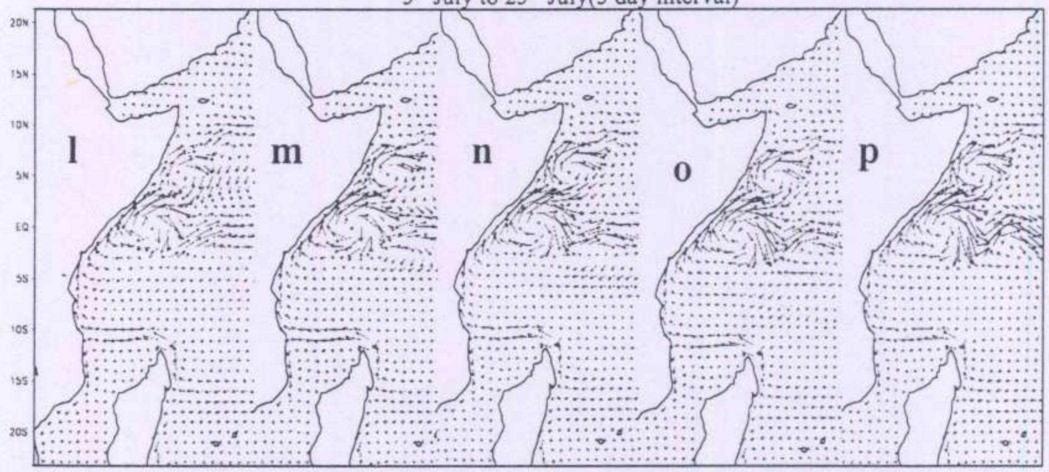

5th August to 30th August(5 day interval)

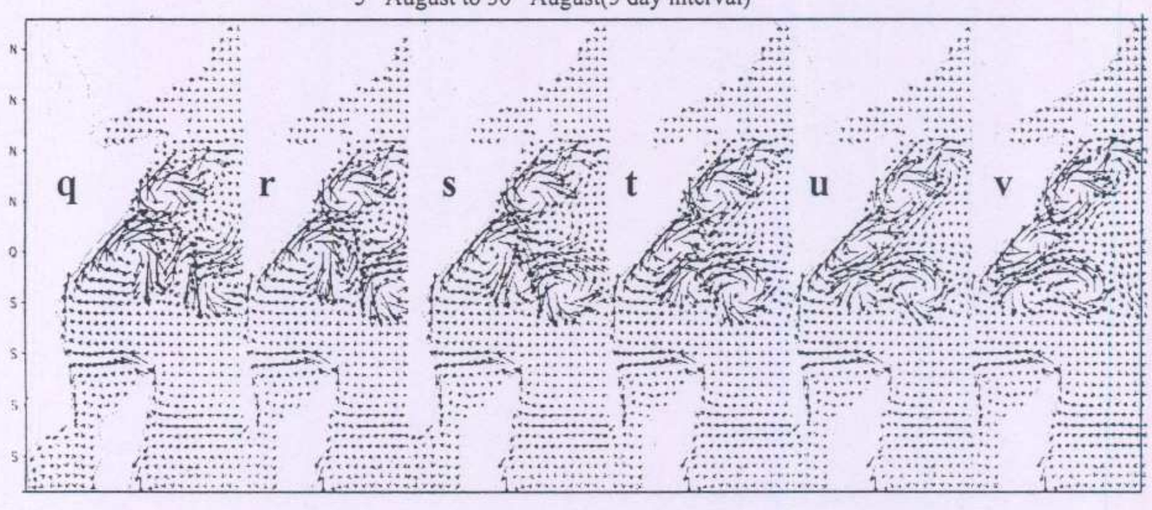

5th September to 22nd September(5 day interval)

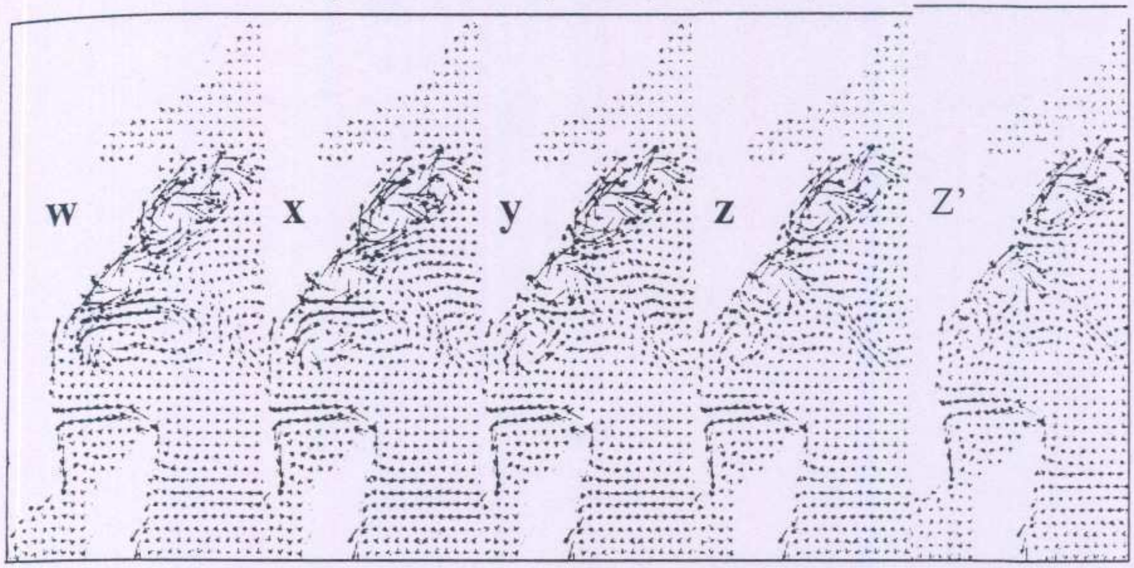

→ 0.8 to 1 m/s

Fig 9.IRG model, five-day simulations (a to z') in the Arabian Sea of the Somali Gyres from May (formation) to September (dissipation) from the 1992-2001(NCEP climatology) obtained by using daily winds as forcings.

(a)10th May

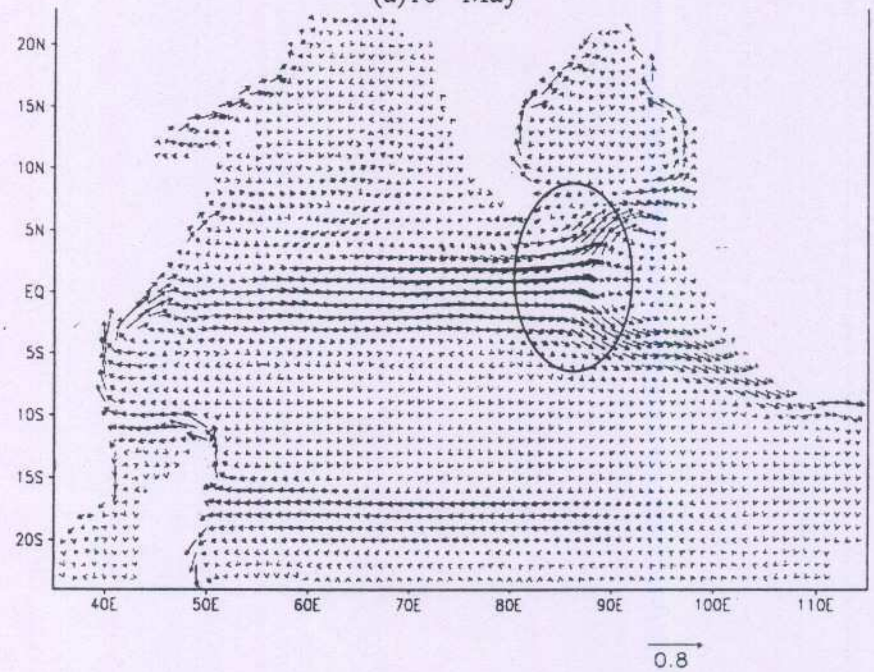
20N
15N
10N
5N
EQ
5S
10S
15S
20S
40E
50E
60E
70E
80E
90E
100E
110E
0.8

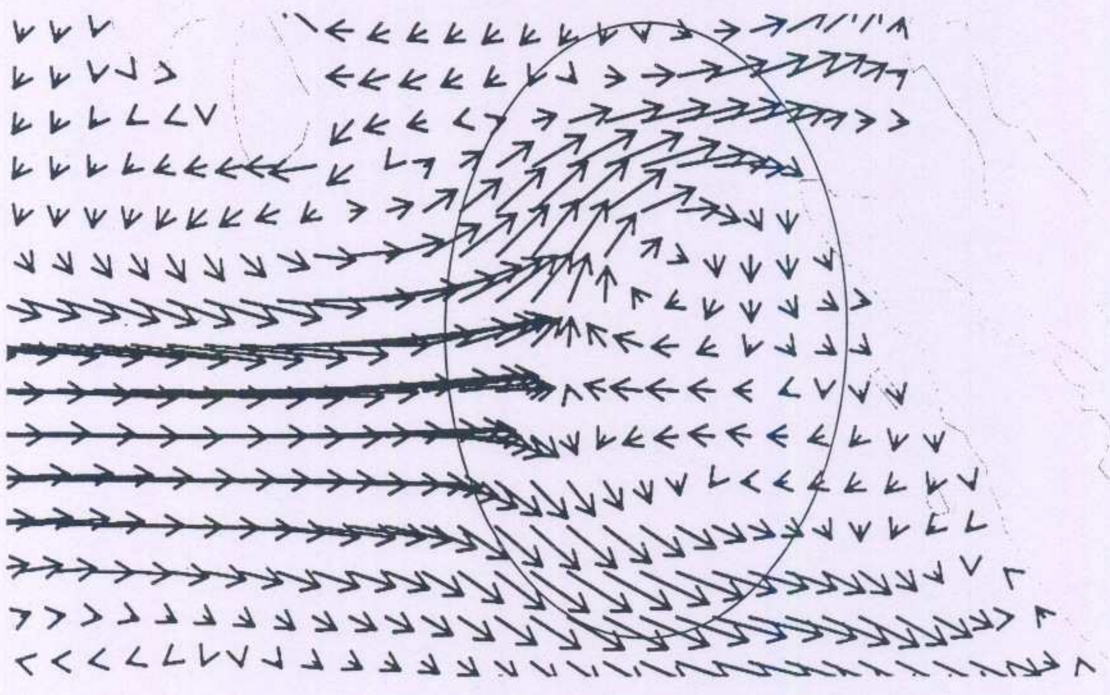

(b) 15th MAY

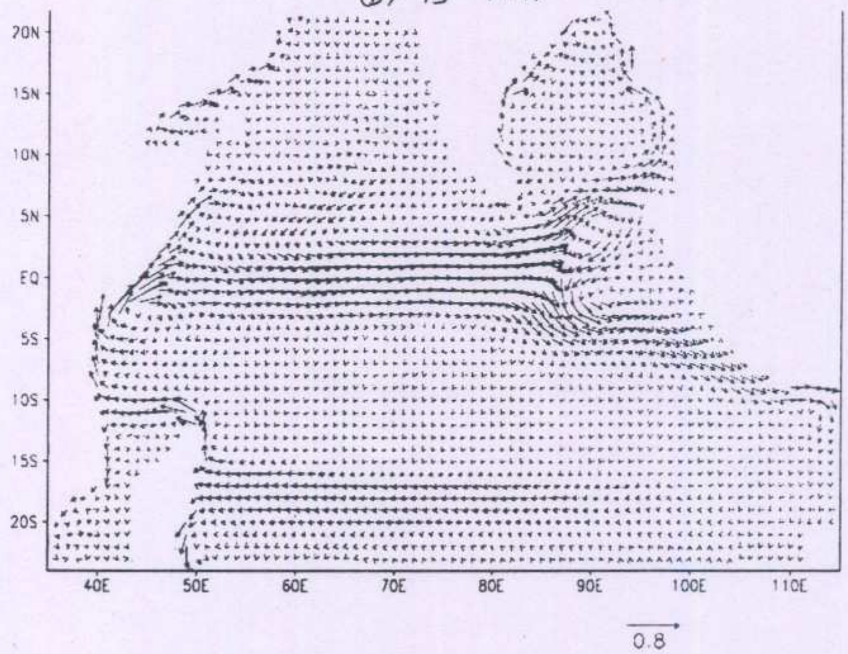
70N
15N
10N
5N
EQ
5S
10S
15S
20S
40E
50E
60E
70E
80E
90E
100E
110E
0.8

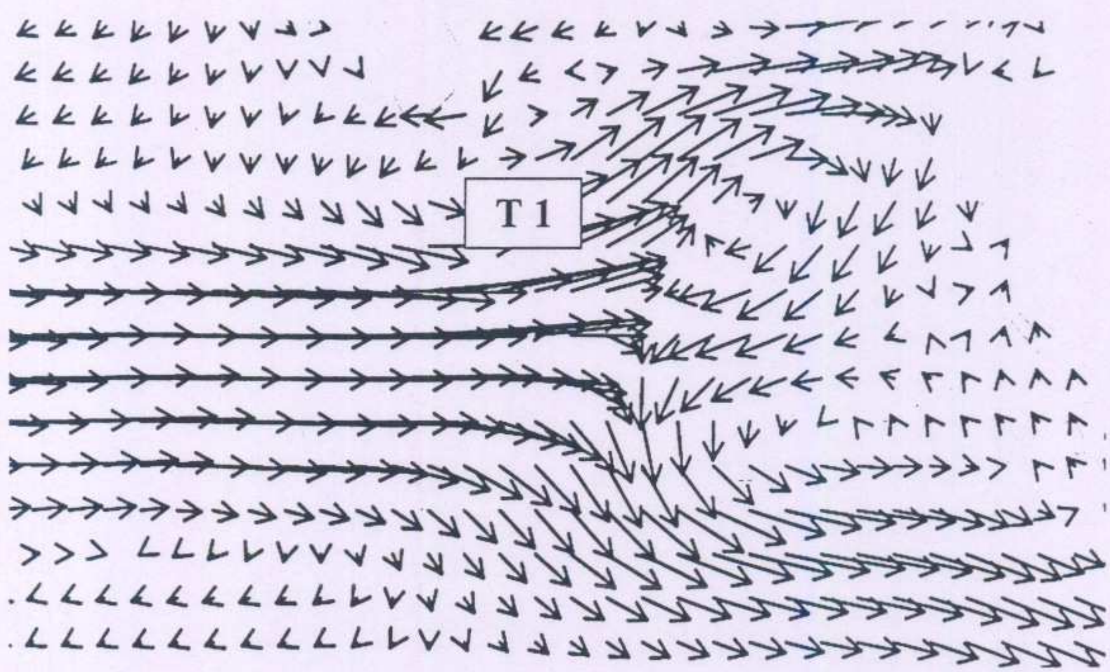
T1

©20th May

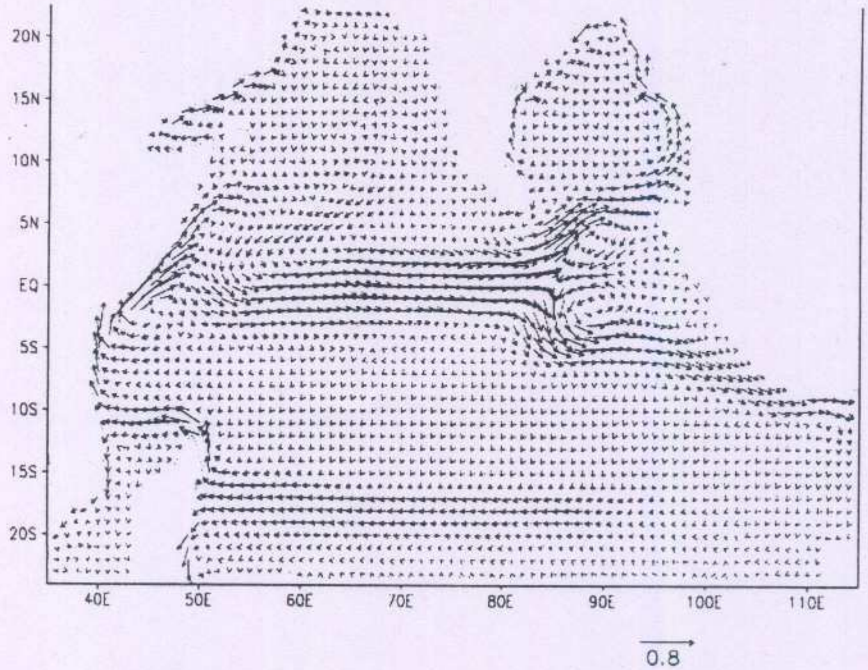
20N
15N
10N
5N
EQ
5S
10S
15S
20S
40E
50E
60E
70E
80E
90E
100E
110E
0.8

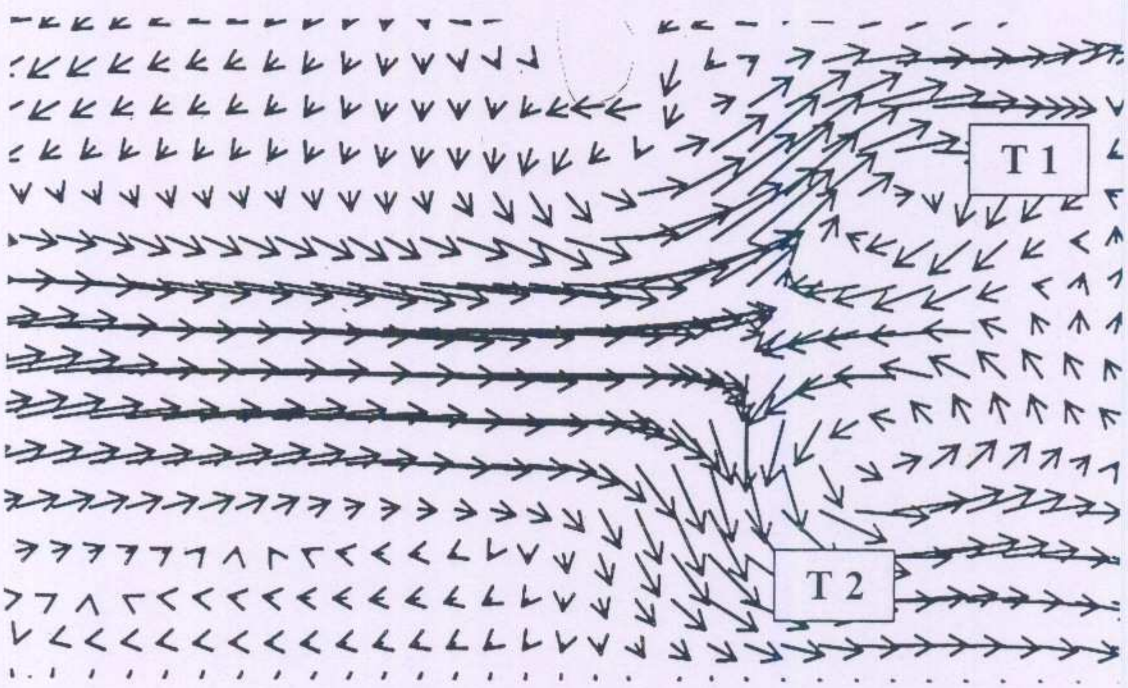
T 1
T 2

(d)25th May

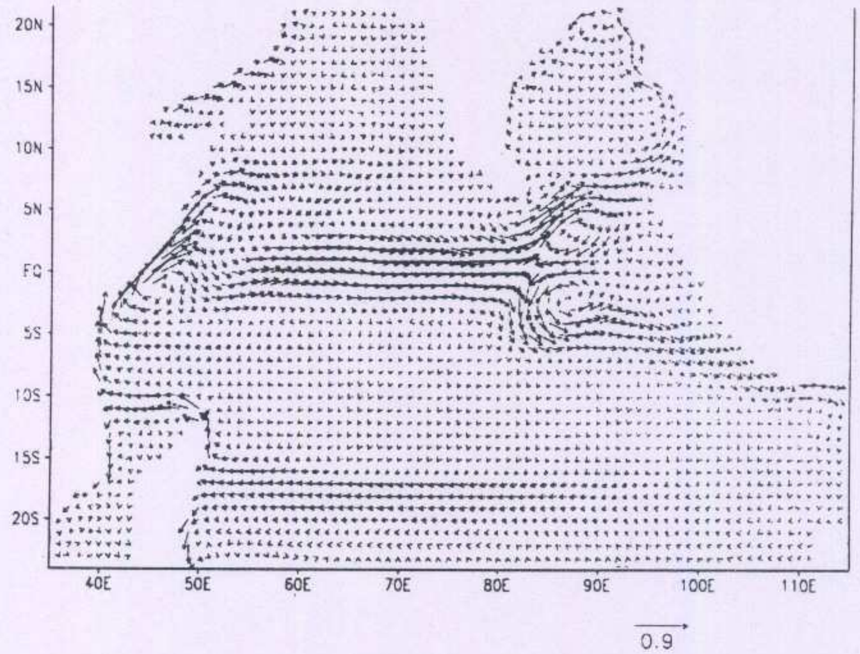
20N
15N
10N
5N
EQ
5S
10S
15S
20S
40E
50E
60E
70E
80E
90E
100E
110E
0.9

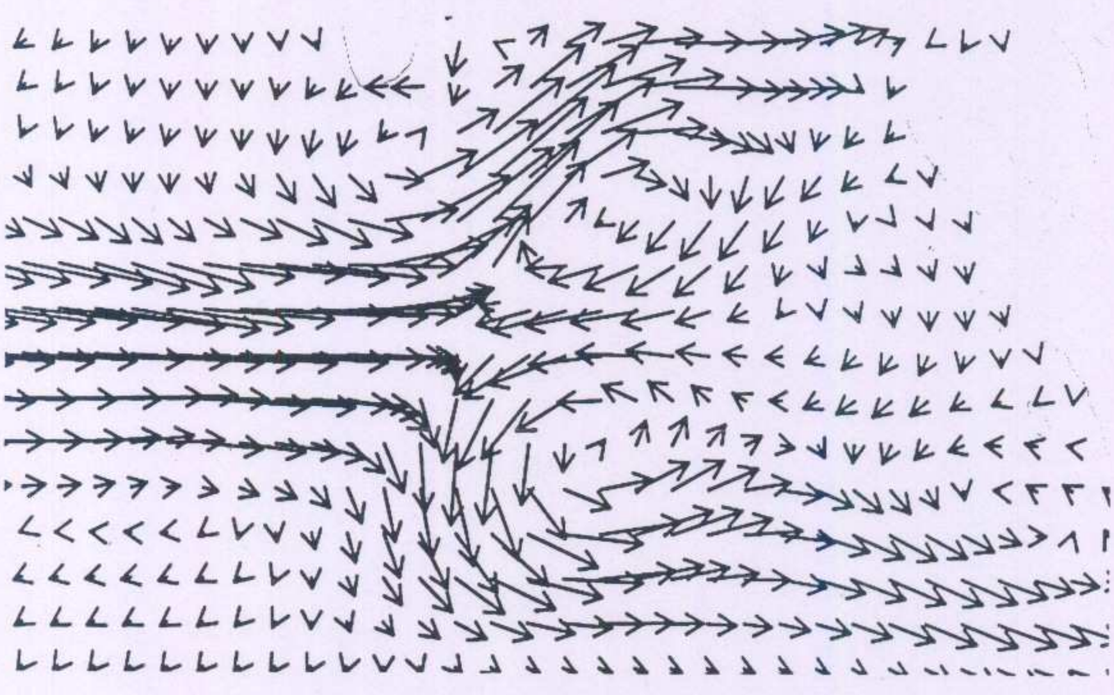

(e)30[th] May

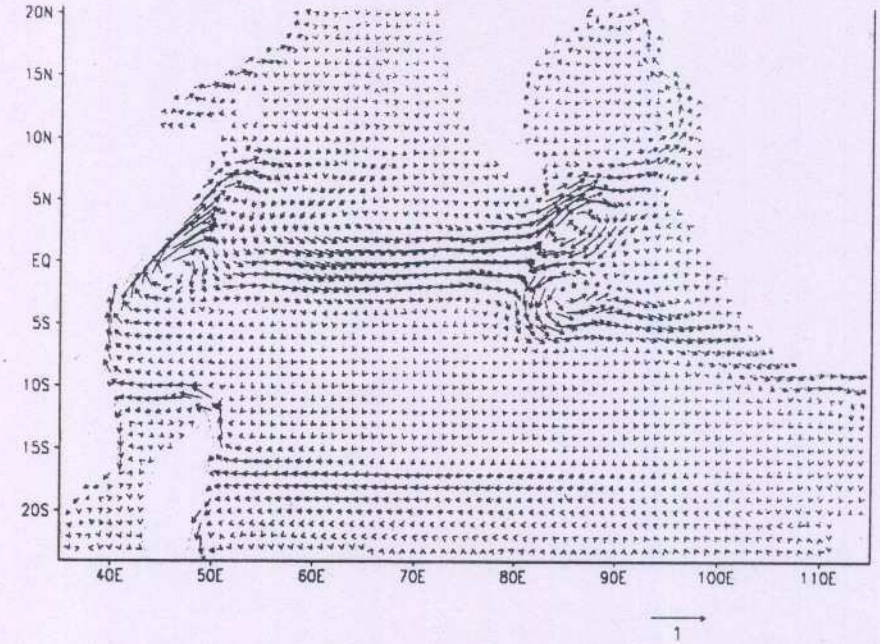

20N
15N
10N
5N
EQ
5S
10S
15S
20S
40E
50E
60E
70E
80E
90E
100E
110E
1

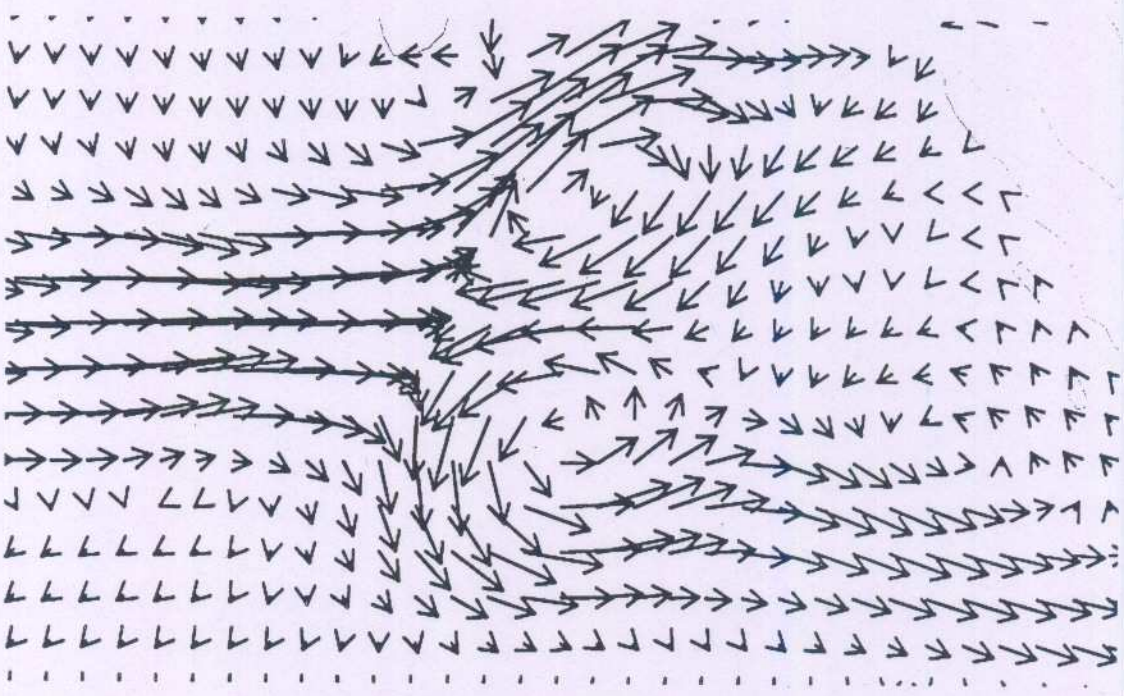

(f) 4th June

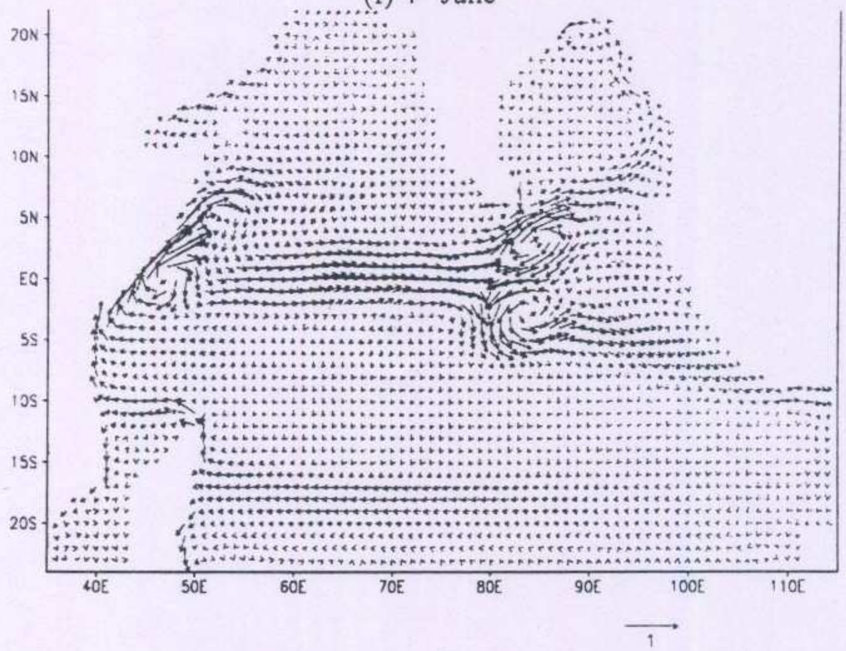

70N
15N
10N
5N
EQ
5S
10S
15S
20S
40E
50E
60E
70E
80E
90E
100E
110E
1

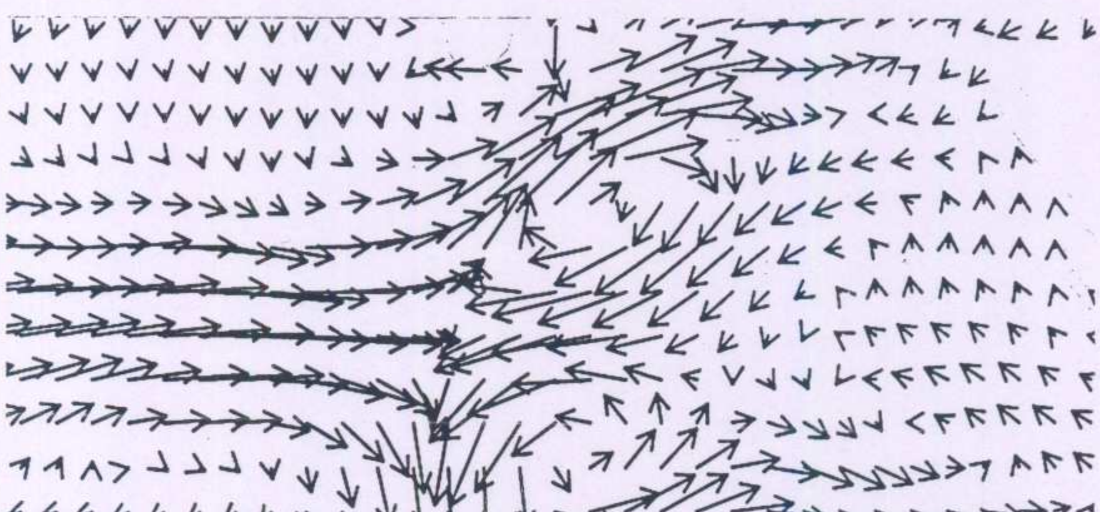

(g)9th June

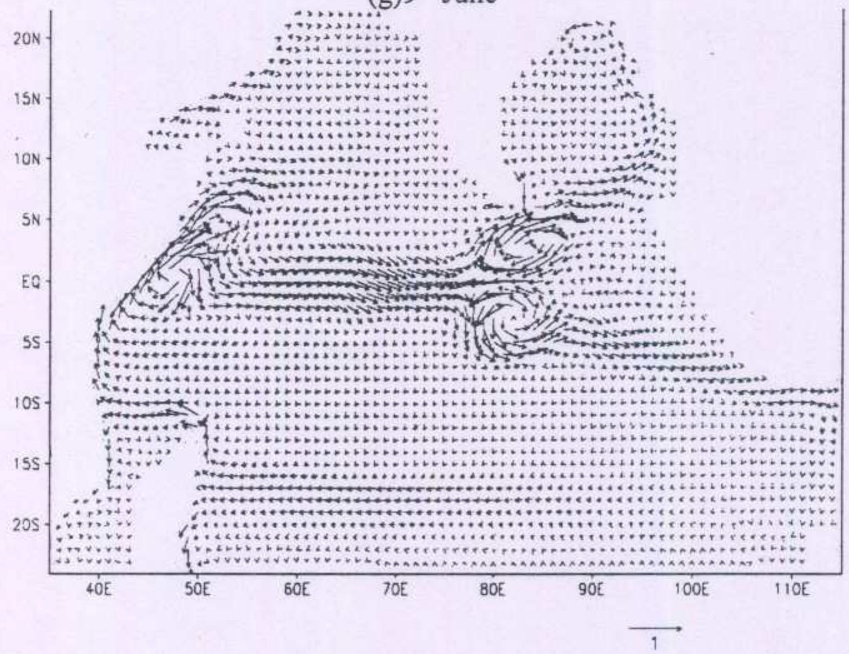
20N
15N
10N
5N
EQ
5S
10S
15S
20S
40E
50E
60E
70E
80E
90E
100E
110E
1

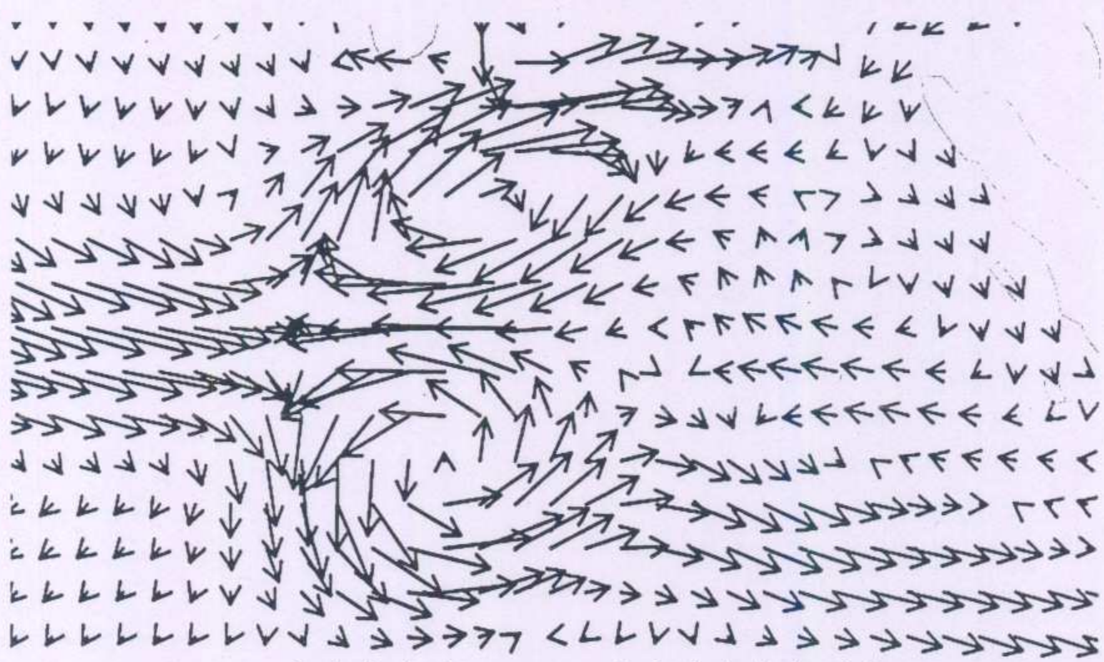

(h)14th June

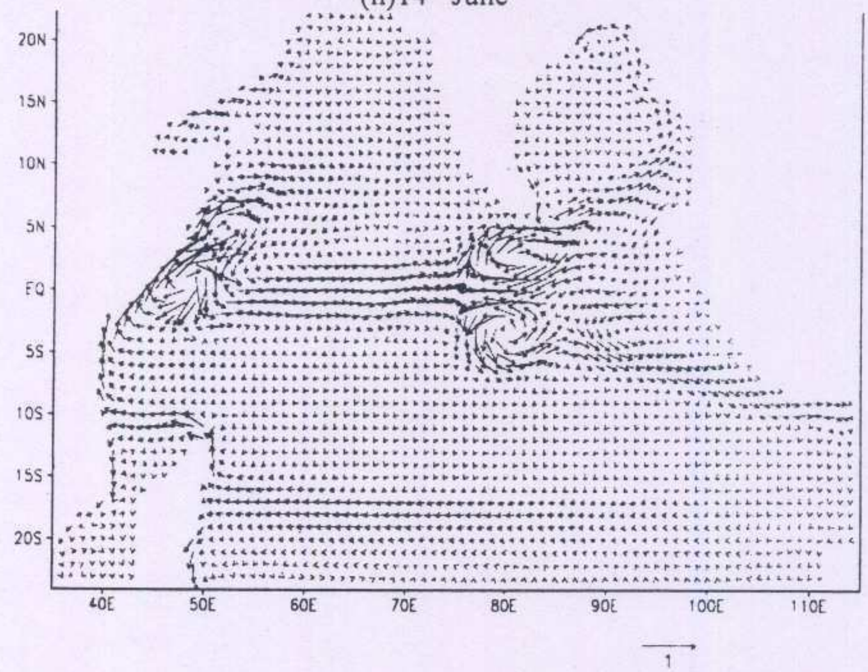
20N
15N
10N
5N
EQ
5S
10S
15S
20S
40E
50E
60E
70E
80E
90E
100E
110E
1

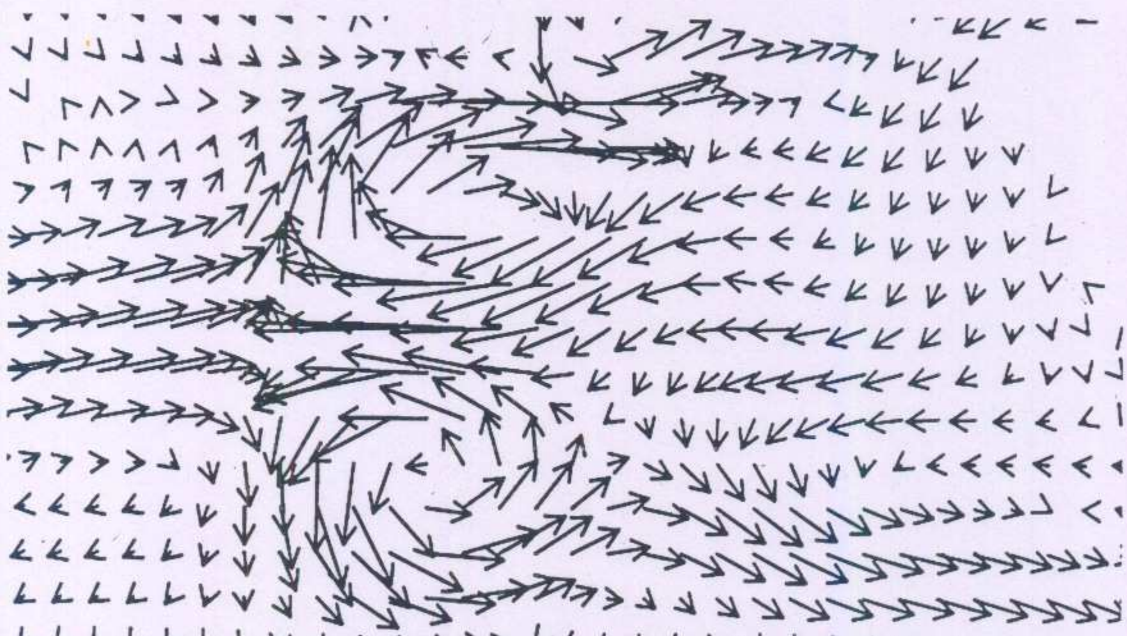

(i)19th June

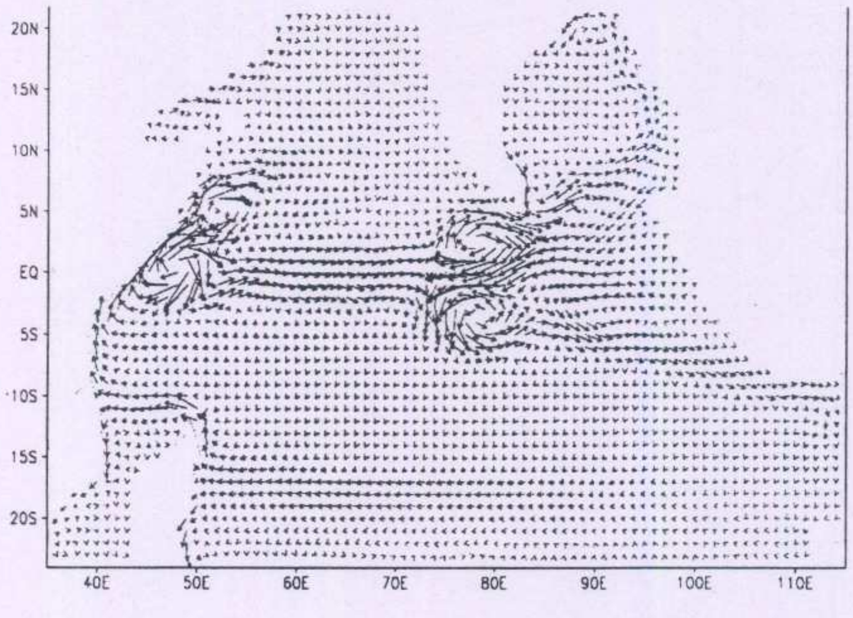
20N
15N
10N
5N
EQ
5S
10S
15S
20S
40E
50E
60E
70E
80E
90E
100E
110E
1

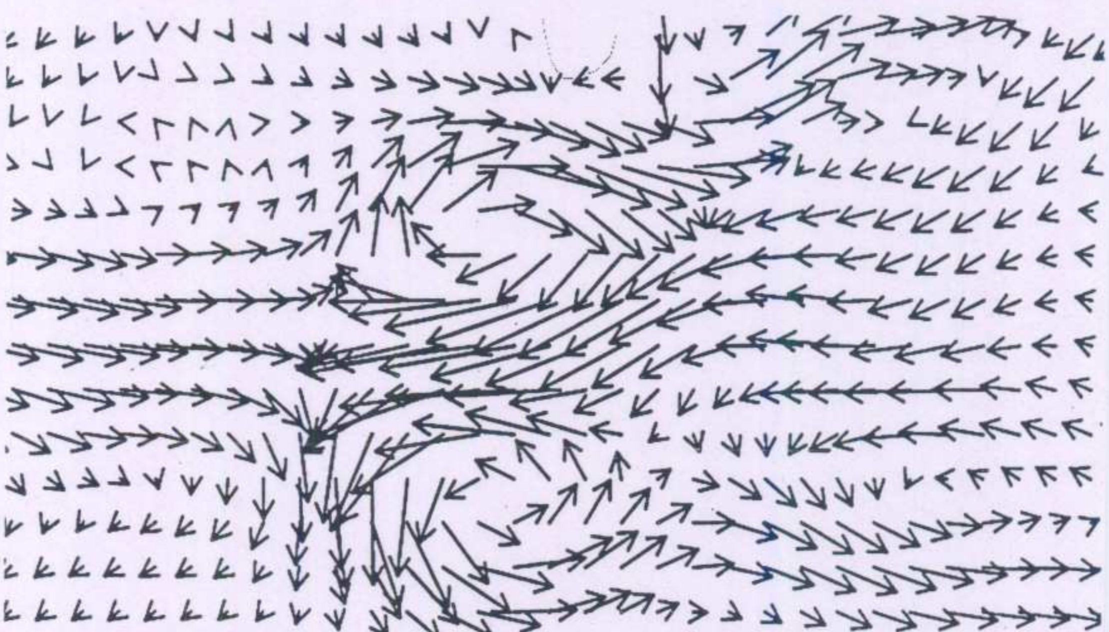

(j)24th June

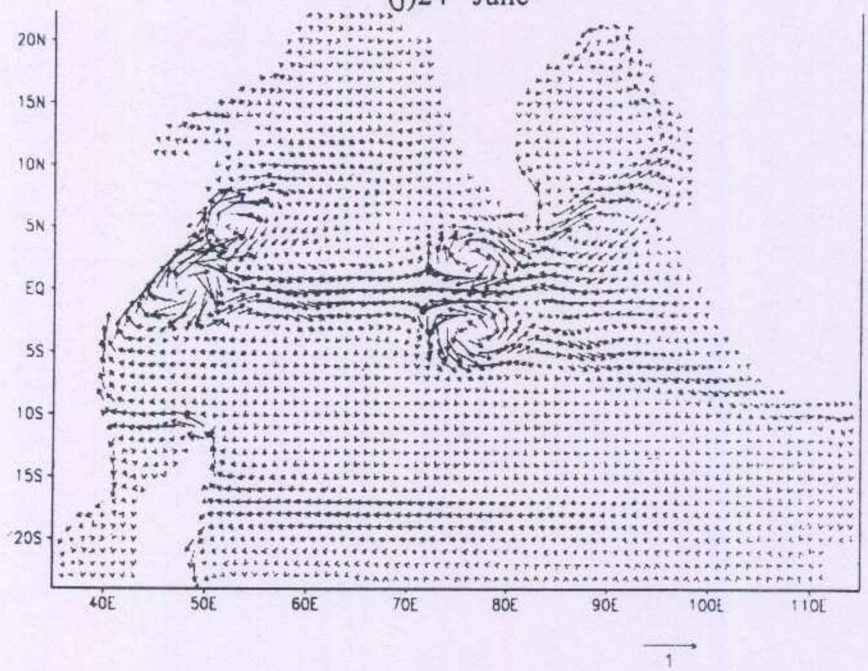
20N
15N
10N
5N
EQ
5S
10S
15S
20S
40E
50E
60E
70E
80E
90E
100E
110E
1

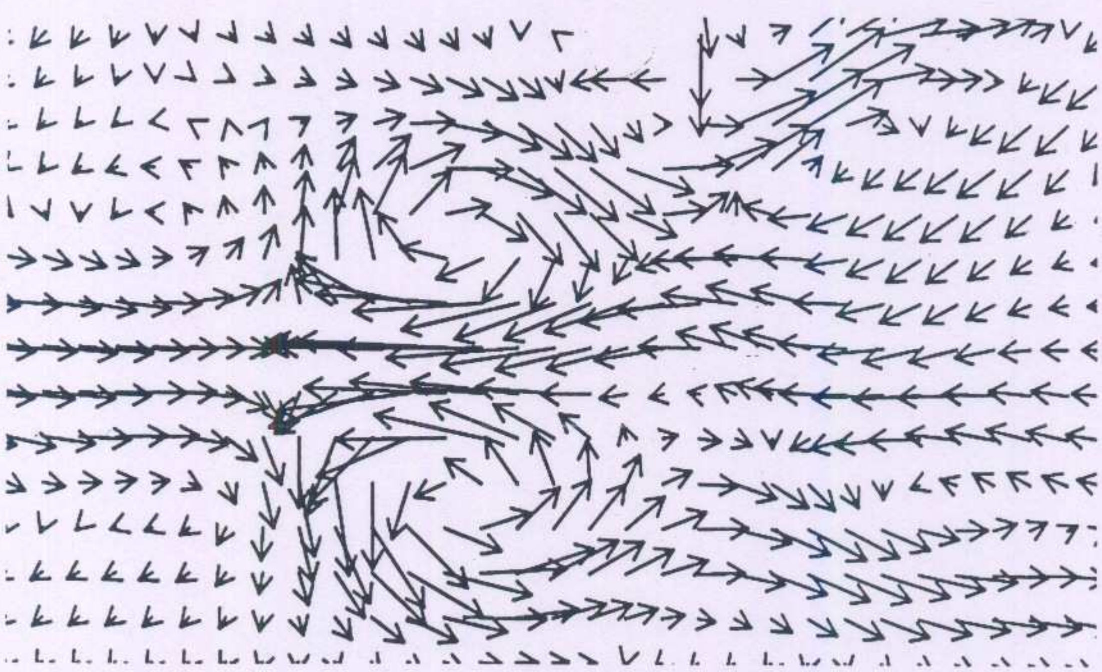

(k) 29th June

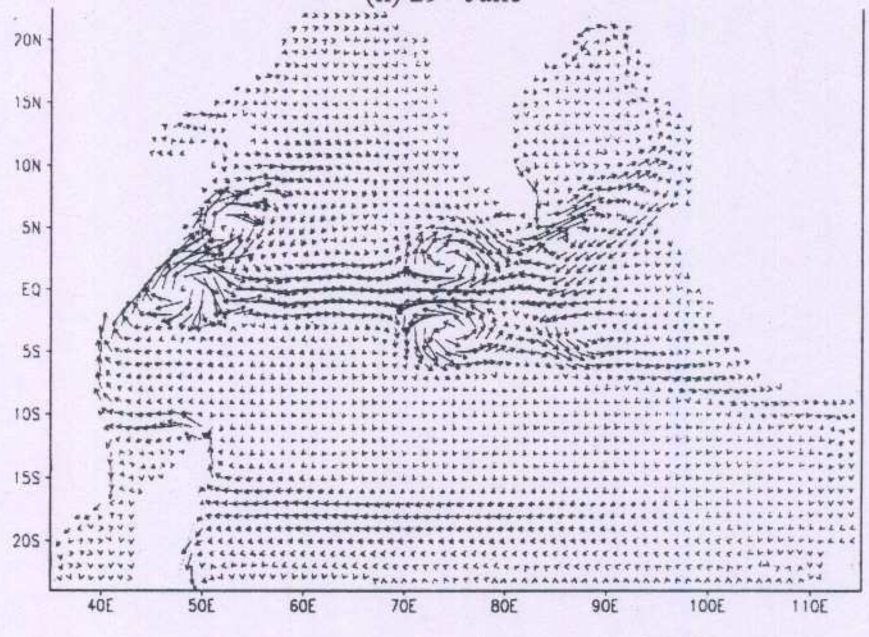

20N
15N
10N
5N
EQ
5S
10S
15S
20S
40E
50E
60E
70E
80E
90E
100E
110E
1

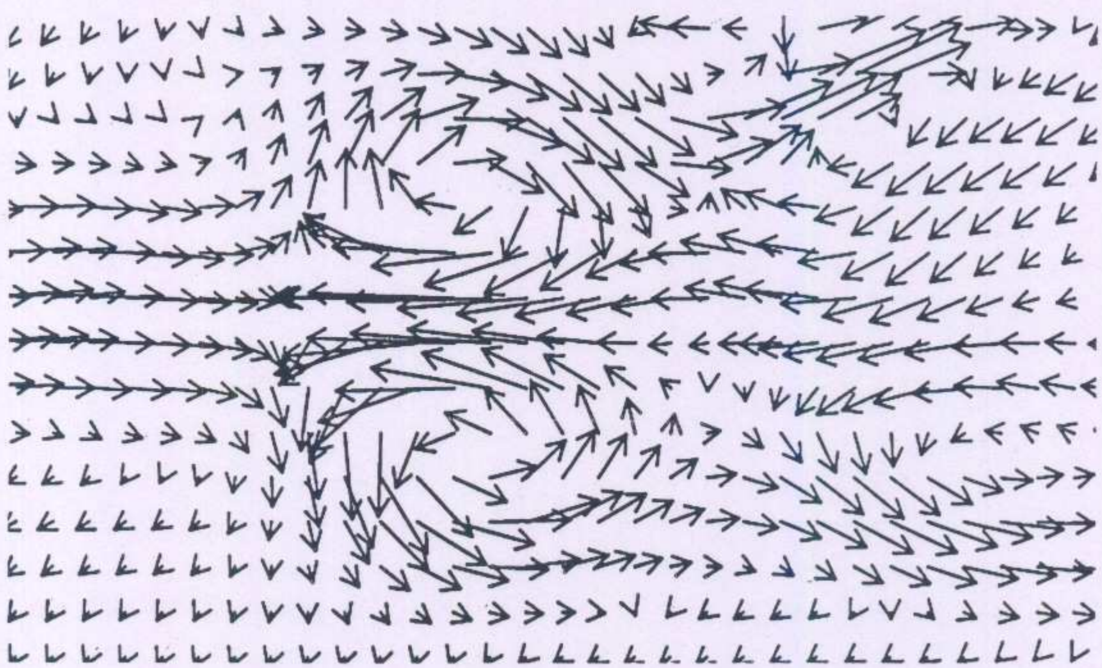

(l)5th July

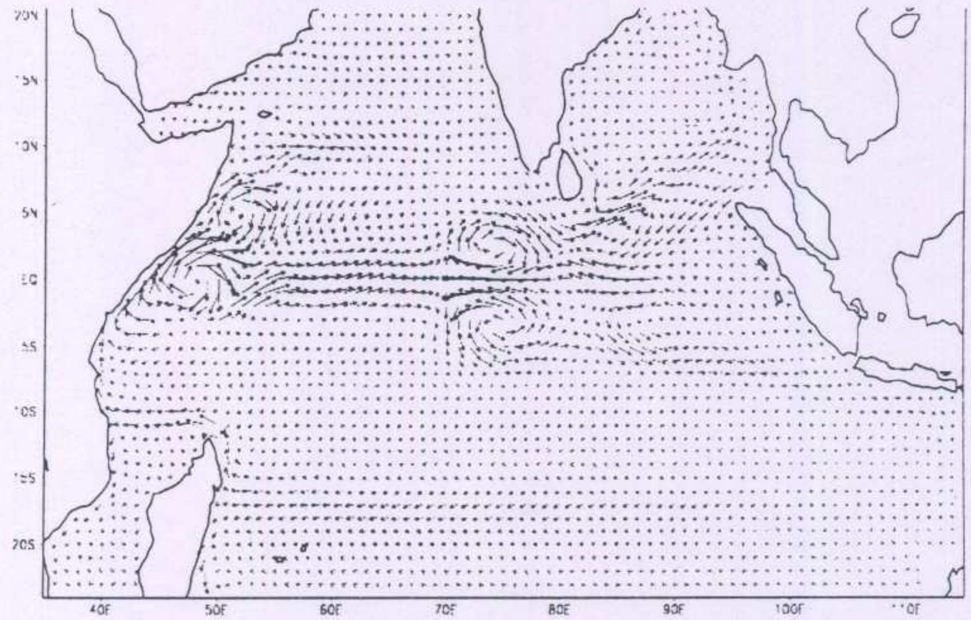
20N
15N
10N
5N
EQ
5S
10S
15S
20S
40E
50E
60E
70E
80E
90E
100E
110E

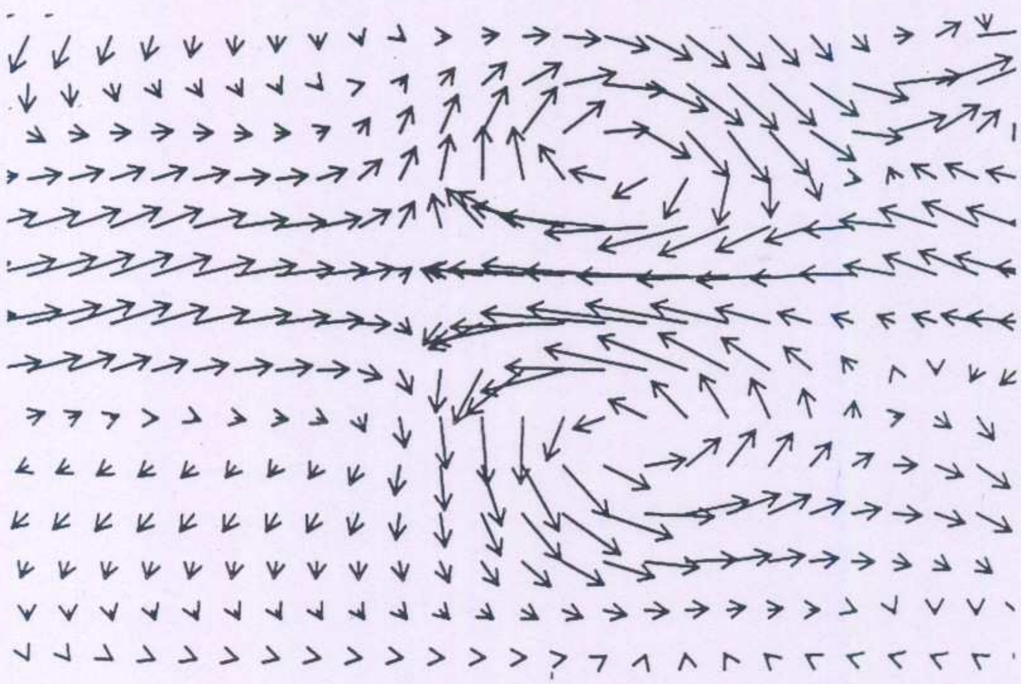

(m)10th July

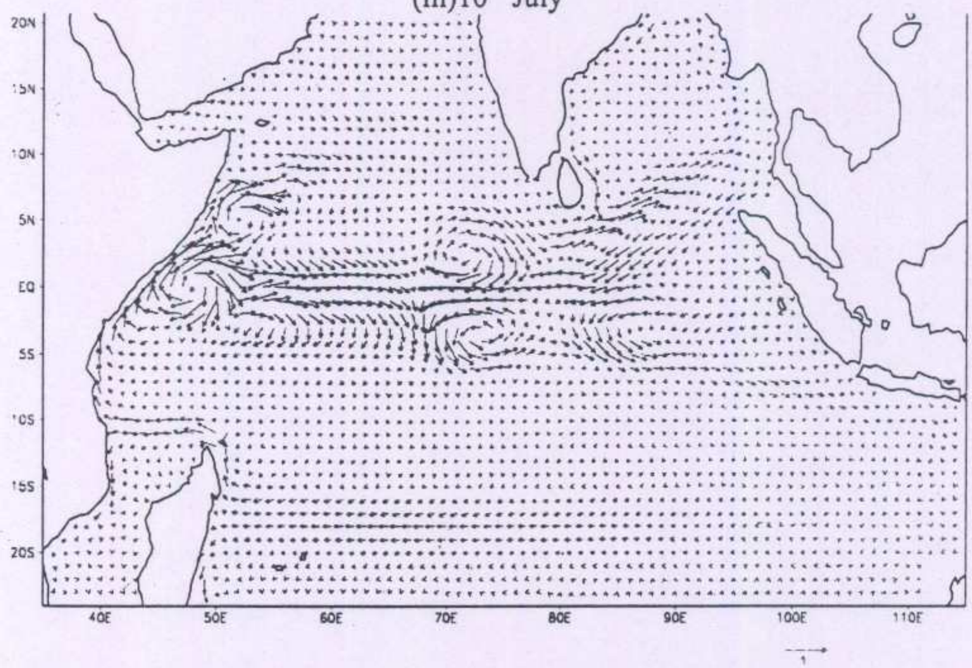
20N
15N
10N
5N
EQ
5S
10S
15S
20S
40E
50E
60E
70E
80E
90E
100E
110E

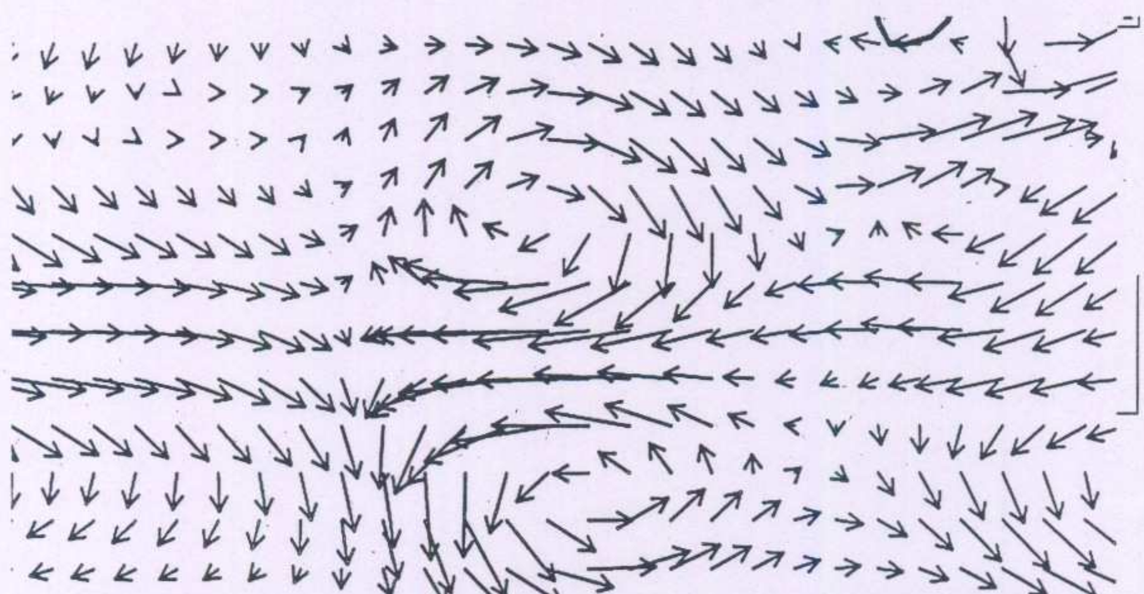

(n)15th July

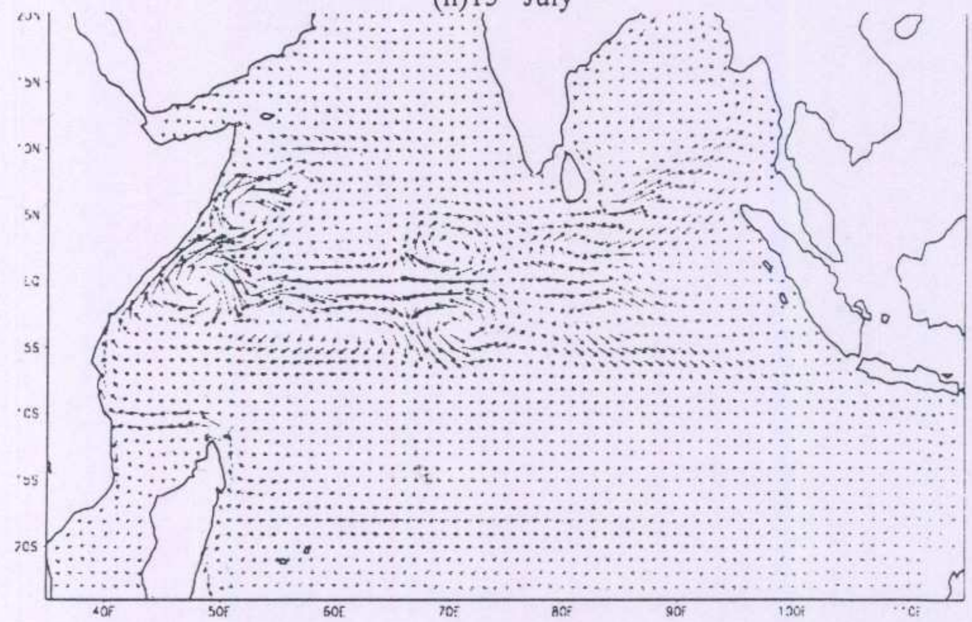

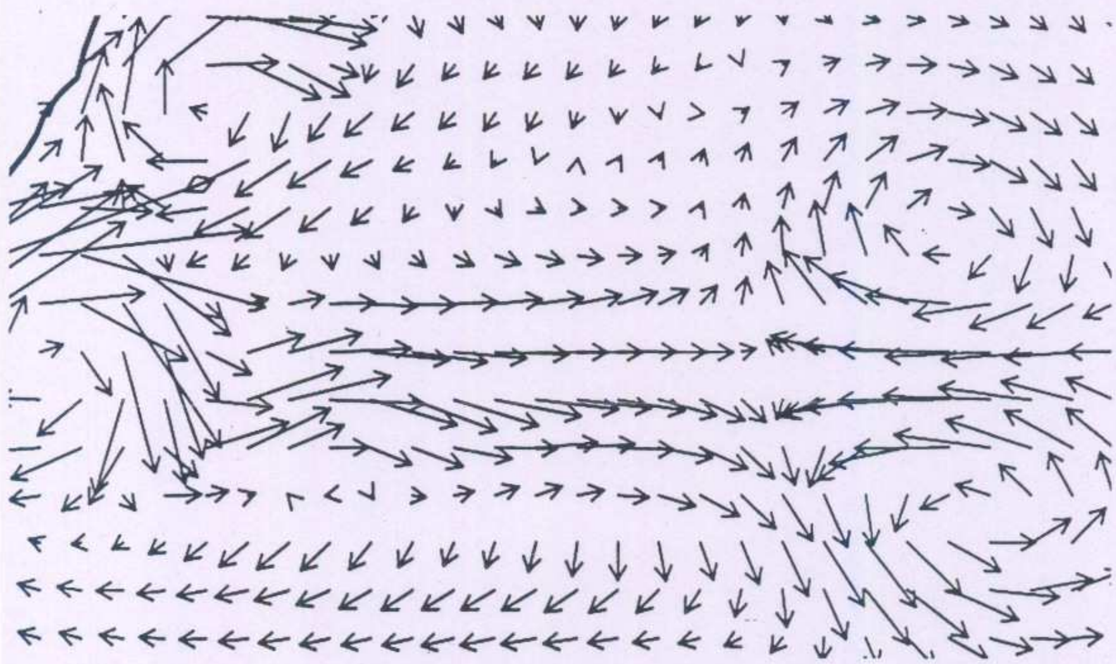

(o)20th July

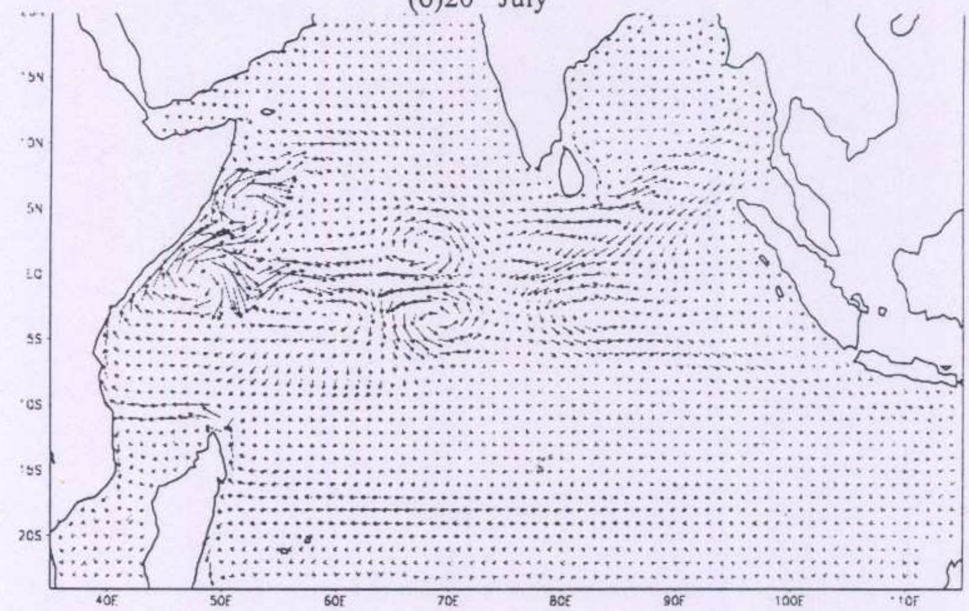

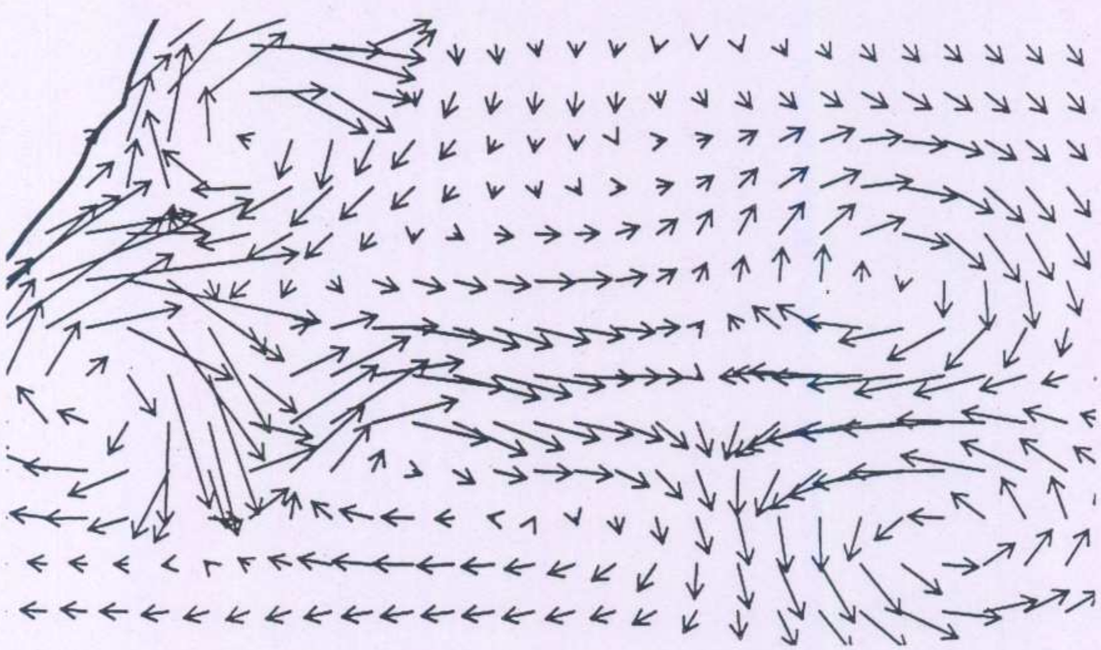

(p)25th July

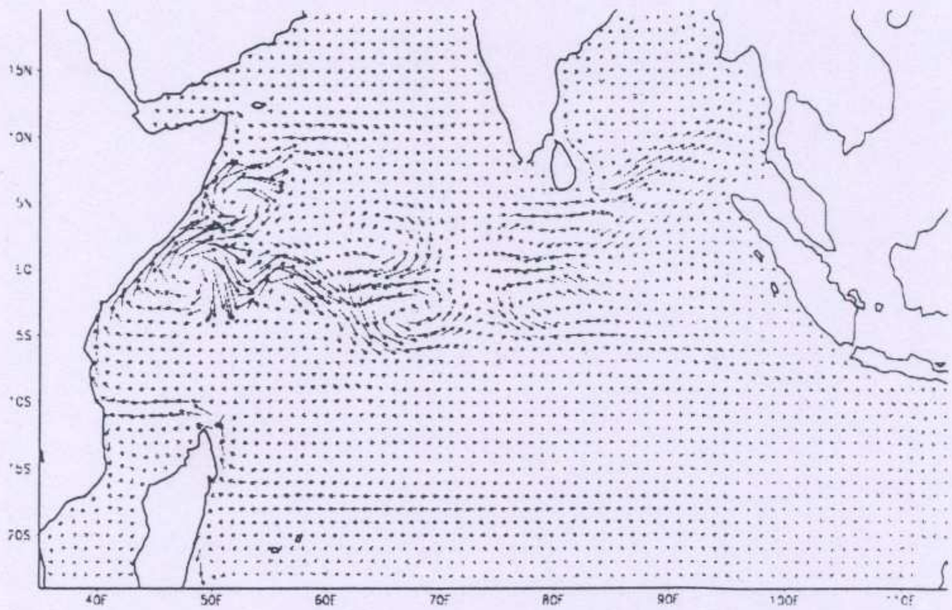

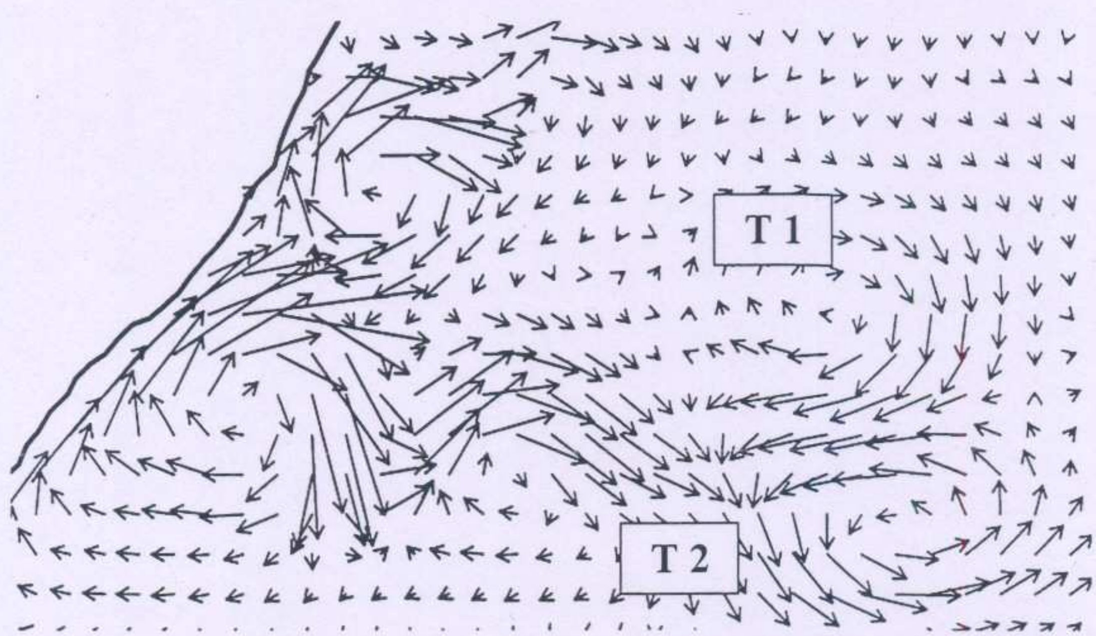

(q) 3rd August

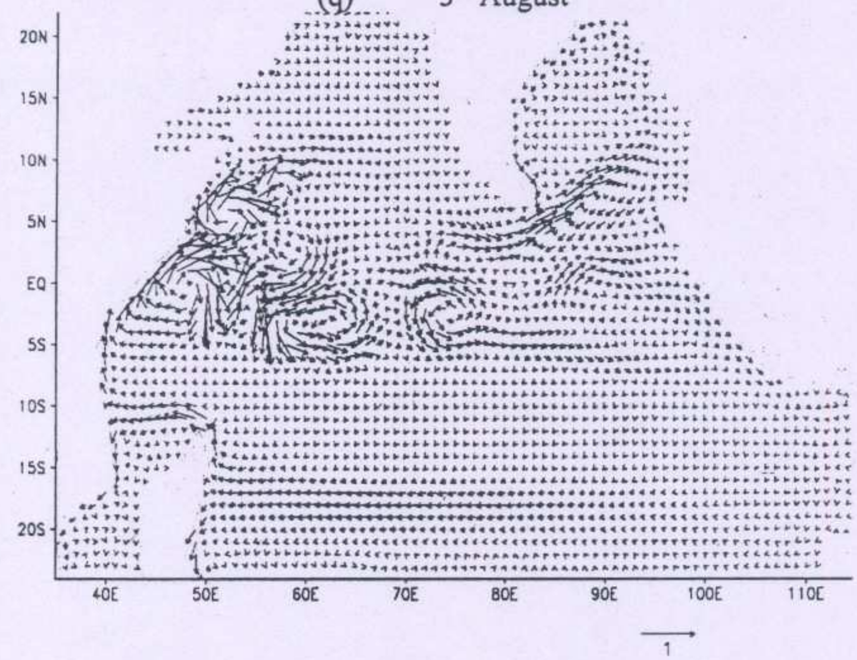

20N
15N
10N
5N
EQ
5S
10S
15S
20S
40E
50E
60E
70E
80E
90E
100E
110E
1

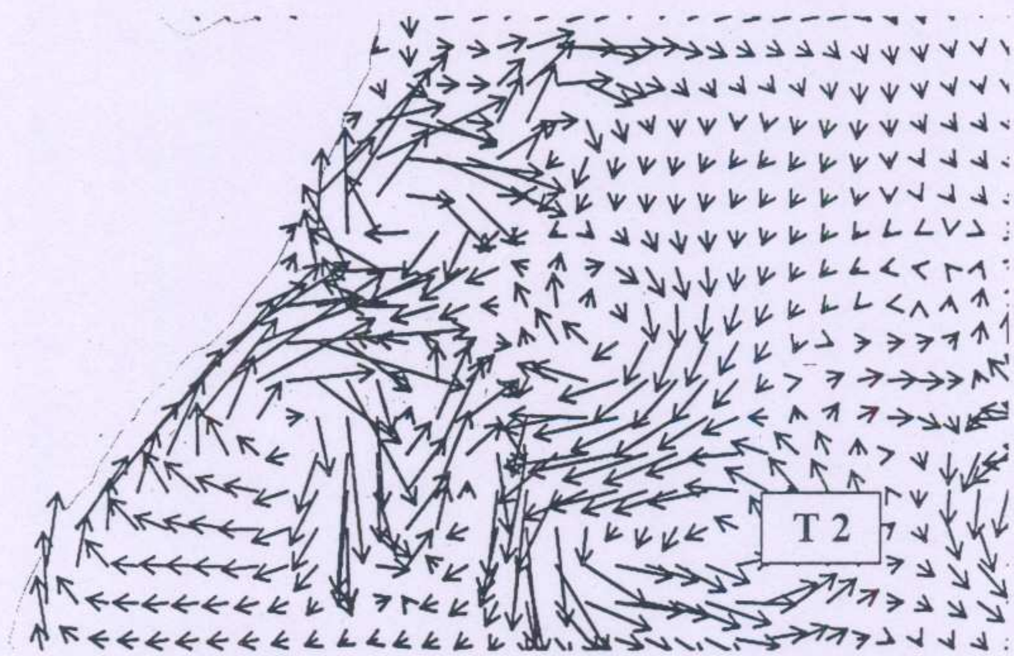

T 2

®8th August

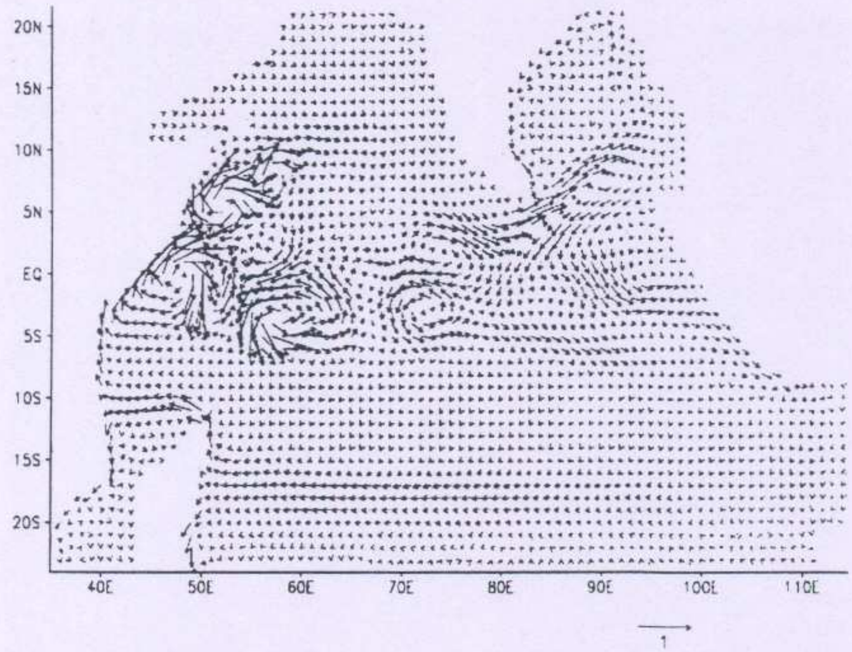
20N
15N
10N
5N
EQ
5S
10S
15S
20S
40E
50E
60E
70E
80E
90E
100E
110E
1

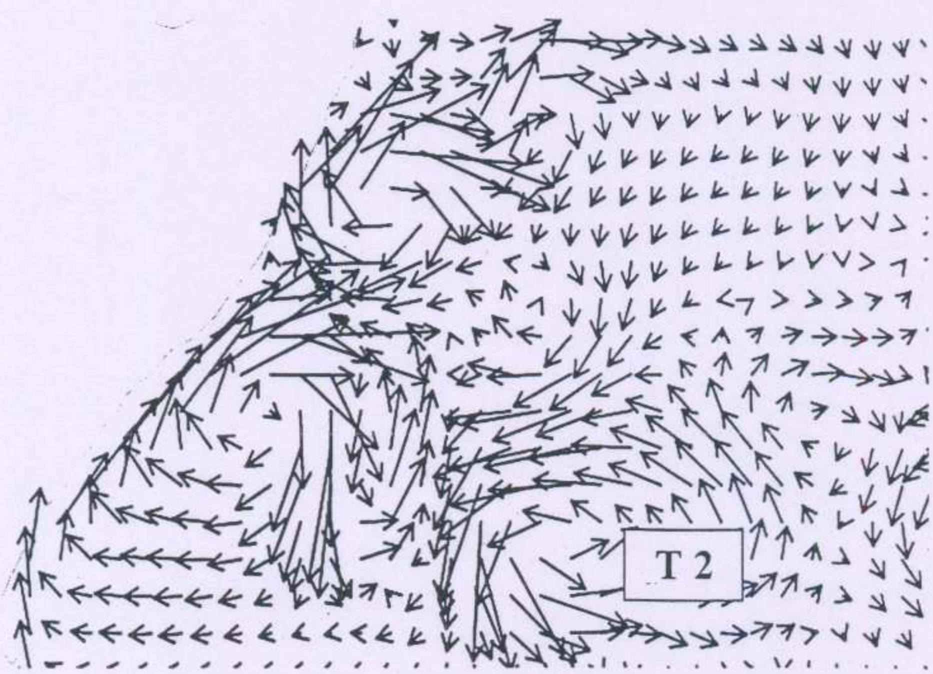
T 2

(s)13[rd] August

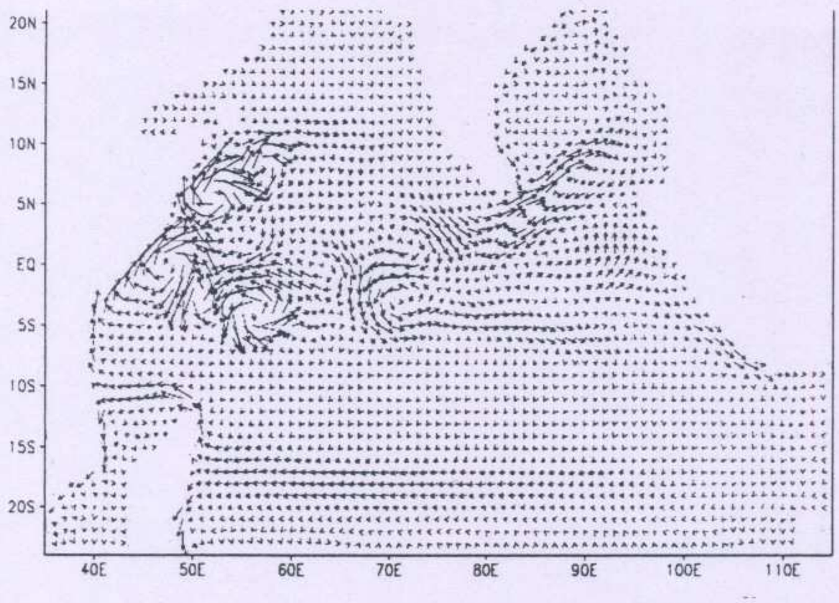

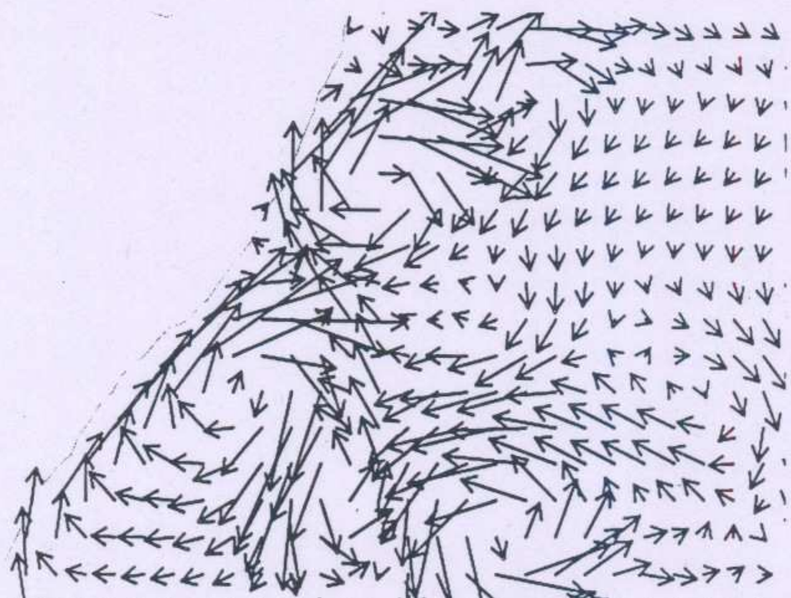

(t)18th August

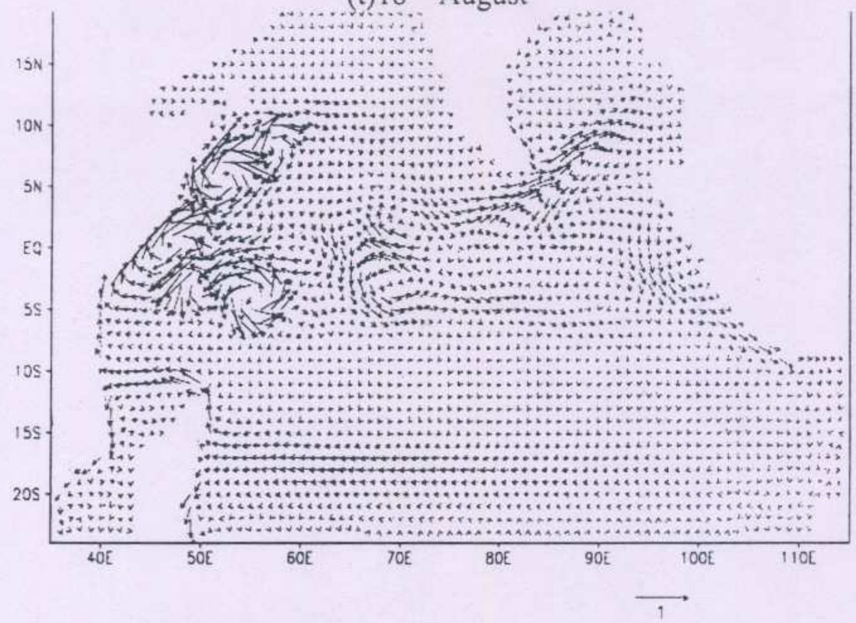

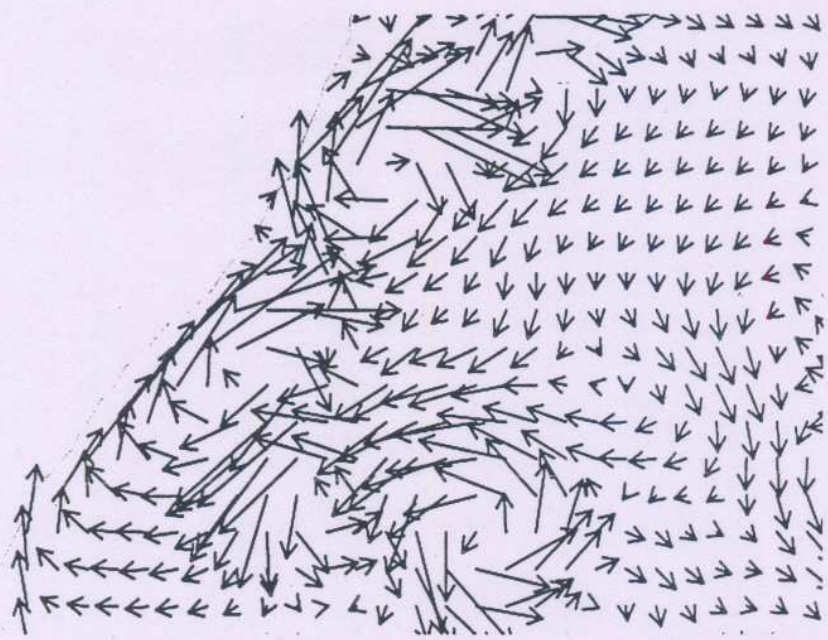

(u)23th August

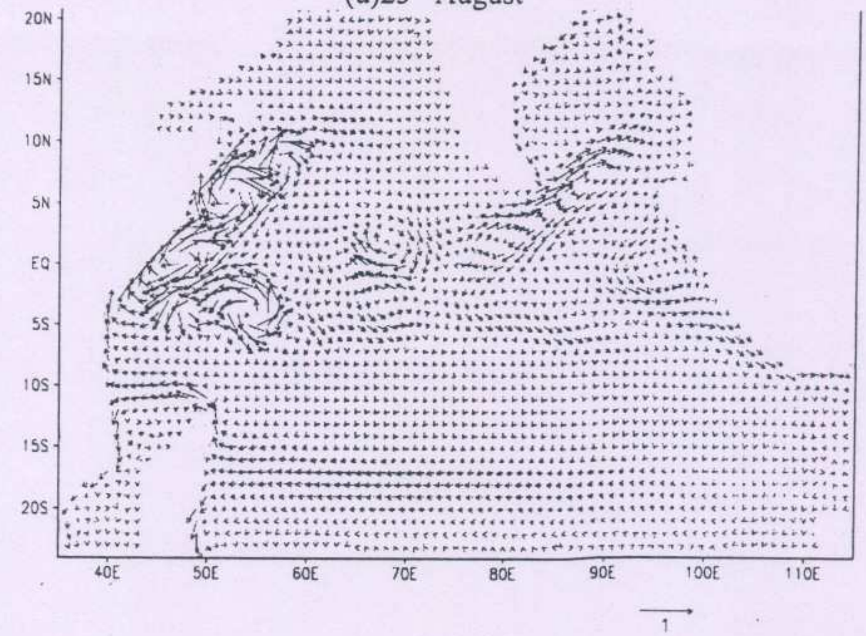

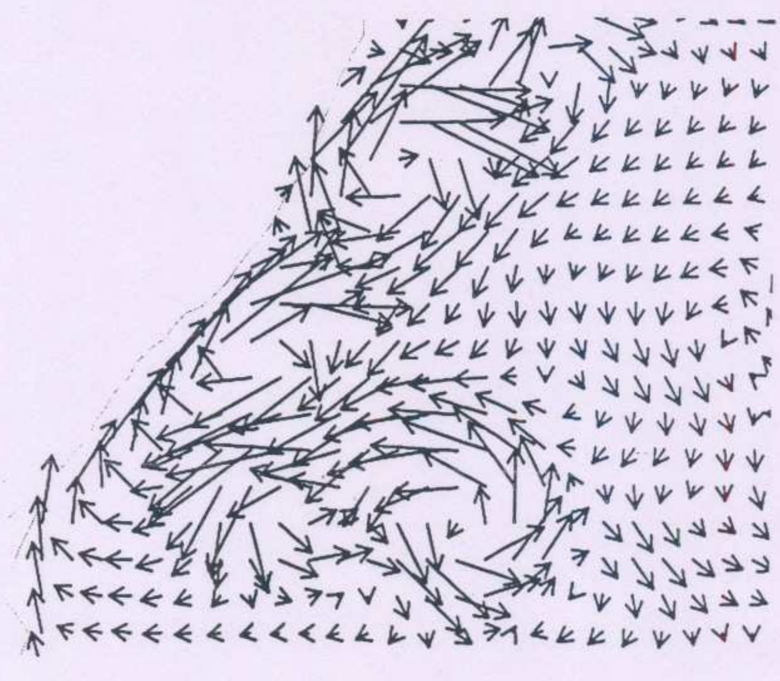

(v)28th August

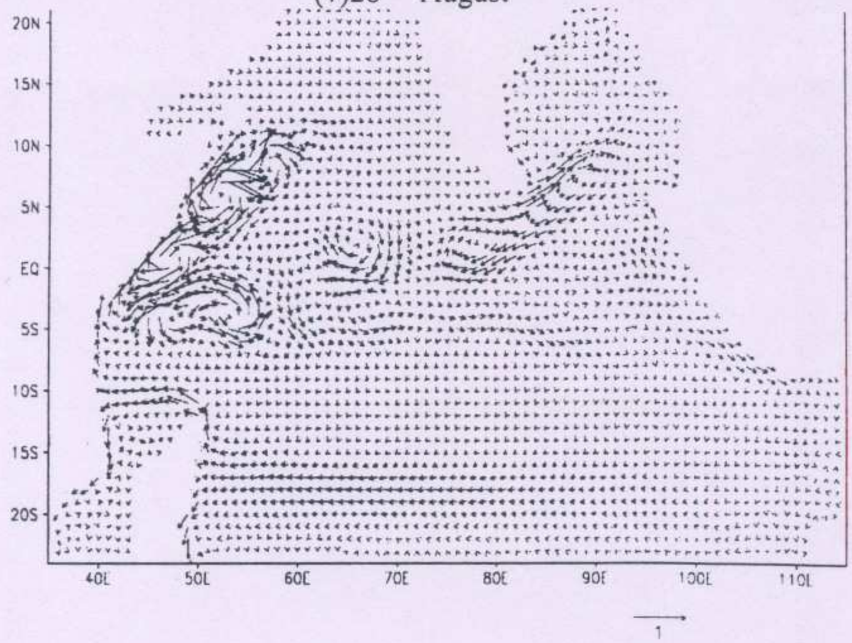

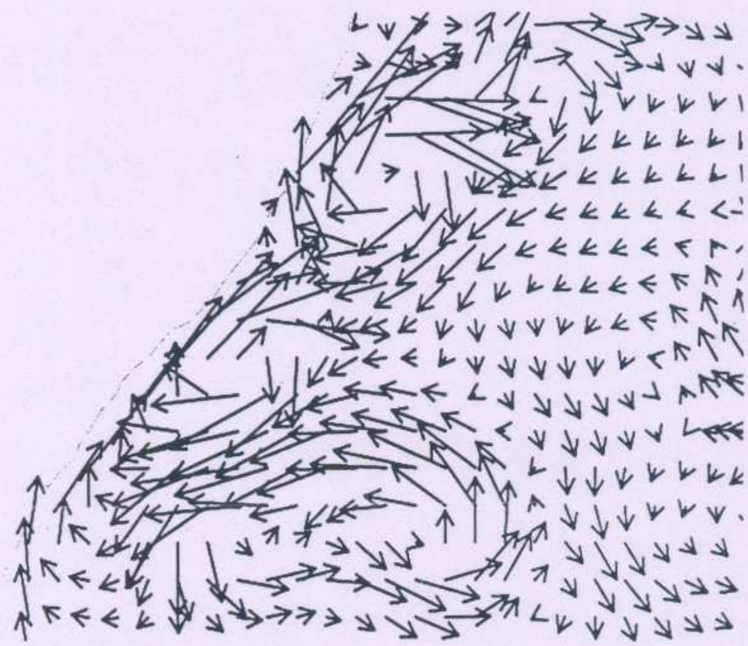

(w)2nd September

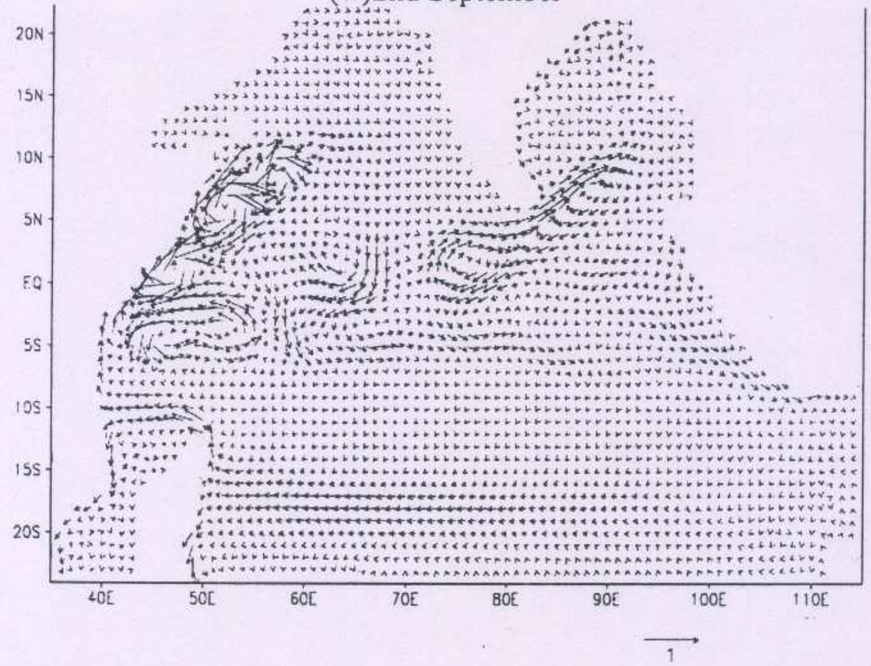

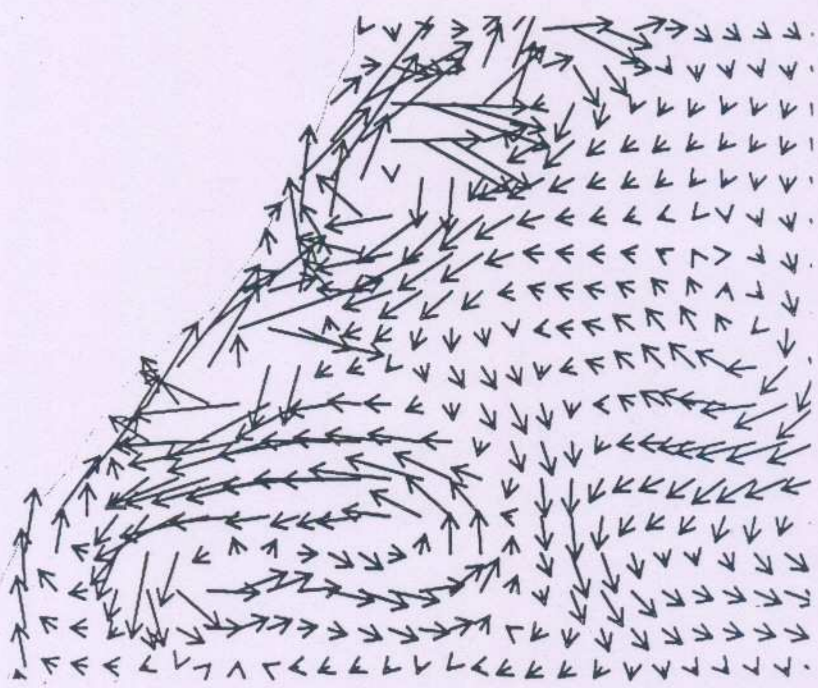

(x)7th September

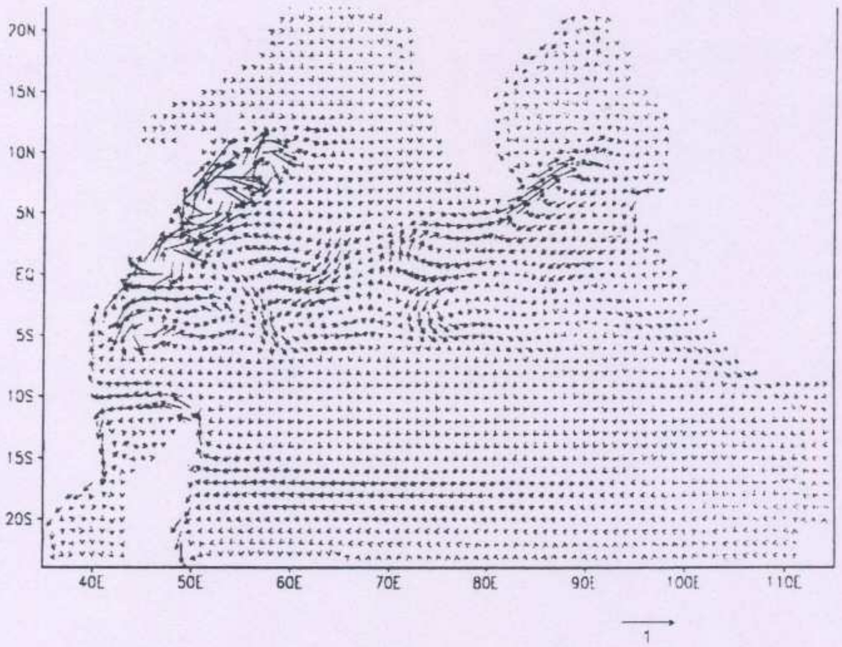

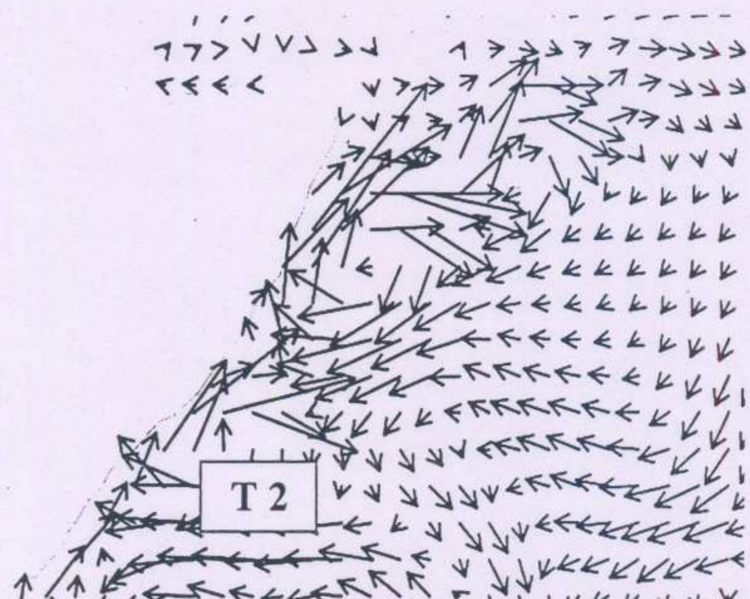

(y)12th September

(y)12th September

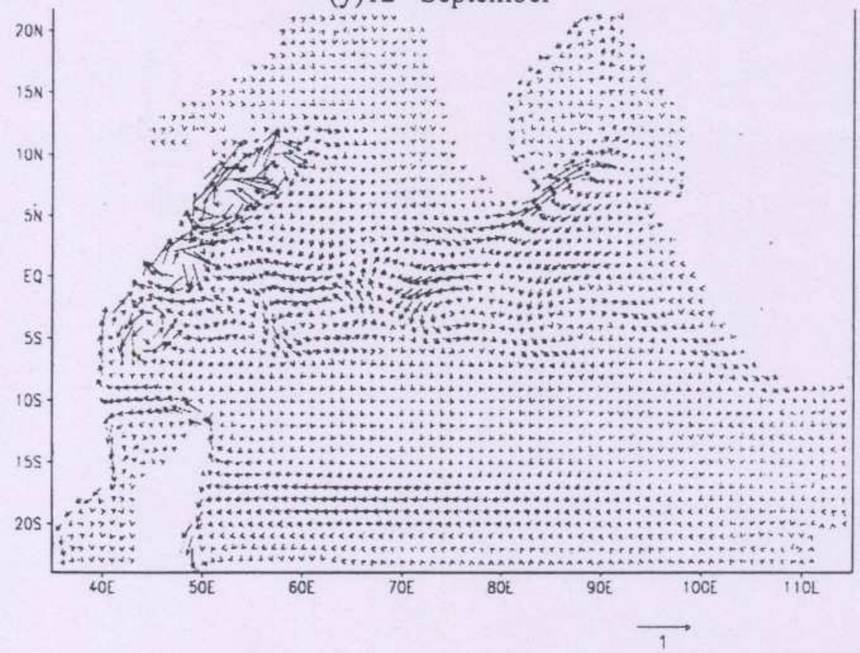

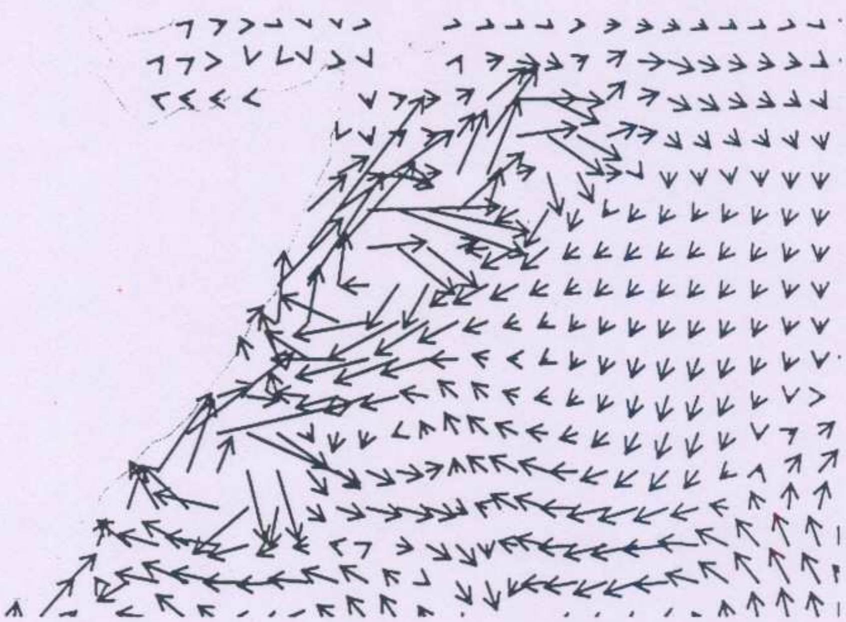

(z) 17th September

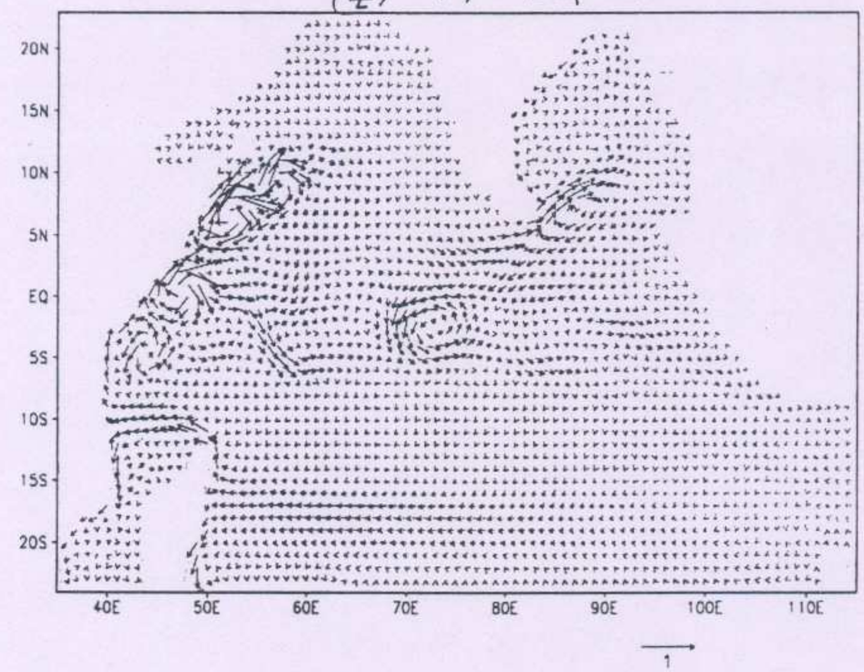

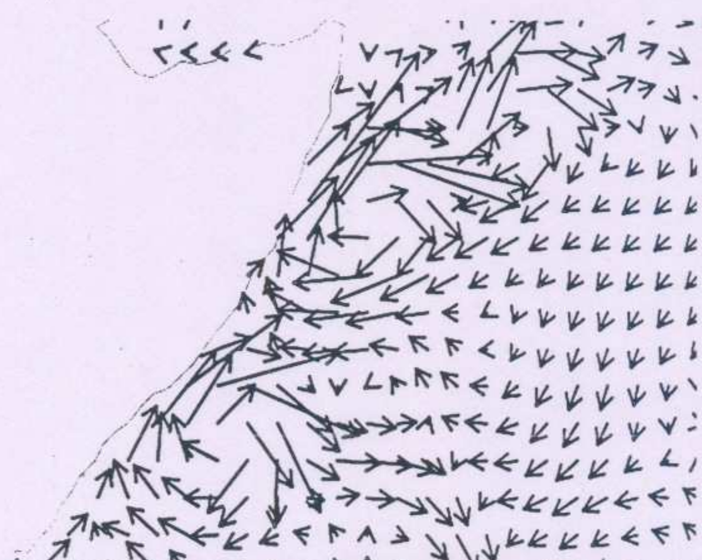

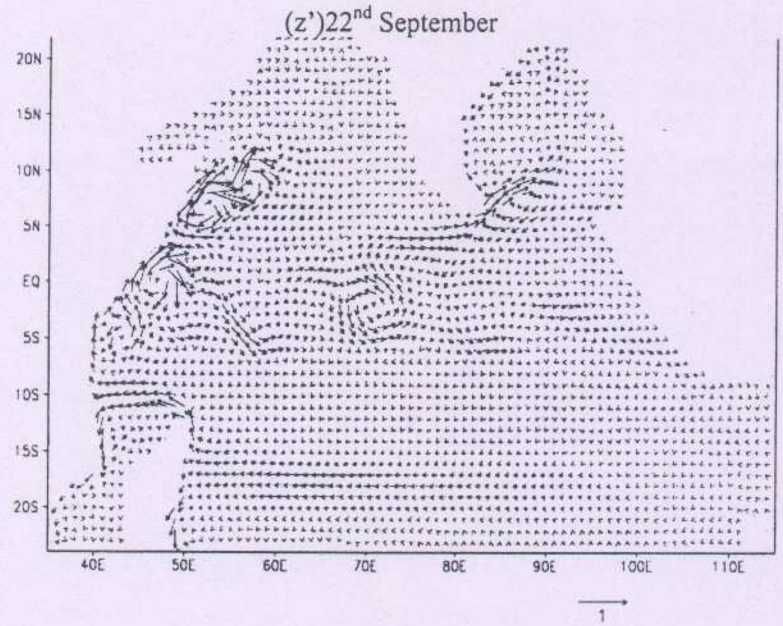

Fig 10. IRG model surface simulations along the equator reveal the T-Gyres with daily winds as forcings. 5-day outputs are presented from the Initial stages to the Final stages of the T-gyres, i.e. from May end to Mid September.

a

05 July 1999 – MSMR

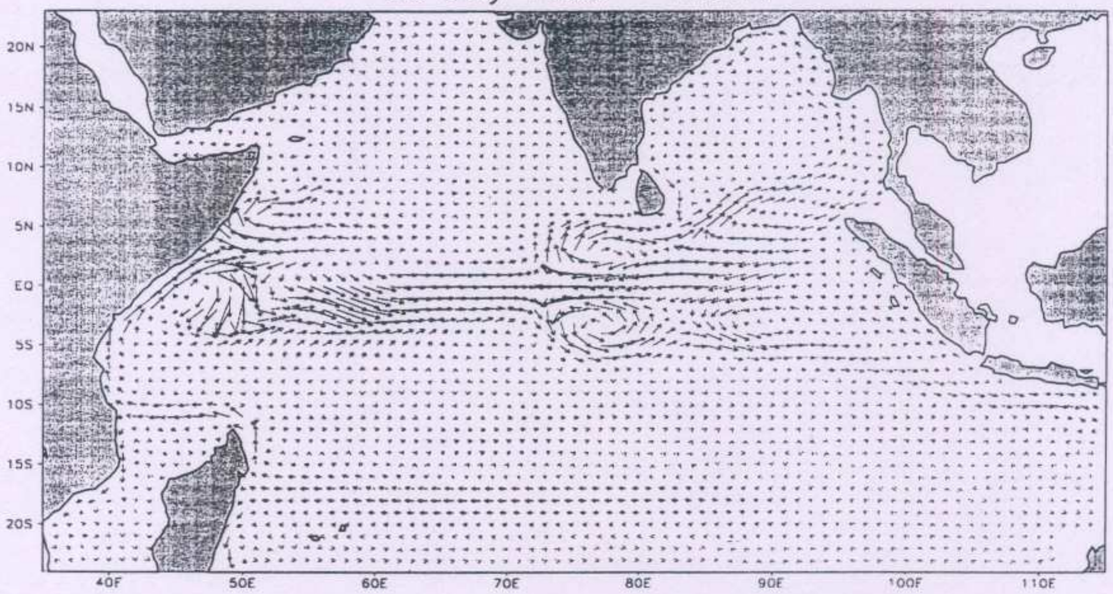

ultd 05 july99(MSMR)

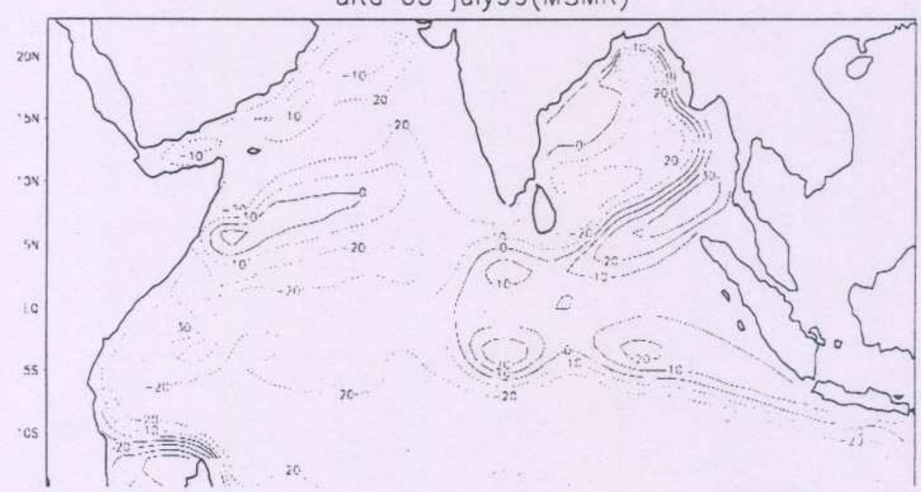

b

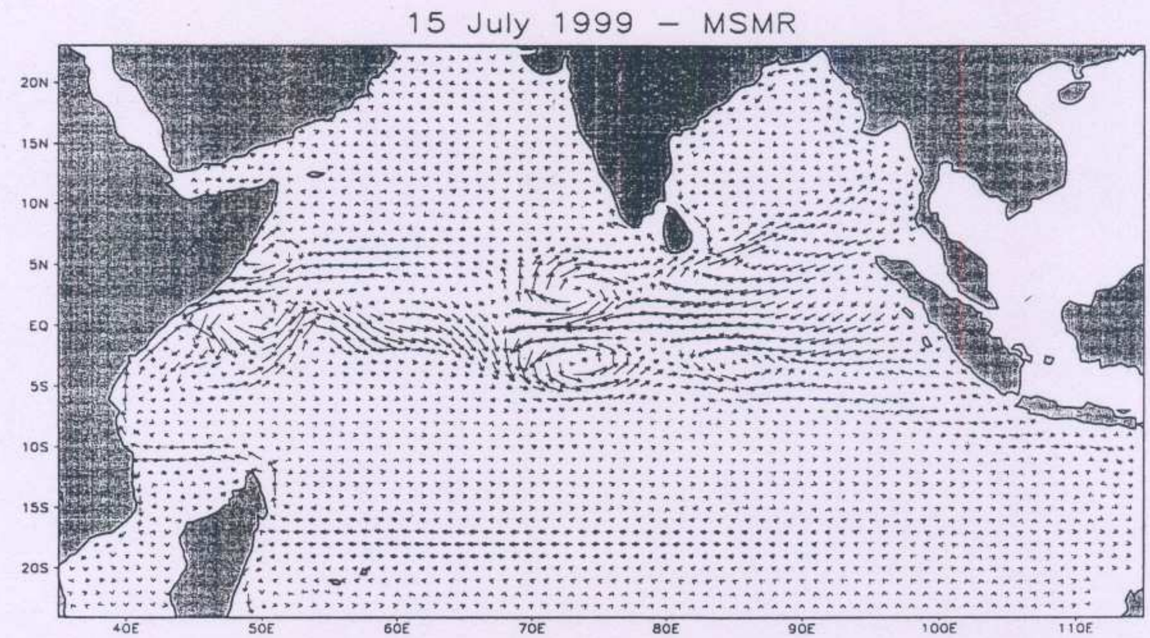
15 July 1999 – MSMR
20N
15N
10N
5N
EQ
5S
10S
15S
20S
40E
50E
60E
70E
80E
90E
100E
110E

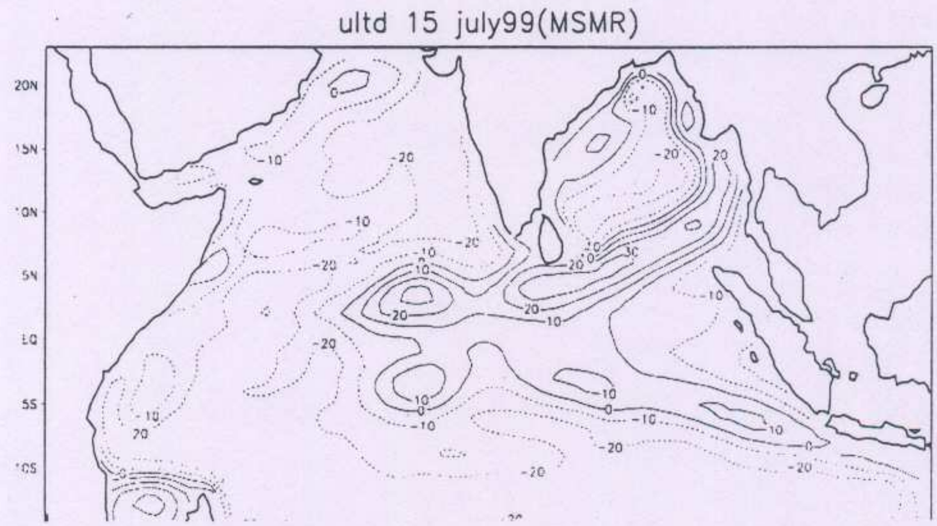
ultd 15 july99(MSMR)
20N
15N
10N
5N
EQ
5S
10S

c

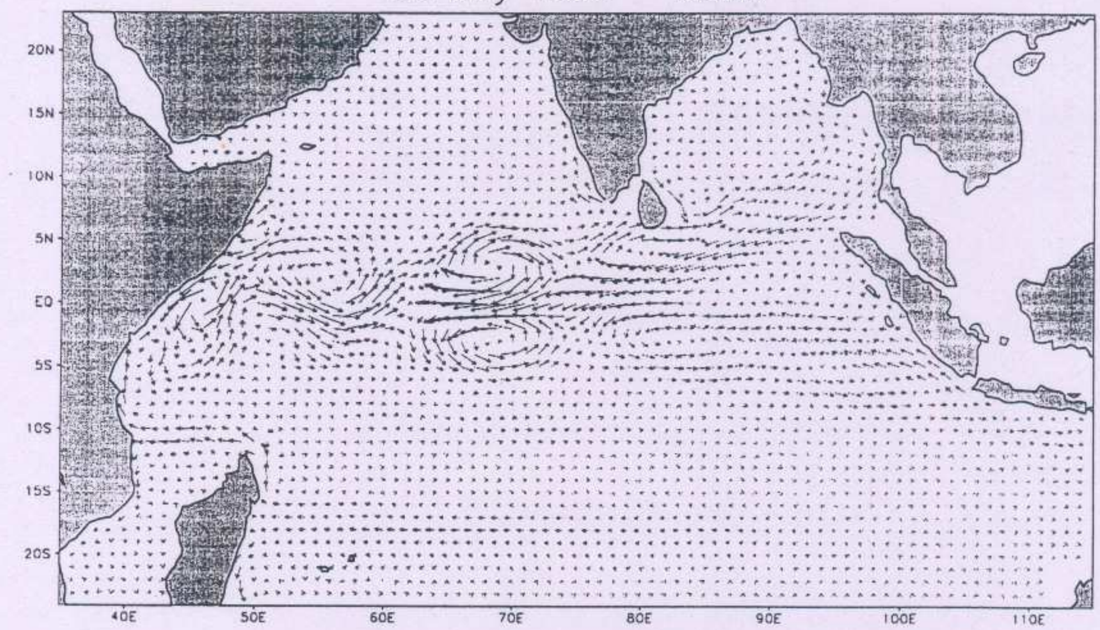

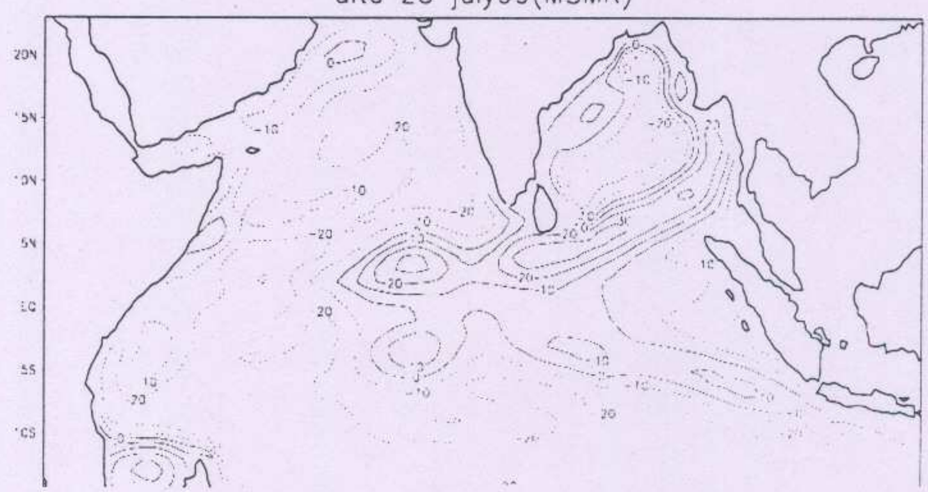

Fig 11 .Currents for the month of July 1999 showing the twin gyres for the dates 05th, 15th and 25th in the upper panel and Upper Layer Thickness Depth (ULTD) in the Lower layer respectively.

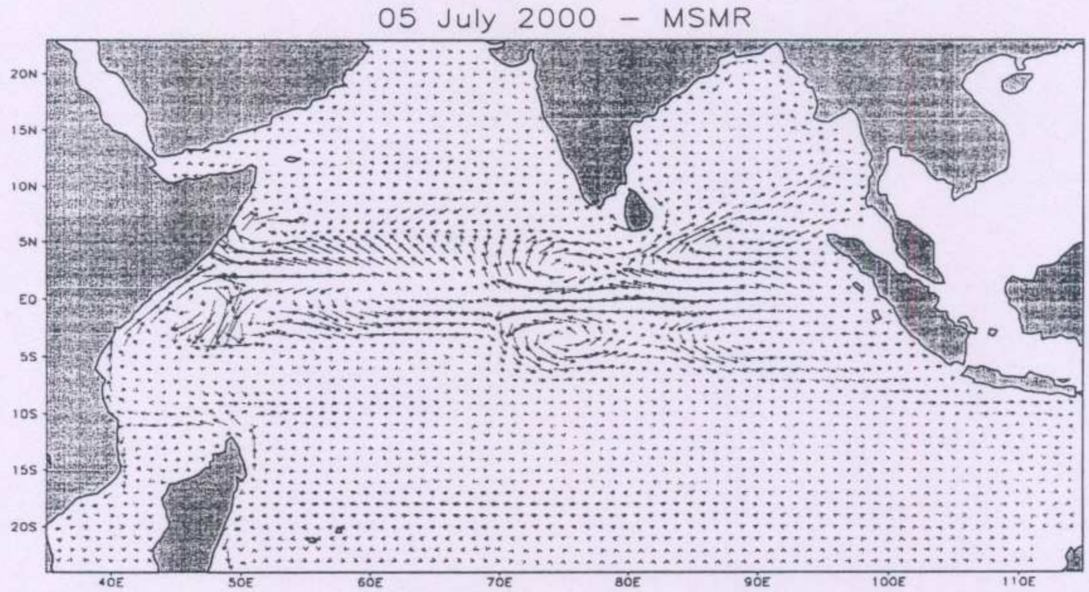
05 July 2000 – MSMR
20N
15N
10N
5N
EQ
5S
10S
15S
20S
40E
50E
60E
70E
80E
90E
100E
110E

a

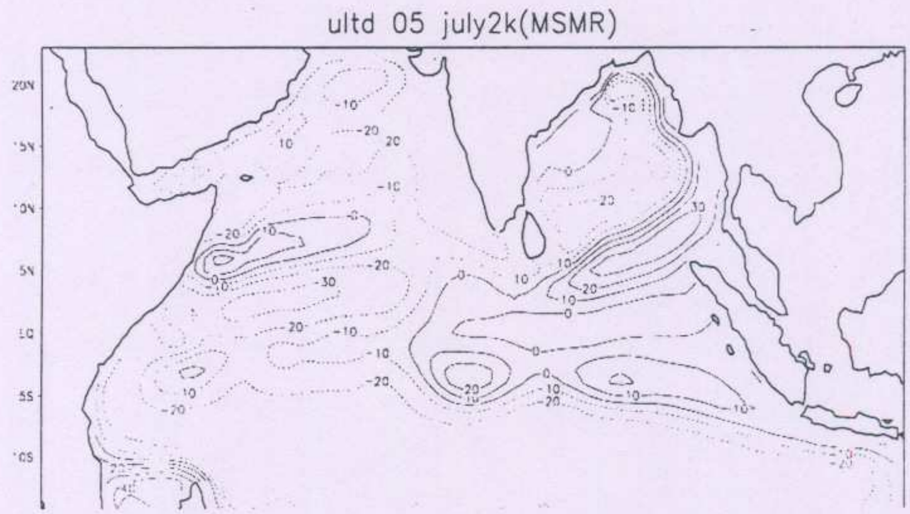
ultd 05 july2k(MSMR)

b

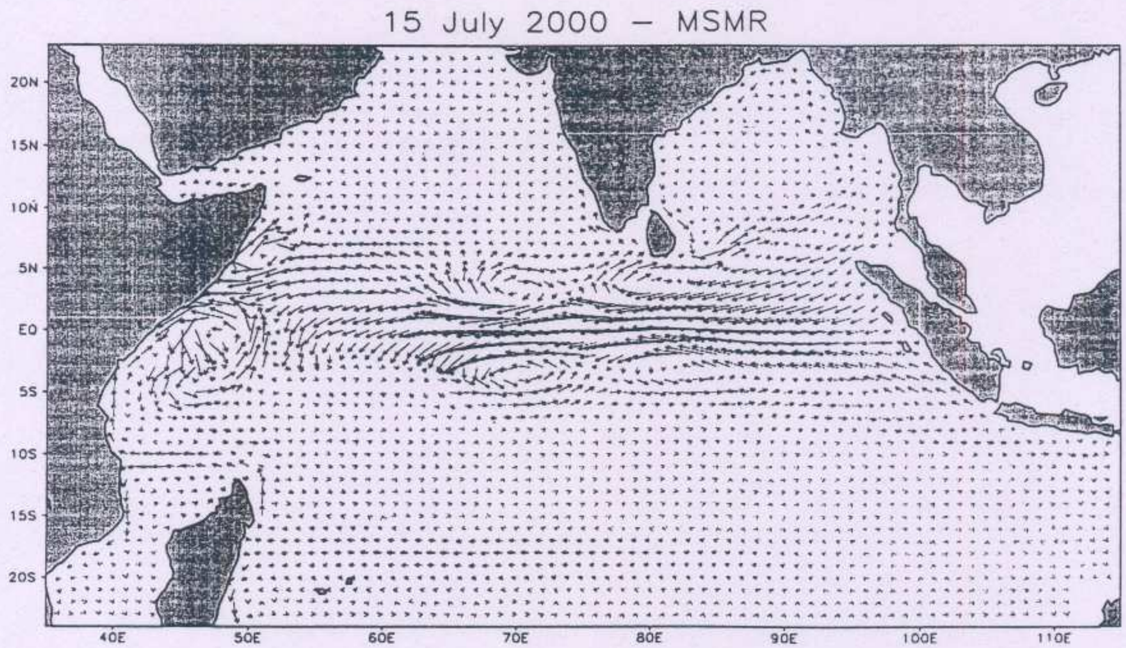
15 July 2000 – MSMR
20N
15N
10N
5N
EQ
5S
10S
15S
20S
40E
50E
60E
70E
80E
90E
100E
110E

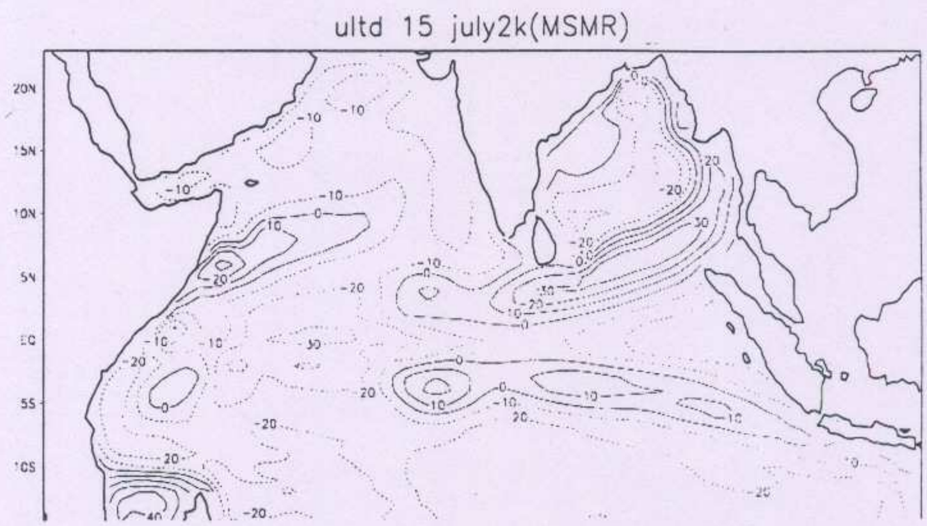
ultd 15 july2k(MSMR)
20N
15N
10N
5N
EQ
5S
10S

c

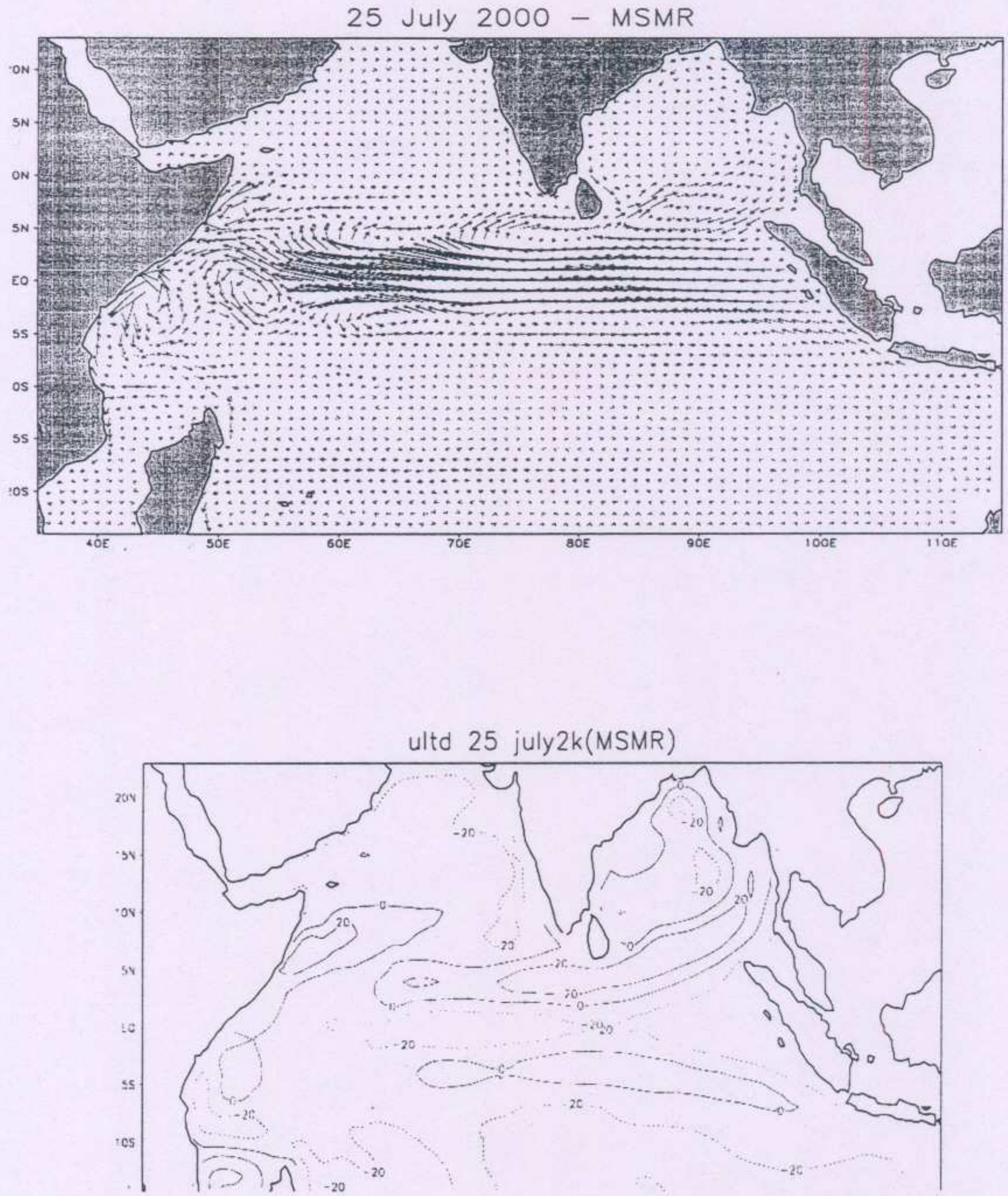

Fig 12. Same as Fig.11 but for the year 2000.

a

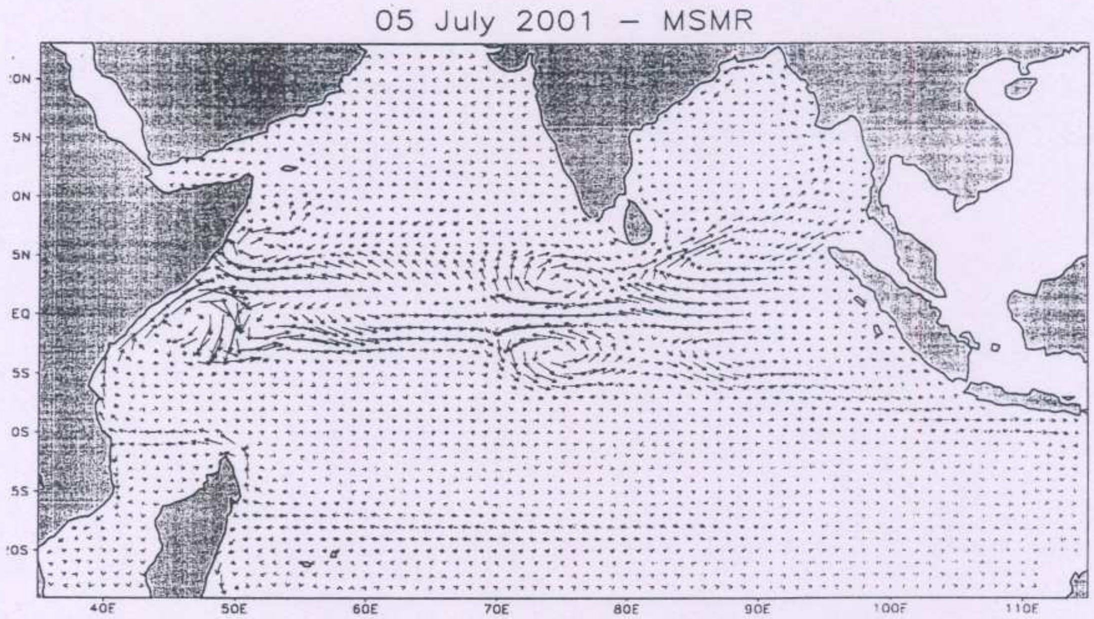
05 July 2001 – MSMR
40E
50E
60E
70E
80E
90E
100E
110E

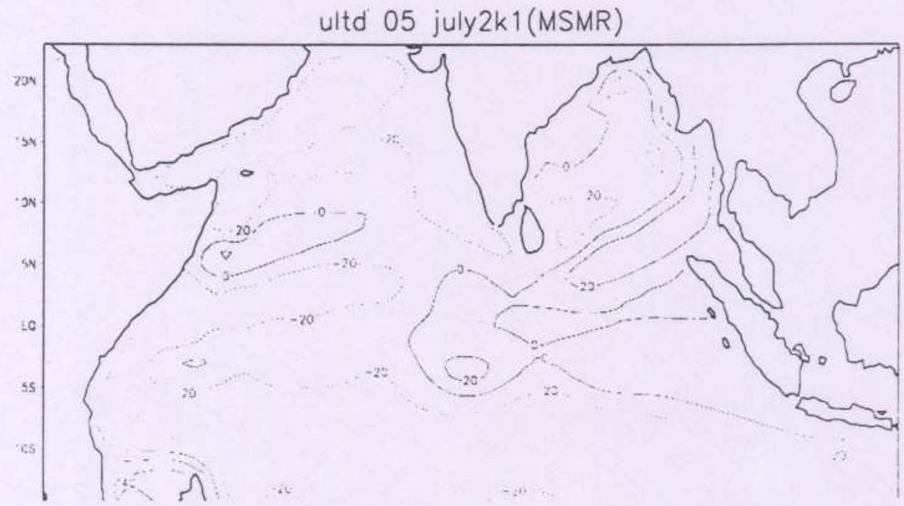
ultd 05 july2k1(MSMR)

b

15 July 2001 – MSMR

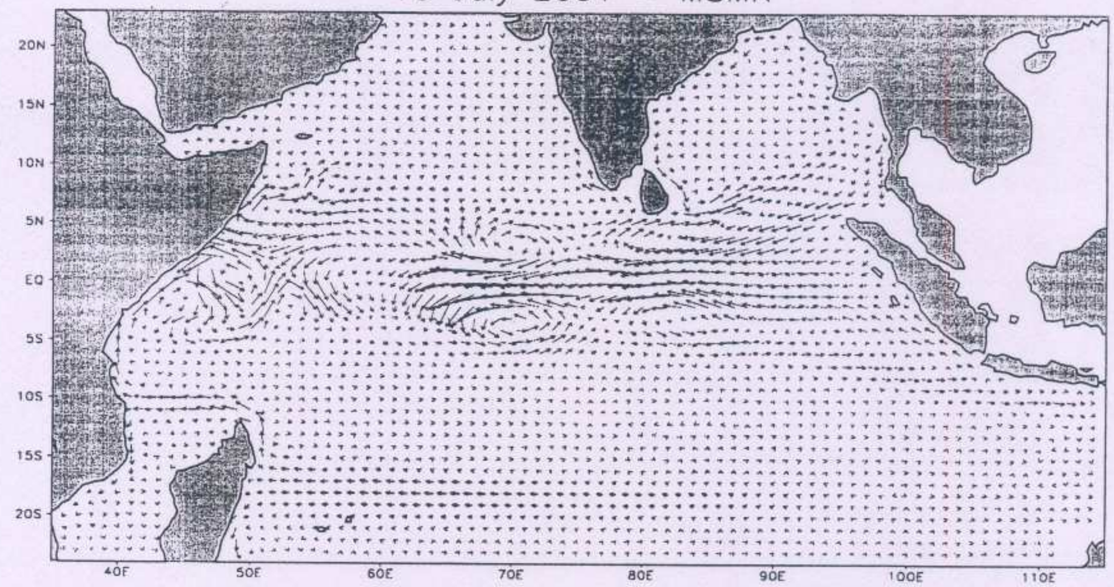

ultd 15 july2k1(MSMR)

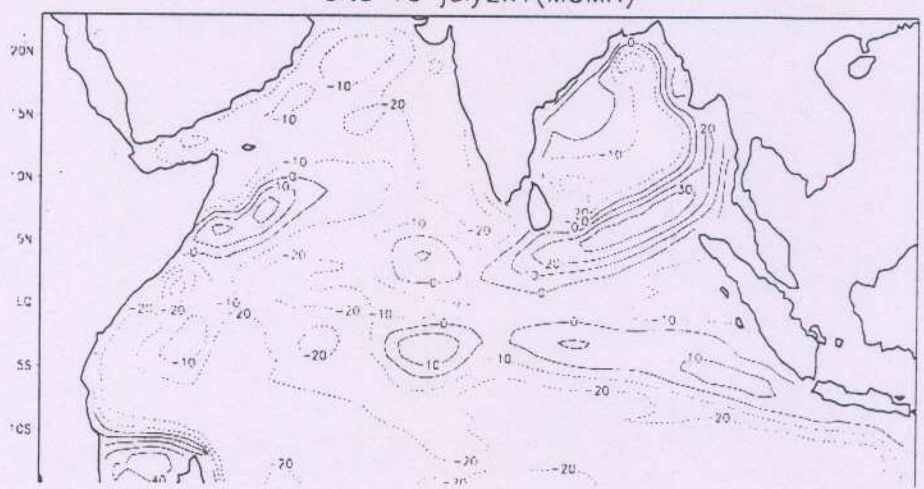

c

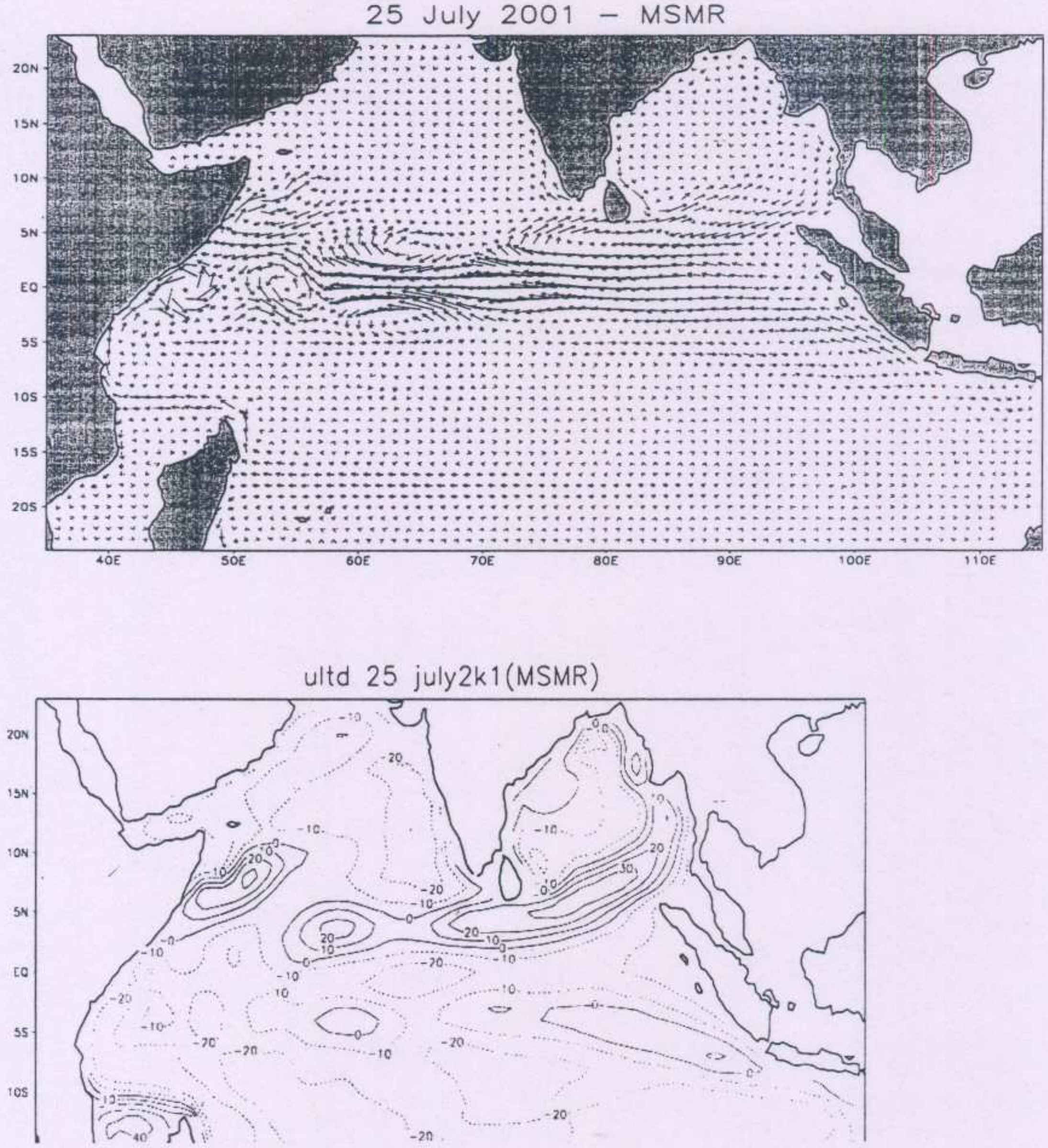

Fig 13. Same as Fig12 but for the year 2001.

a

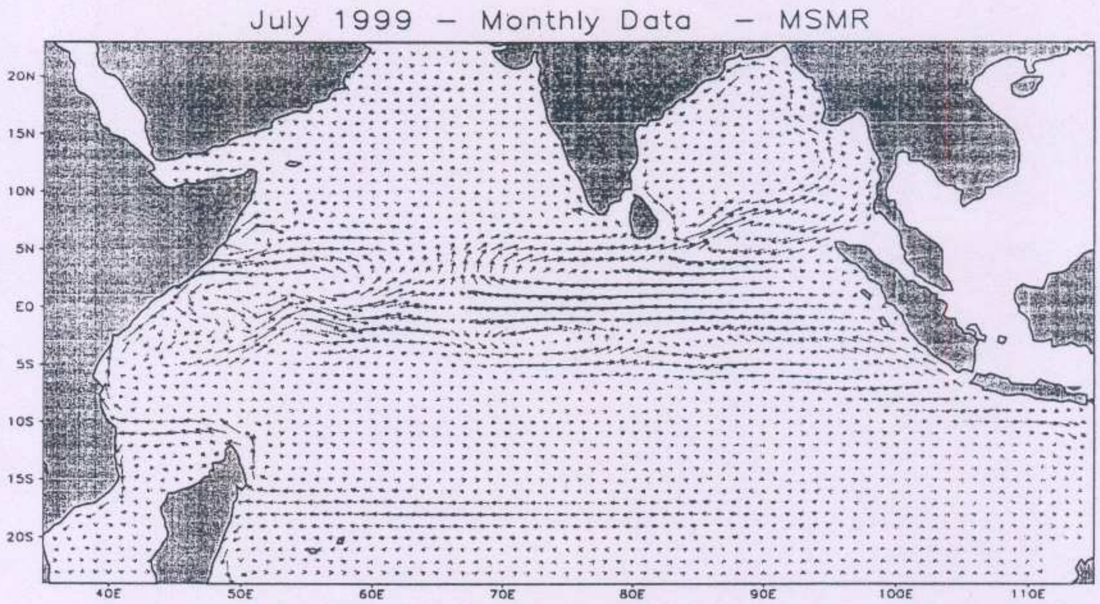

July 1999 – Monthly Data – MSMR
20N
15N
10N
5N
EO
5S
10S
15S
20S
40E
50E
60E
70E
80E
90E
100E
110E

b

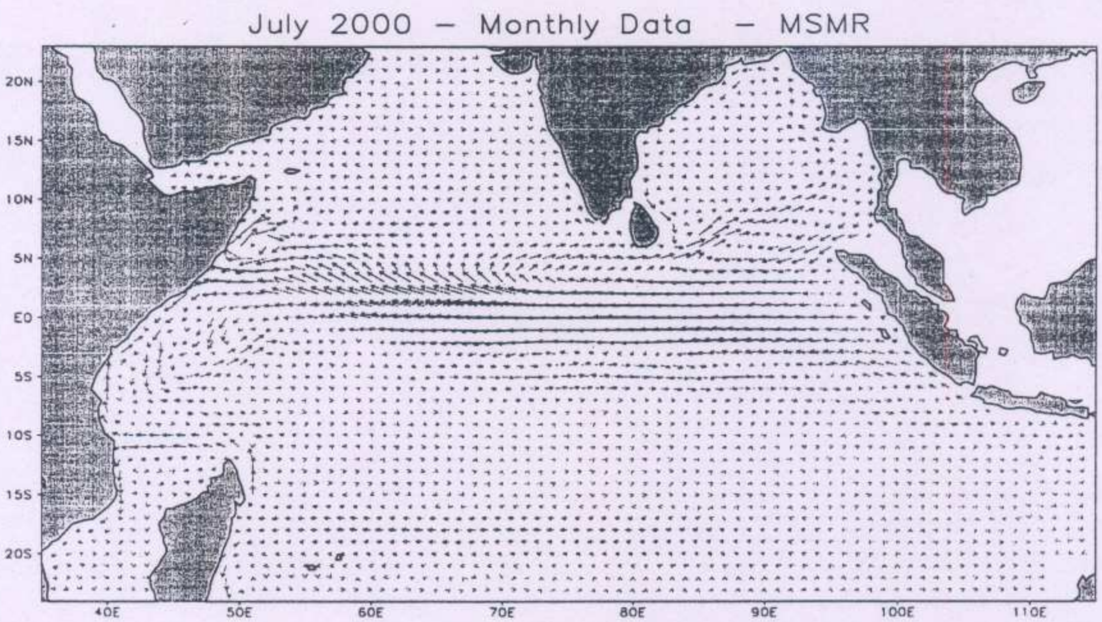

July 2000 – Monthly Data – MSMR
20N
15N
10N
5N
EO
5S
10S
15S
20S
40E
50E
60E
70E
80E
90E
100E
110E

c

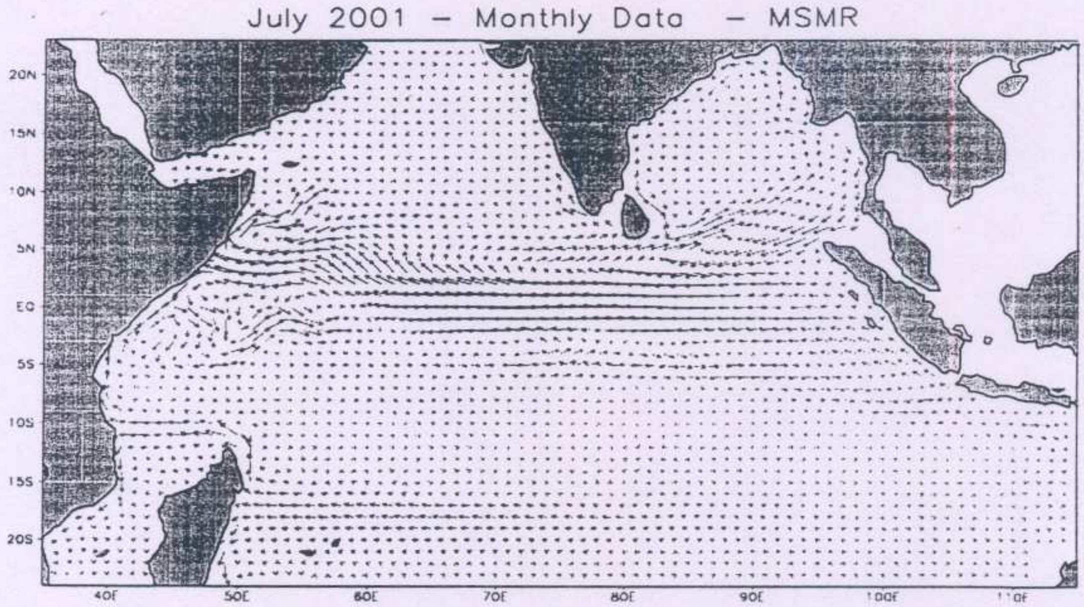

d

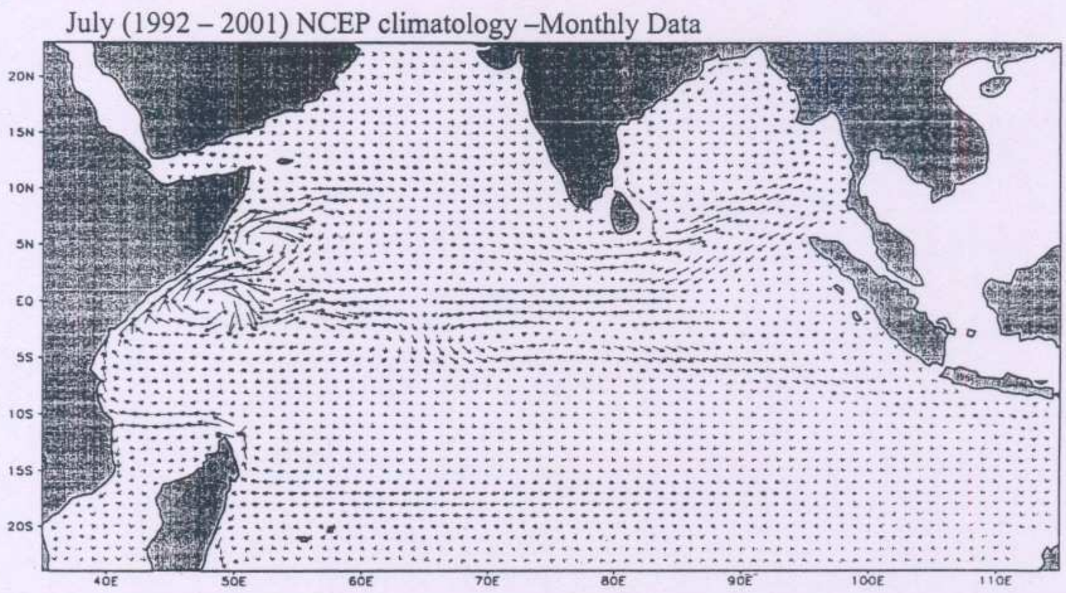

Fig 14. The Twin Gyres are not seen when the Monthly winds are used to force the model, this clearly seen in **a**, **b**, **c** when MSMR winds are used and in **d** when NCEP winds are used.

a

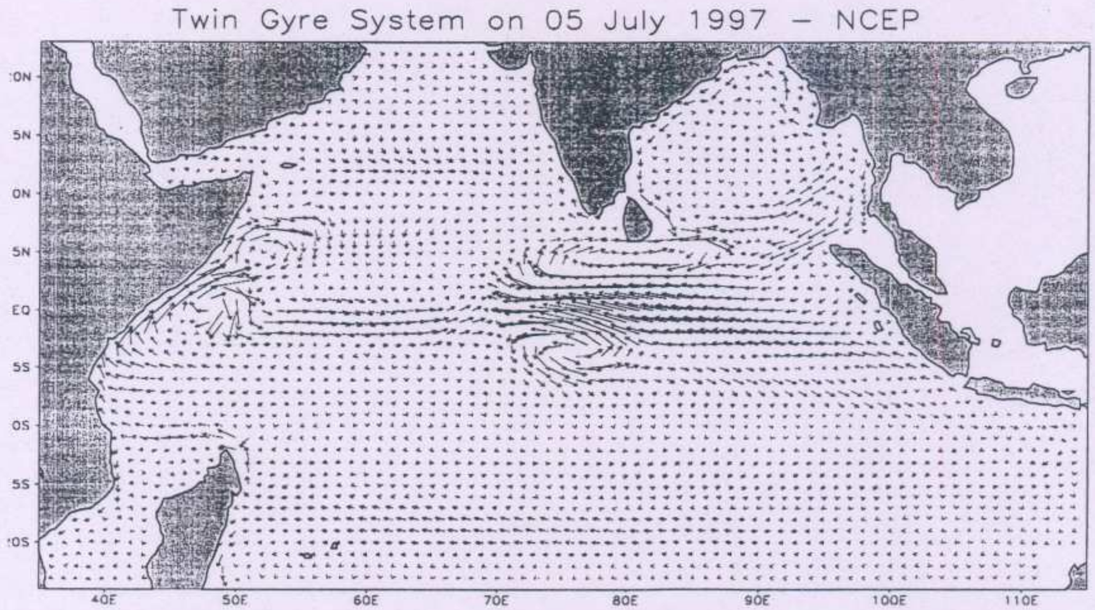

b

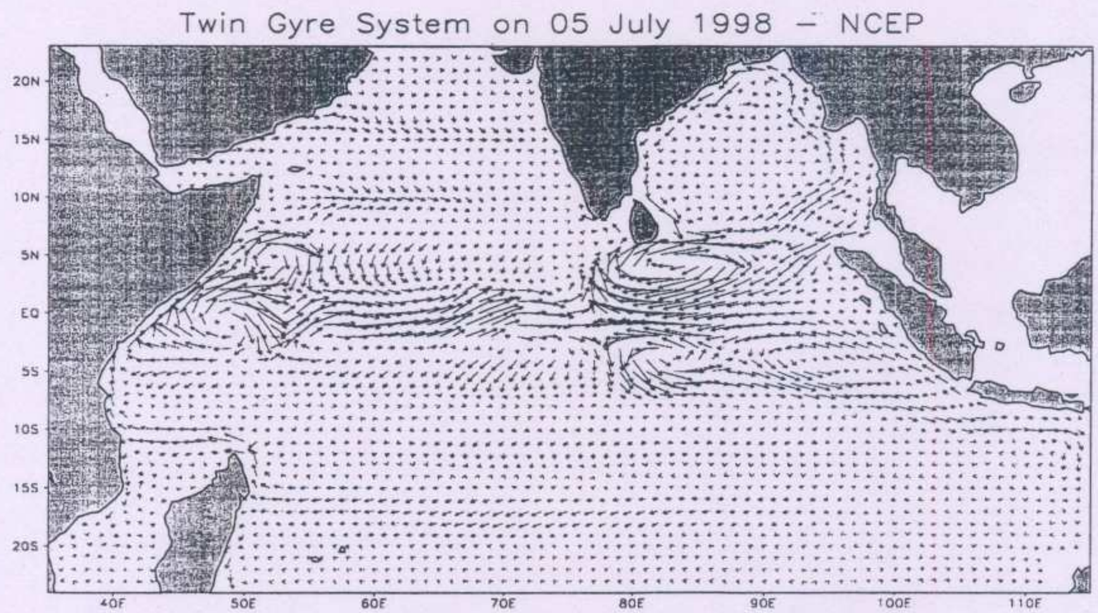

Fig 15. Twin gyres as seen the contrasting ElNino years of 1997 and 1998 in **a** and **b** respectively.

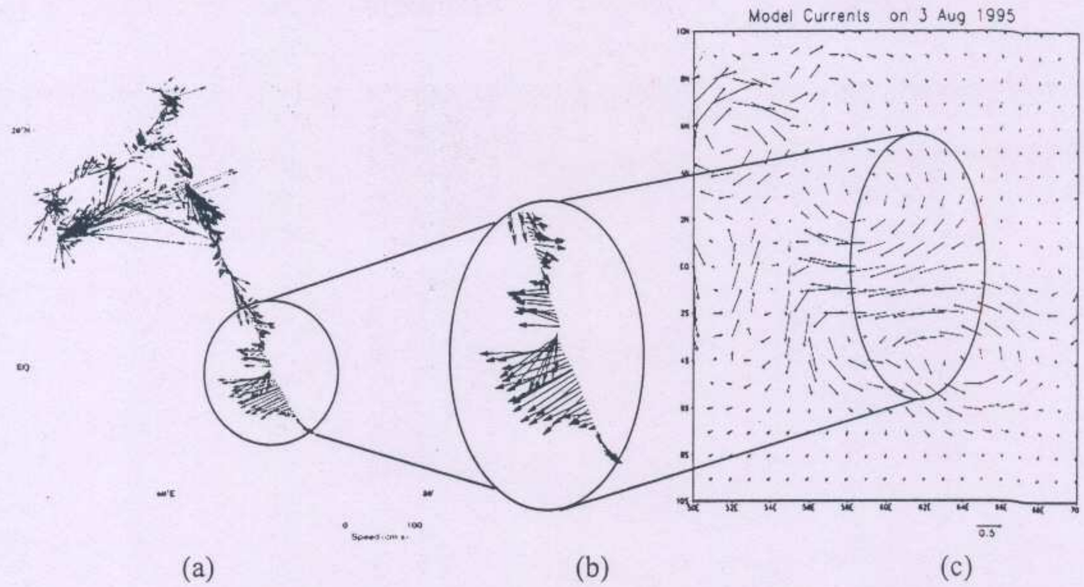

Fig 16. (a) Is the vector plots of surface circulations (25m to 35m) from the WOCE along 50E-80E, 10S-30N during 7th July – 26th August 1995. (b) A closer view (65E-70E,Eq-5N) from 1st to 3rd Aug1995 (c) The model simulated surface currents along 64E-70E,Eq-5N for 3/08/1995.

(A) TOPEX SSH 09/05 –19/05 1993

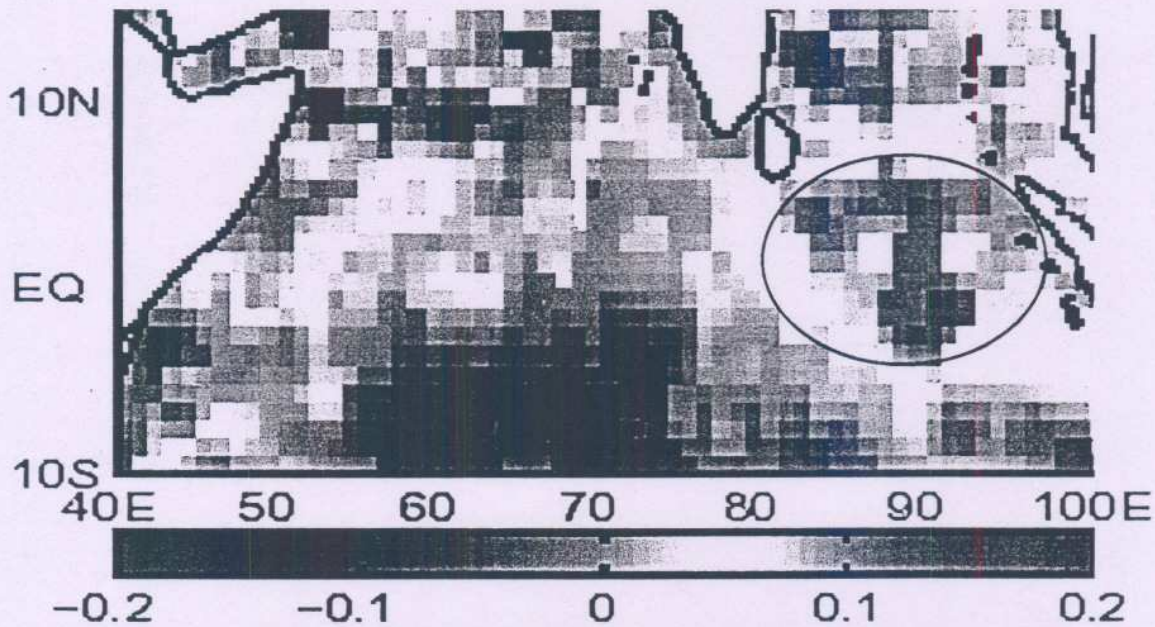

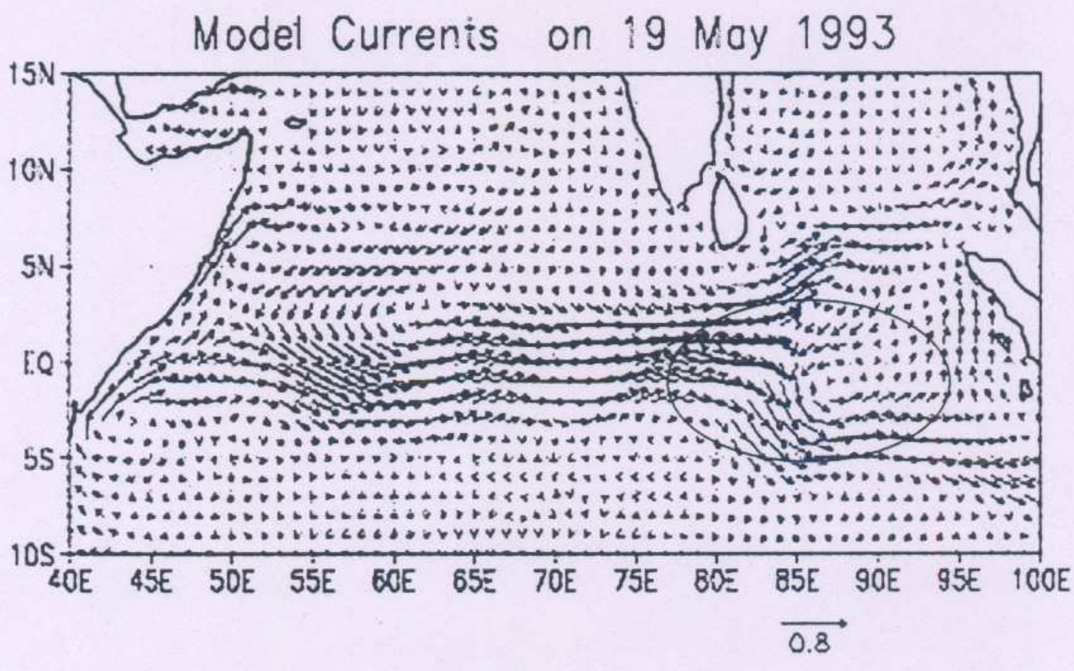

(B) TOPEX SSH 19/05 – 29/05 1993

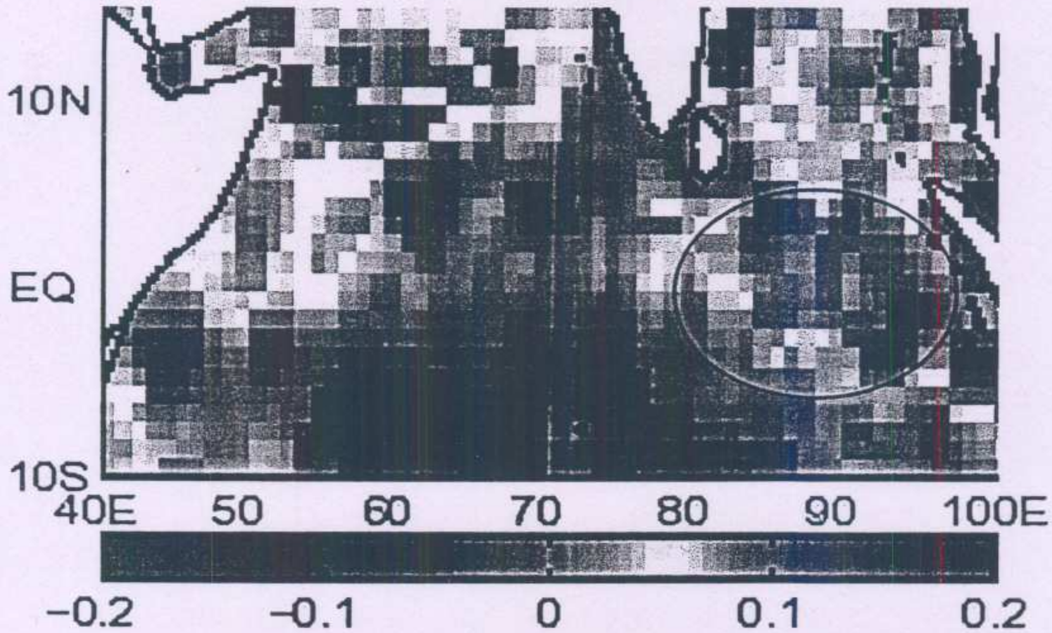

Model Currents on 30 May 1993

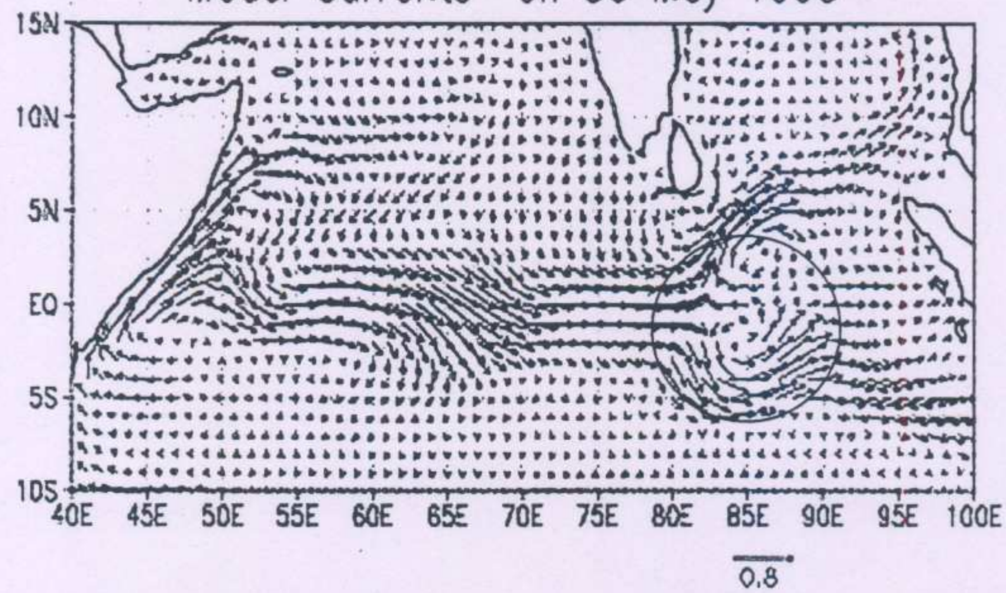

(C) TOPEX SSH 29/05 – 07/06 1993

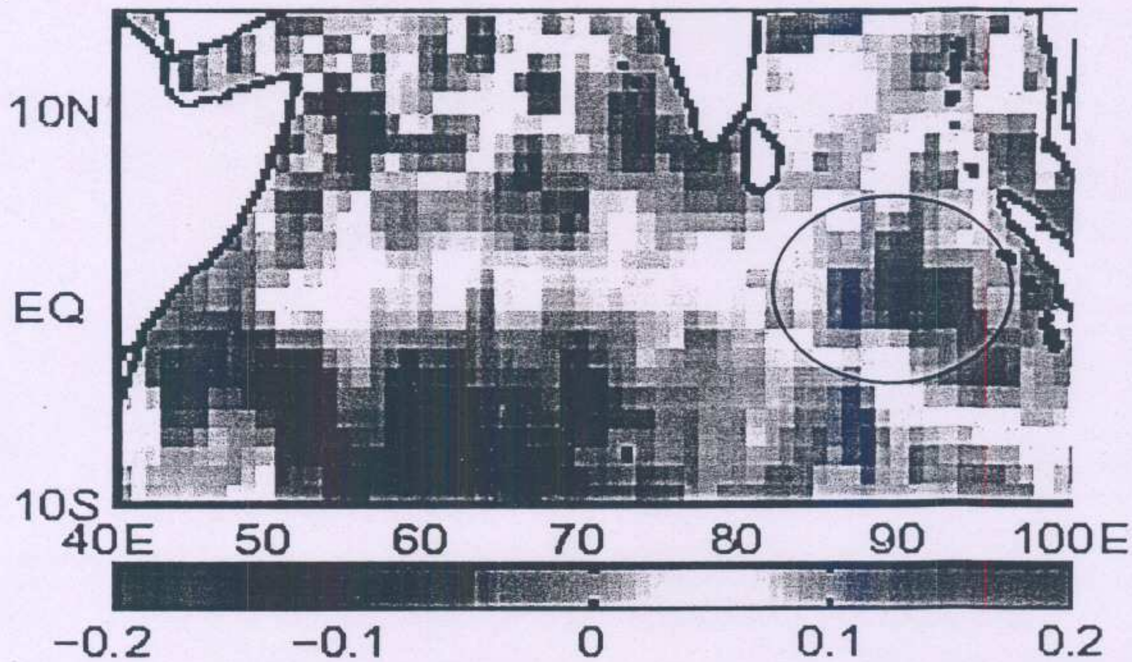

Model Currents on 9 Jun 1993

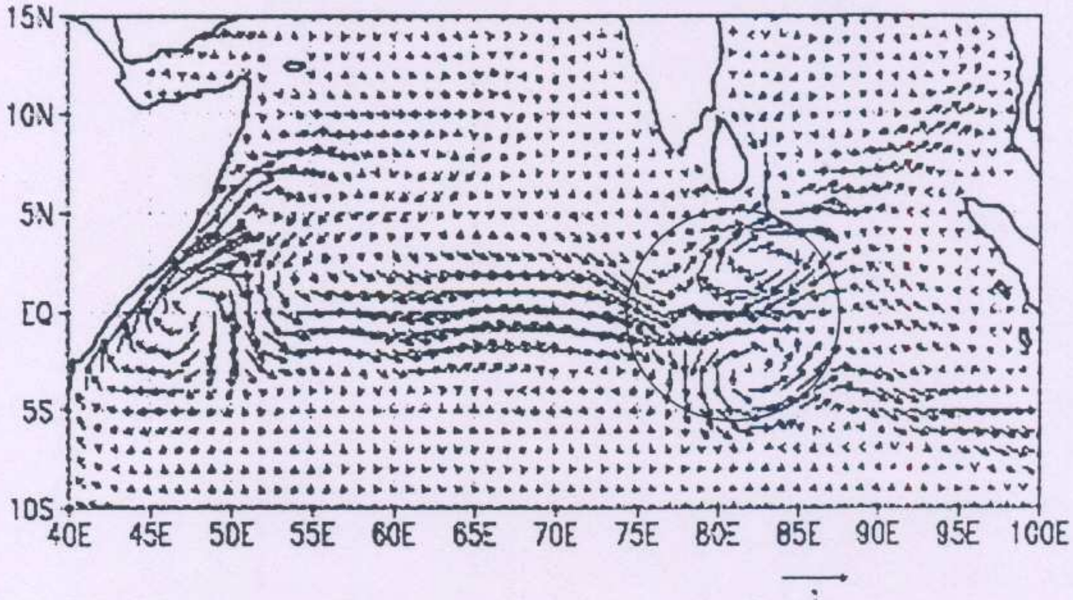

(D) TOPEX SSH 07/06 – 17/06 1993

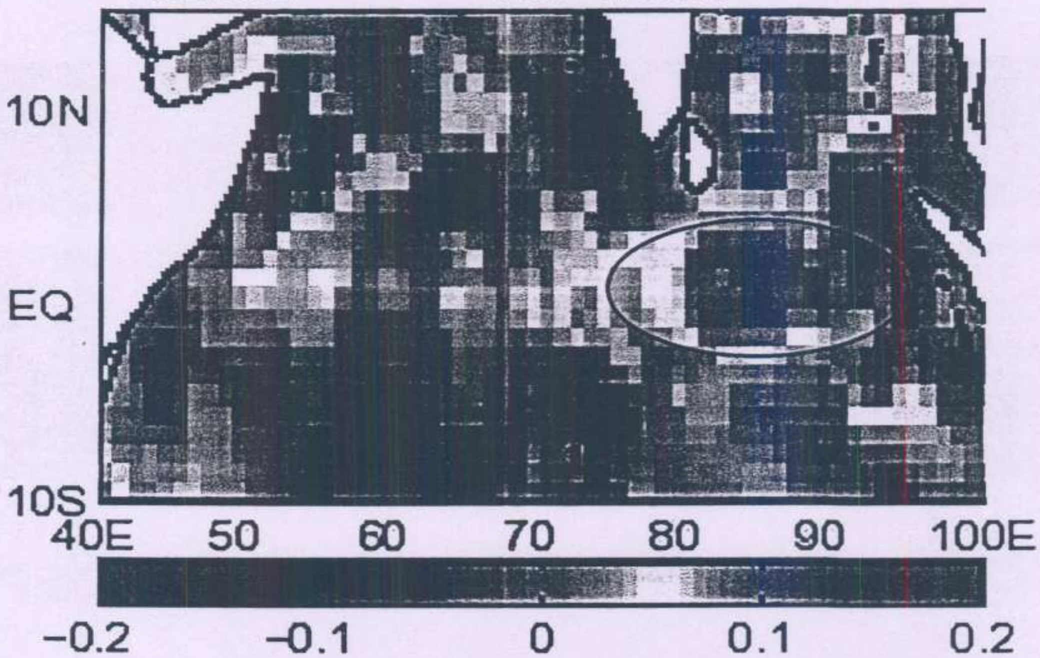

Model Currents on 19 Jun 1993

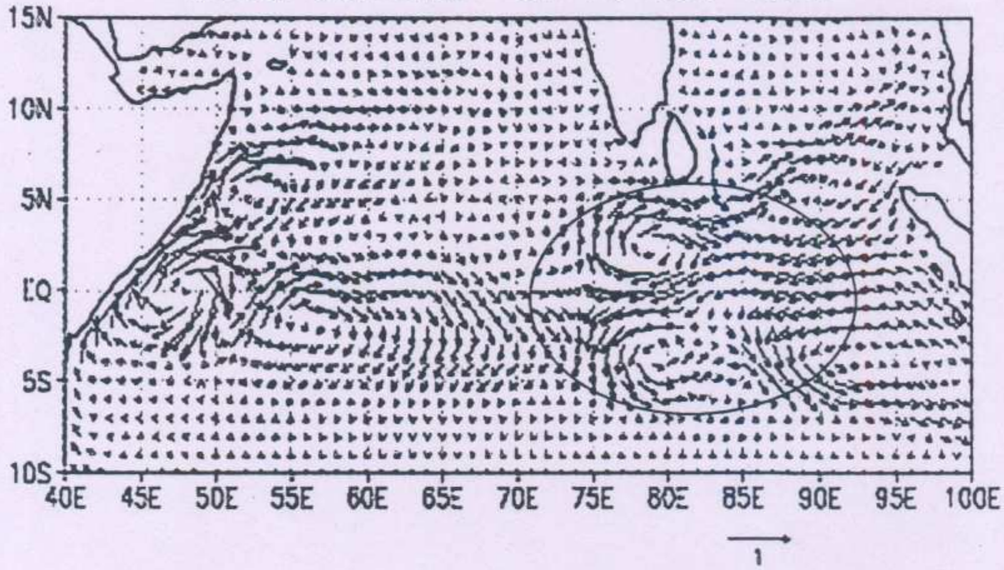

(E) TOPEX SSH 27/06 –07/07 1993

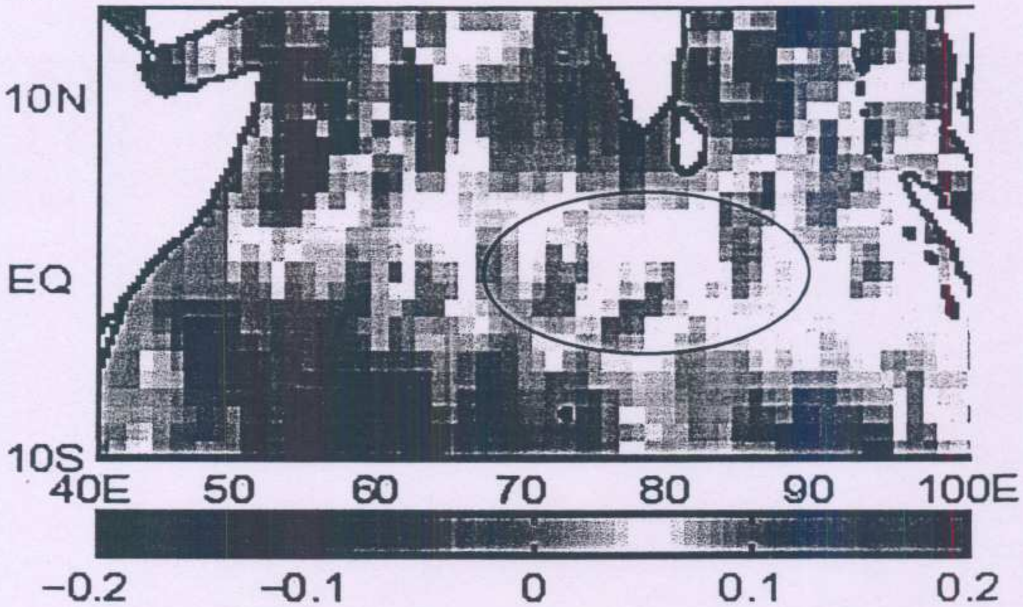

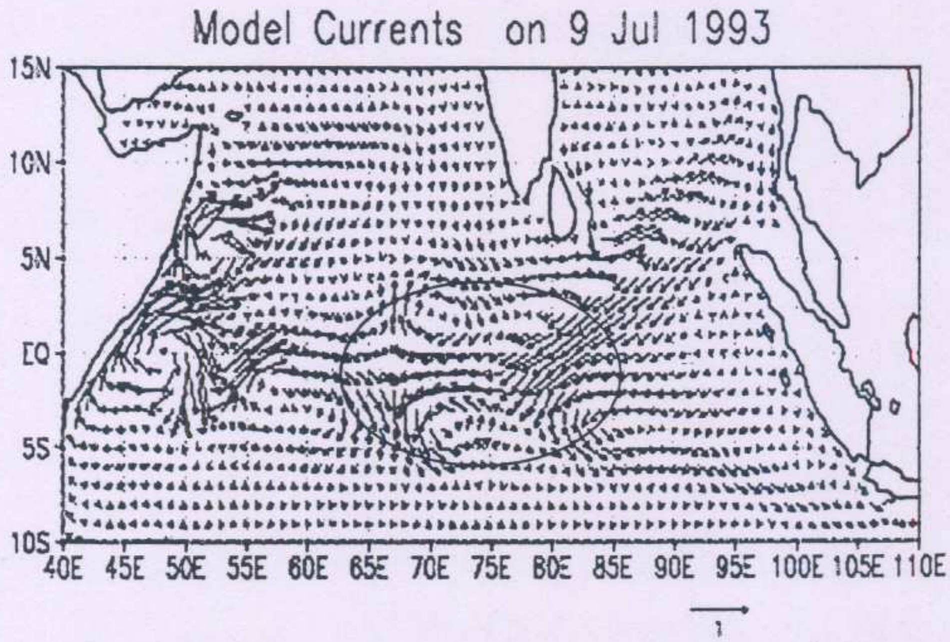

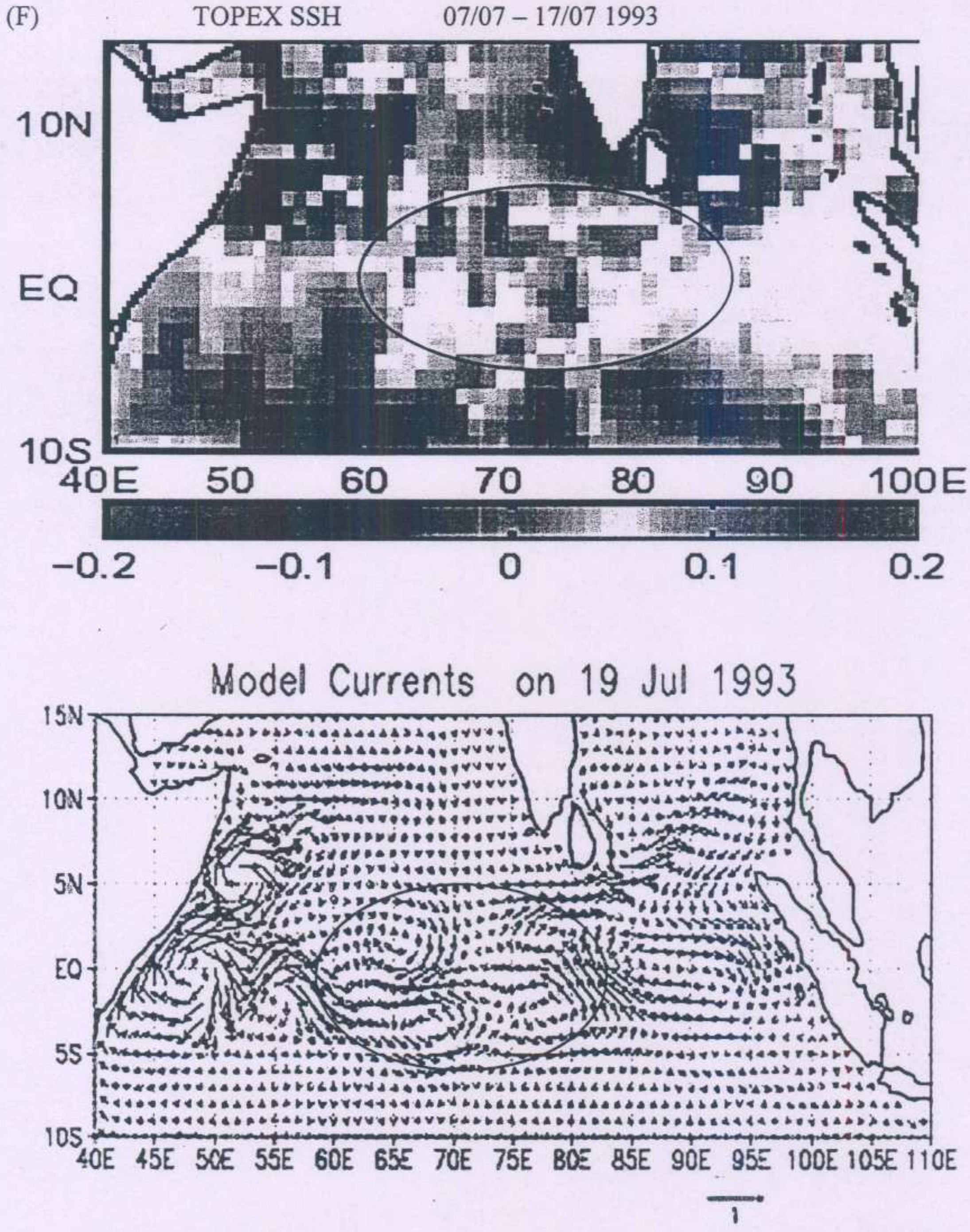

Fig.17.TOPEX/POSEIDON Sea Surface height residuals (Upper Panel) in the Equatorial Indian Ocean from 19th May to 19th July1993 and model simulations (Lower panel) for the same year (A to F). The circles in the Figures show evolution and westward propagation of the Twin Gyres that are reflected subsequently in the rise of SSH.

T- Gyres

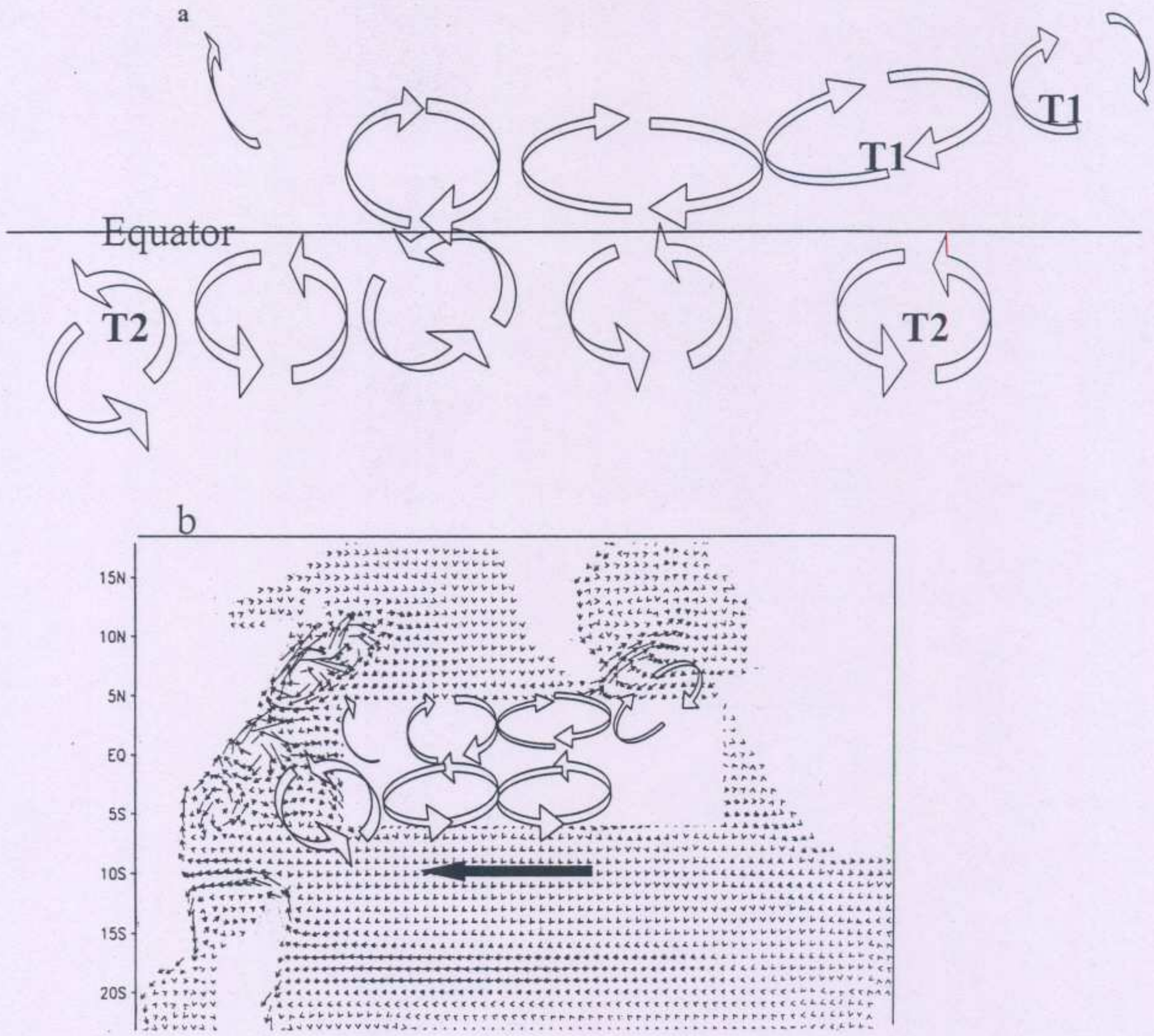

Fig 18. a & b represent the formation and westward propagation and dissipation stages of the Twin (T) gyres.T1 and T2 are the northern and southern gyre respectively.

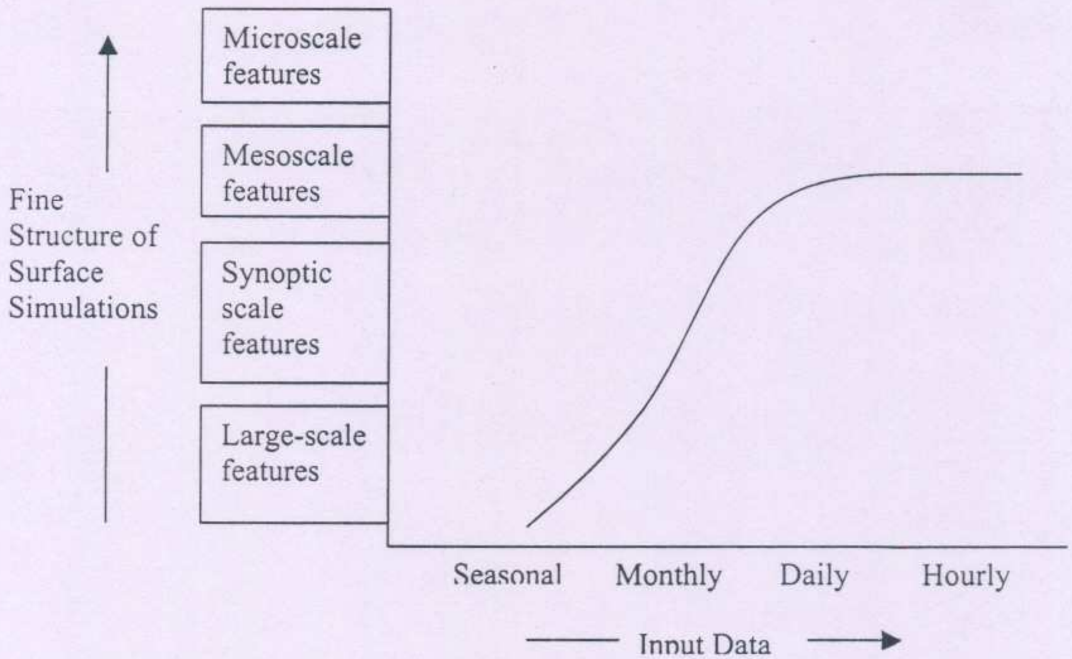

Fig 19.The variations in the Fine structures of surface simulations with Input Data.

I. I. T. M. RESEARCH REPORTS

- Energetic consistency of truncated models, *Asnani G.C.*, August 1971, RR-001.
- Note on the turbulent fluxes of heat and moisture in the boundary layer over the Arabian Sea, *Sinha S.*, August 1971, RR-002.
- Simulation of the spectral characteristics of the lower atmosphere by a simple electrical model and using it for prediction, *Sinha S.*, September 1971, RR-003.
- Study of potential evapo-transpiration over Andhra Pradesh, *Rakhecha P.R.*, September 1971, RR-004.
- Climatic cycles in India-1: Rainfall, *Jagannathan P. and Parthasarathy B.*, November 1971, RR-005.
- Tibetan anticyclone and tropical easterly jet, *Raghavan K.*, September 1972, RR-006.
- Theoretical study of mountain waves in Assam, *De U.S.*, February 1973, RR-007.
- Local fallout of radioactive debris from nuclear explosion in a monsoon atmosphere, *Saha K.R. and Sinha S.*, December 1972, RR-008.
- Mechanism for growth of tropical disturbances, *Asnani G.C. and Keshavamurty R.N.*, April 1973, RR-009.
- Note on "Applicability of quasi-geostrophic barotropic model in the tropics", *Asnani G.C.*, February 1973, RR-010.
- On the behaviour of the 24-hour pressure tendency oscillations on the surface of the earth, Part-I: Frequency analysis, Part-II: Spectrum analysis for tropical stations, *Misra B.M.*, December 1973, RR-011.
- On the behaviour of the 24 hour pressure tendency oscillations on the surface of the earth, Part-III : Spectrum analysis for the extra-tropical stations, *Misra B.M.*, July 1976, RR-011A.
- Dynamical parameters derived from analytical functions representing Indian monsoon flow, *Awade S.T. and Asnani G.C.*, November 1973, RR-012.
- Meridional circulation in summer monsoon of Southeast Asia, *Asnani G.C.*, November 1973, RR-014.
- Energy conversions during weak monsoon, *Keshavamurty R.N. and Awade S.T.*, August 1974, RR-015.
- Vertical motion in the Indian summer monsoon, *Awade S.T. and Keshavamurty R.N.*, August 1974, RR-016.
- Semi-annual pressure oscillation from sea level to 100mb in the northern hemisphere, *Asnani G.C. and Verma R.K.*, August 1974, RR-017.
- Suitable tables for application of gamma probability model to rainfall, *Mooley D.A.*, November 1974, RR-018.

- Annual and semi-annual thickness oscillation in thenorthern hemisphere, *Asnani G.C. and Verma R.K.*, January 1975, RR-020.

- Spherical harmonic analysis of the normal constant pressure charts in the northern hemisphere, *Awade S.T., Asnani G.C. and Keshavamurty R.N.*, May 1978, RR-021.

- Dynamical parameters derived from analytical function representing normal July zonal flow along 87.5 °E, *Awade S.T. and Asnani G.C.*, May 1978, RR-022.

- Study of trends and periodicities in the seasonal and annual rainfall of India, *Parthasarathy B. and Dhar O.N.*, July 1975, RR-023.

- Southern hemisphere influence on Indian rainfall, *Raghavan K.., Paul D.K. and Upasani P.U.*, February 1976, RR-024.

- Climatic fluctuations over Indian region - Rainfall : A review, *Parthasarathy B. and Dhar O.N.*, May 1978, RR-025.

- Annual variation of meridional flux of sensible heat, *Verma R.K. and Asnani G.C.*, December 1978, RR-026.

- Poisson distribution and years of bad monsoon over India, *Mooley D.A and Parthasarathy B.*, April 1980, RR-027.

- On accelerating the FFT of Cooley and Tukey, *Mishra S.K.*, February 1981, RR-028.

- Wind tunnel for simulation studies of the atmospheric boundary layer, *Sivaramakrishnan S.*, February 1981, RR-029.

- Hundred years of Karnataka rainfall, *Parthasarathy B. and Mooley D.A.*, March 1981, RR-030.

- Study of the anomalous thermal and wind patterns during early summer season of 1979 over the Afro-Asian region in relation to the large-scale performance of the monsoon over India, *Verma R.K. and Sikka D.R.*, March 1981, RR-031.

- Some aspects of oceanic ITCZ and its disturbances during the onset and established phase of summer monsoon studied with Monex-79 data, *Sikka D.R., Paul D.K. and Singh S.V.*, March 1981, RR- 032.

- Modification of Palmer drought index, *Bhalme H.N. and Mooley D.A.*, March 1981, RR-033.

- Meteorological rocket payload for Menaka-II/Rohini 200 and its developmental details, *Vernekar K.G. and Brij Mohan*, April 1981, RR-034.

- Harmonic analysis of normal pentad rainfall of Indian stations, *Anathakrishnan R. and Pathan J.M.*, October 1981, RR-035.

- Pentad rainfall charts and space-time variations of rainfall over India and the adjoining areas, *Anathakrishnan R. and Pathan J.M.*, November 1981, RR-036.

- Dynamic effects of orography on the large scale motion of the atmosphere Part I : Zonal flow and elliptic barrier with maximum height of one km., *Bavadekar S.N. and Khaladkar R.M.*, January 1983, RR-037.

- Limited area five level primitive equation model, *Singh S.S.*, February 1983, RR-038.
- Developmental details of vortex and other aircraft thermometers, *Vernekar K.G., Brij Mohan and Srivastava S.*, November 1983, RR-039.
- Note on the preliminary results of integration of a five level P.E. model with westerly wind and low orography, *Bavadekar S.N., Khaladkar R.M., Bandyopadhyay A. and Seetaramayya P.*, November 1983, RR-040.
- Long-term variability of summer monsoon and climatic change, *Verma R.K., Subramaniam K. and Dugam S.S.*, December 1984, RR-041.
- Project report on multidimensional initialization for NWP models, *Sinha S.*, February 1989, RR-042.
- Numerical experiments with inclusion of orography in five level P.E. Model in pressure-coordinates for interhemispheric region, *Bavadekar S.N. and Khaladkar R.M.*, March 1989, RR-043.
- Application of a quasi-lagrangian regional model for monsoon prediction, *Singh S.S. and Bandyopadhyay A.*, July 1990, RR-044.
- High resolution UV-visible spectrometer for atmospheric studies, *Bose S., Trimbake H.N., Londhe A.L. and Jadhav D.B.*, January 1991, RR-045.
- Fortran-77algorithm for cubic spline interpolation for regular and irregular grids, *Tandon M.K.*, November 1991, RR-046.
- Fortran algorithm for 2-dimensional harmonic analysis, *Tandon M.K.*, November 1991, RR- 047.
- 500 hPa ridge and Indian summer monsoon rainfall : A detailed diagnostic study, *Krishna Kumar K., Rupa Kumar K. and Pant G.B.*, November 1991, RR-048.
- Documentation of the regional six level primitive equation model, *Singh S.S. and Vaidya S.S.*, February 1992, RR-049.
- Utilisation of magnetic tapes on ND-560 computer system, *Kripalani R.H. and Athale S.U.*, July 1992, RR-050.
- Spatial patterns of Indian summer monsoon rainfall for the period 1871-1990, *Kripalani R.H., Kulkarni A.A., Panchawagh N.V. and Singh S.V.*, August 1992, RR-051.
- FORTRAN algorithm for divergent and rotational wind fields, *Tandon M.K.*, November 1992, RR-052.
- Construction and analysis of all-India summer monsoon rainfall series for the longest instrumental period: 1813-1991, *Sontakke N.A., Pant G.B. and Singh N.*, October 1992, RR-053.
- Some aspects of solar radiation, *Tandon M.K.*, February 1993, RR-054.
- Design of a stepper motor driver circuit for use in the moving platform, *Dharmaraj T. and Vernekar K.G.*, July 1993, RR-055.

- Experimental set-up to estimate the heat budget near the land surface interface, *Vernekar K.G., Saxena S., Pillai J.S., Murthy B.S., Dharmaraj T. and Brij Mohan*, July 1993, RR-056.

- Identification of self-organized criticality in atmospheric total ozone variability, *Selvam A.M. and Radhamani M.*, July 1993, RR-057.

- Deterministic chaos and numerical weather prediction, *Selvam A.M.*, February 1994, RR-058.

- Evaluation of a limited area model forecasts, *Singh S.S., Vaidya S.S Bandyopadhyay A., Kulkarni A.A, Bawiskar S.M.,Sanjay J., Trivedi D.K. and Iyer U.*, October 1994, RR-059.

- Signatures of a universal spectrum for atmospheric interannual variability in COADS temperature time series, *Selvam A.M., Joshi R.R. and Vijayakumar R.*, October 1994, RR-060.

- Identification of self-organized criticality in the interannual veriability of global surface temperature, *Selvam A.M. and Radhamani M.*, October 1994, RR-061.

- Identification of a universal spectrum for nonlinear veriability of solar-geophysical parameters, *Selvam A.M., Kulkarni M.K., Pethkar J.S. and Vijayakumar R.*, October 1994, RR-062.

- Universal spectrum for fluxes of energetic charged particles from the earth's magnetosphere, *Selvam A.M. and Radhamani M.*, June 1995, RR-063.

- Estimation of nonlinear kinetic energy exchanges into individual triad interactions in the frequency domain by use of the cross-spectral technique, *Chakraborty D.R.*, August 1995, RR-064.

- Monthly and seasonal rainfall series for all-India homogeneous regions and meteorological subdivisions: 1871-1994, *Parthasarathy B., Munot A.A. and Kothawale D.R.*, August 1995, RR-065.

- Thermodynamics of the mixing processes in the atmospheric boundary layer over Pune during summer monsoon season, *Morwal S.B. and Parasnis S.S.*, March 1996, RR-066.

- Instrumental period rainfall series of the Indian region: A documentation, *Singh N. and Sontakke N.A.*, March 1996, RR-067.

- Some numerical experiments on roundoff-error growth in finite precision numerical computation, *Fadnavis S.*, May 1996, RR-068.

- Fractal nature of MONTBLEX time series data, *Selvam A.M. and Sapre V.V.*, May 1996, RR-069.

- Homogeneous regional summer monsoon rainfall over India: Interannual variability and teleconnections, *Parthasarathy B., Rupa Kumar K. and Munot A.A.*, May 1996, RR-070.

- Universal spectrum for sunspot number variability, *Selvam A.M. and Radhamani M.*, November 1996, RR-071.

- Development of simple reduced gravity ocean model for the study of upper north Indian ocean, *Behera S.K. and Salvekar P.S.*, November 1996, RR-072.

- Study of circadian rhythm and meteorological factors influencing acute myocardial infraction, *Selvam A.M., Sen D. and Mody S.M.S.*, April 1997, RR-073.

- Signatures of universal spectrum for atmospheric gravity waves in southern oscillation index time series, *Selvam A.M., Kulkarni M.K., Pethkar J.S. and Vijayakumar R.*, December 1997, RR-074.

- Some example of X-Y plots on Silicon Graphics, *Selvam A.M., Fadnavis S. and Gharge S.P.*, May 1998, RR-075.

- Simulation of monsoon transient disturbances in a GCM, *Ashok K., Soman M.K. and Satyan V.*, August 1998, RR-076.

- Universal spectrum for intraseasonal variability in TOGA temperature time series, *Selvam A.M., Radhamani M., Fadnavis S. and Tinmaker M.I.R.*, August 1998, RR-077.

- One dimensional model of atmospheric boundary layer, *Parasnis S.S., Kulkarni M.K., Arulraj S. and Vernekar K.G.*, February 1999, RR-078.

- Diagnostic model of the surface boundary layer - A new approach, *Sinha S.*, February 1999, RR-079.

- Computation of thermal properties of surface soil from energy balance equation using force - restore method, *Sinha S.*, February 1999, RR-080.

- Fractal nature of TOGA temperature time series, *Selvam A.M. and Sapre V.V.*, February 1999, RR-081.

- Evolution of convective boundary layer over the Deccan Plateau during summer monsoon, *Parasnis S.S.*, February 1999, RR-082.

- Self-organized criticality in daily incidence of acute myocardial infarction, *Selvam A.M., Sen D., and Mody S.M.S.*, Feburary 1999, RR-083.

- Monsoon simulation of 1991 and 1994 by GCM : Sensitivity to SST distribution, *Ashrit R.G., Mandke S.K. and Soman M.K.*, March 1999, RR-084.

- Numerical investigation on wind induced interannual variability of the north Indian Ocean SST, *Behera S.K., Salvekar P.S. and Ganer D.W.*, April 1999, RR-085.

- On step mountain eta model, *Mukhopadhyay P., Vaidya S.S., Sanjay J. and Singh S.S.*, October 1999, RR-086.

- Land surface processes experiment in the Sabarmati river basin: an overview and early results, *Vernekar K.G., Sinha S., Sadani L.K., Sivaramakrishnan S., Parasnis S.S., Brij Mohan, Saxena S., Dharamraj T., Pillai, J.S., Murthy B.S., Debaje, S.B., Patil, M.N. and Singh A.B.*, November 1999, RR-087.

- Reduction of AGCM systematic error by Artificial Neural Network: A new approach for dynamical seasonal prediction of Indian summer monsoon rainfall, *Sahai A.K. and Satyan V.*, December 2000, RR-088.

- Ensemble GCM simulations of the contrasting Indian summer monsoons of the 1987 and 1988, *Mujumdar M. and Krishnan R.*, February 2001, RR-089.

- Aerosol measurements using lidar and radiometers at Pune during INDOEX field phases, Maheskumar R.S., Devara P.C.S., Raj P.E., Jaya Rao Y.,Pandithurai G., Dani K.K., Saha S.K., Sonbawne S.M. and Tiwari Y.K., December 2001, RR-090.

- Modelling studies of the 2000 Indian summer monsoon and extended analysis, Krishnan R., Mujumdar M., Vaidya V., Ramesh K.V. and Satyan V., December 2001, RR-091.

- Intercomparison of Asian summer monsoon 1997 simulated by atmospheric general circulation models, Mandke S.K., Ramesh K.V. and Satyan V., December 2001, RR-092.

- Prospects of prediction of Indian summer monsoon rainfall using global SST anomalies, Sahai A.K, Grimm A.M., Satyan V. and Pant G.B., April 2002, RR-093.

- Estimation of nonlinear heat and momentum transfer in the frequency domain buy the use of frequency co-spectra and cross-bispectra, Chakraborty D.R. and Biswas M.K., August 2002, RR-094

- Real time simulations of surface circulations by a simple ocean model, P Rahul Chand Reddy, Salvekar P.S., Ganer D.W. and Deo A.A., January 2003, RR-095

RR-96.
24.4.03